Dissertation zur Erlangung des Doktorgrades

der Fakultät für Chemie und Pharmazie der

Ludwig-Maximilians-Universität München

Design of an anti-inflammatory coating for invasive medical devices

Eva Barbara Reinauer

aus Tübingen, Deutschland

2018

Erklärung

Diese Dissertation wurde im Sinne von §7 der Promotionsordnung vom 28. November 2011 von Herrn Prof. Dr. Gerhard Winter betreut.

Eidesstattliche Versicherung

Diese Dissertation wurde selbstständig und ohne unerlaubte Hilfe erarbeitet.

München, den 22.01.2018

_____

Eva Reinauer

Dissertation eingereicht am: 22.01.2018

1. Gutachter: Prof. Dr. Gerhard Winter

2. Gutachter: Prof. Dr. Wolfgang Frieß

Mündliche Prüfung am: 12.03.2018

FÜR MEINE FAMILIE

IN LIEBE UND DANKBARKEIT

. ...

ABSTRACT

The prevention of material-mediated innate immune responses, which may lead to severe side effects, is an unsolved issue in invasive medicine. Neutrophil granulocytes are activated upon contact of blood with artificial material surfaces in medical devices. This unappreciated non-specific immune response provides a challenge for invasive medicine, since it may cause systemic inflammatory reactions and severe sequelae such as organ failure or even death.

This thesis investigates the design an anti-inflammatory surface coating, which avoids or reduces material-mediated innate immune responses on the example of the material polymethylpentene (PMP). PMP is a polymer, which is used as hollow fibers in medical devices like oxygenators enabling the exchange of oxygen and carbon dioxide in the blood.

Therefore, a biofunctional anti-inflammatory coating has been developed to avoid material-mediated neutrophil activation during respiratory support. The biofunctional anti-inflammatory coating is based on the covalent coupling of the agonistic FasL-molecule APO010, the covalent coupling of albumin (Recombumin® alpha) to passivate the coating and an amino acid-based stabilizing formulation to enable stability and functionality of the coating even after ethylenoxid (EtO)-sterilization and subsequent storage of the device.

To investigate the stability and functionality of the coating, different methods were established: an ELISA to investigate the stable coupling of the biofunctional coating, a sandwich ELISA to detect detached APO010 and a chemotaxis assay to investigate the reduction of neutrophil activity after incubation with the coating.

The novel coating has been upscaled from laboratory scale (bench setting) to a serial production scale, whereby the methods from this work were able to show a rapid reduction of neutrophil activation by approx. 10 % after contacting the surface in the second serial production run and the stability of the surface coating even after accelerated aging for up to 82 days at 55 °C in the third serial production run. Three upscaling steps were performed to generate homogeneous distribution of the coating on the PMP matrix.

The biofunctional anti-inflammatory coating is a new technology to reduce unappreciated material-induced immunogenic responses. In principle, it should be possible to transfer this technology to other surfaces. This could allow for expansion of the positive effects to other medical devices in direct blood contact and can possibly show the way for new biofunctional coatings in the medical device sector.

TABLE OF CONTENTS

LIST OF FIGURES

LIST OF TABLES

ABBREVIATIONS

AA	Amino acid
AAF	Accelerated aging factor
AAT	Accelerated aging time
Ala	Alanine, L-
API	Active Pharmaceutical Ingredient
Arg	Arginine, L-
Asp	Aspartic acid, L-
BSA	Bovines Serum Albumin
C3	Complement component 3
CD	Cluster of Differentiation
CPB	Cardiopulmonary bypass
Da	Dalton
DISC	Death-inducing signaling complex
DMEM	Dulbecco´s Modified Eagle Medium
DMSO	Dimethyl sulfoxide
DNA	Deoxyribonucleic acid
DSF	Differential Scanning Fluorimetry
EDC	1-ethyl-3-(3-dimethylaminopropyl)carbodiimide hydrochloride
EDTA	Ethylenediaminetetraacetic acid
ELISA	Enzyme-linked Immunosorbent Assay
EP	European Pharmacopoeia
EtO	Ethylene oxide
FACS	Fluorescence-activated cell sorting
FADD	Fas-associated death domain protein
FasL	FasLigand
FasR	FasReceptor
FBS	Fetal bovine serum
FITC	Fluorescein isothiocyanate
FTIR	Fourier transform infrared spectroscopy
Glu	Glutamic acid, L-
Gly	Glycine
GMP	Good Manufacturing Practice
h	Hour
H_2O	Water

H$_2$SO$_4$	Sulfuric acid
HCl	Hydrochloric acid
HCMV	Human cytomegalovirus
HEPES	2-[4-(2-hydroxyethyl)piperazin-1-yl]ethanesulfonic acid
His	Histidine, L-
HPLC	High performance liquid chromatography
HRP	Horseradish peroxidase
IL	Interleukin
Ile	Isoleucine, L-
JP	Japanese Pharmacopoeia
kDa	Kilo Dalton
Leu	Leucine, L-
LIM	Leukocyte inhibition module
LL	Lower left
LR	Lower right
Lys-Acetate	Lysine acetate salt
Lys-HCl	Lysine, L-, HCl
MC	Monocyte
Met	Methionine, L-
min	Minute
MTP	Microtiter plate
N(2)-Gly-Gln	Glycyl-L-glutamine monohydrate
N(2)-Gly-L-Tyr	Glycyl-L-tyrosine
NaOH	Sodium hydroxide
nc	Negative control
NETs	Neutrophil extracellular traps
NF	National Formulary
o/n	Overnight
PBS	Phosphate buffered saline
PC	Polycarbonate
PCR	Polymerase chain reaction
PCR	Polymerase Chain Reaction
PE	Phycoerythrin
PEI	Polyethyleneimine
Phe	Phenylalanine, L-
pHEMA	Poly(hydroxyethylmethacrylate)

PI	Propidium Iodide
PMA	Phorbol 12-myristate 13-acetate
PMN	Polymorphonuclear Leukocytes
PMP	Polymethylpentene
PP	Polypropylene
Pro	Proline, L-
PS	Phosphatidylserine
PSU	Polysulfone
PU	Polyurethane
Q	Quadrant
Q_{10}	Aging factor
QC	Quality control
q-PCR	Real-time quantitative Polymerase Chain Reaction
ROS	Reactive oxygen species
RPE	Retinal pigment epithelial
RPMI	Roswell Park Memorial Institute
RT or T_{RT}	Room temperature (range from 22 to 25°C in this thesis)
SDS-PAGE	Sodium dodecyl sulfate polyacrylamide gel electrophoresis
sec	Second
SEM	Scanning electron microscope
Ser	Serine, L-
SIRS	Systemic inflammatory response syndrome
T_{AA}	Accelerated aging temperature
Thr	Threonine, L-
T_m	Melting point
TMB	3,3',5,5'-Tetramethylbenzidine
TNFSF13	Tumor necrosis factor ligand superfamily member 13
Tyr	Tryptophan, L-
UL	Upper left
UR	Upper right
USP	United States Pharmacopeia
Val	Valine, L-
w/	With
w/o	Without
wt	Wild type
XTT	Tetrazolium salt

1 General Introduction

1.1 Medical need

The prevention of material-mediated innate immune responses, which may lead to severe side effects, is an unsolved issue in invasive medicine. Neutrophil granulocytes are activated upon contact of blood with artificial material surfaces in medical devices [1-3]. This unappreciated non-specific immune response provides a challenge for invasive medicine, since it may cause systemic inflammatory reactions and severe sequelae such as organ failure or even death [1-5].

This thesis investigates the design an anti-inflammatory surface coating, which avoids or reduces material-mediated innate immune responses.

1.2 Medical devices with blood contact

1.2.1 The development of the heart-lung machine as an example

In 1931, John H. Gibbon started with animal experiments to substitute the functions of heart and lung by a machine [6]. 20 years later, the first successful open heart operation was performed using a heart-lung machine [7]. Another team of surgeons worked on a different approach: the team of Clarence Walton Lillehei established a method of cross-circulation, where a healthy person served as a donor for a sick person like a biological oxygenator [8,

9]. Thus, the first operation in March of 1954 on a sick boy was successful, but the boy died after 11 days due to pneumonia. Later, Lillehei used dog lungs as oxygenator, because it was not always possible to find a donor. To decrease the risk for two persons he moved on to use the heart-lung-machine [9]. Many scientists worked on this issue for a long period of time, but were not successful. However, Gibbon and Lillehei achieved success with different approaches. Thus, 60 years later the foundation in cardiac surgery was born and today open heart surgery is a routine procedure, which is performed on a daily basis [10].

Even through the success of the first surgeries, which forms an important milestone in medicine, related problems of inflammation and thrombus formation during and after the surgeries are still leading to the dead of many patients. Therefore, to date many scientists work on the issue to reduce systemic inflammation and thrombus formation during surgeries.

1.2.2 Biocompatibility of artificial material

Artificial surfaces of medical devices may consist of different material like metal, ceramic, glass, synthetic materials (plastics), or biopolymers depending on their application [11]. A high number of medical devices consist of plastics, because plastic is cheap and easy to handle in the manufacturing process and can be adapted to any application. Whereas polypropylene (PP) is often utilized for syringes, filters, etc. due to its thermal stability during sterilization, silicon is often used for breast implants, and polycarbonate is often used for housings due to its robustness. Most medical devices consist of several materials, for example the housing of a membrane oxygenator comprises polycarbonate, whereby the inner membrane for the gas exchange may consist of polypropylene (PP) or polymethylpentene (PMP) [11, 12].

In literature, many investigations to generate biocompatible materials are published. Cao et al. (2007) demonstrated a reduction of protein adsorption, platelet adhesion and thrombus formation in *in vitro* models by using a tetraglyme coated material compared to the untreated materials. They assume that one main advantage of improved blood compatibility of plasma-deposited tetraglyme, a hydrophilic polymer, comes from a generalized reduction in blood interactions [13, 14].

Ishihara et al. (1994) showed on grafts that the zwitterionic phosphorcholine, consisting of a hydrophilic side chain with phospholipid polar groups and a hydrophobic tail, decreases

protein adsorption compared to the original graft coating. Thus, blood cell activation and aggregation on the surface were inhibited [15].

However, more or less the same materials have been used in the clinic for more than 50 years. The reason is the lack of understanding of the biology and physicochemistry of the interaction between blood proteins, cells, and artificial materials [16]. One of the main issues for using basically the same materials is the difficulty in analyzing and evaluating the new biomaterials in the relevant biological environment [16].

Some researchers suggest that only the uppermost layer of a biomaterial is in direct physicochemical contact with the biological system, which means that the distance of the liquid biointerface is just some atomic bond long [17, 18]. Therefore, it is important not only to study the biocompatibility of a material by microscopic or spectroscopic data, but the aqueous milieu of the bio-system in contact with the biomaterial [16, 17].

1.2.3 Blood-contacting medical devices induce inflammatory response and thrombus formation

Through the interaction of air, blood, synthetic components, and mechanical stress in the cardiopulmonary bypass (CPB) device, an inflammatory response is mediated. This inflammatory response gets enhanced by the physical trauma of surgery and effects of ischaemia and reperfusion [19-22]. Therefore, the stress by the artificial surface and the biomaterials should be kept as low as possible. Blood-contacting medical devices, such as vascular grafts, stents, and heart valves are necessary in cardiovascular treatment. For patients with cancer, venous catheters and ports are required to get access to the veins. In these devices not only inflammation but also thrombus formation is a common cause of failure. Due to the complexity of the different aspects, which have influence in the health of patients, it is of major importance to understand how blood-contacting medical devices induce coagulation and inflammation and how to prevent it [23].

When blood comes in contact with surfaces of medical devices, there is a fast adsorption of plasma proteins on the surface. The formation of the protein adhesion is related to the physicochemical properties of the surface and is the first step for a potential inflammatory response and thrombus formation [24].

In Figure 1-1, the activation of thrombus formation and inflammation via the medical device surface is shown. Protein adsorption to the artificial surface activates several cascades. Platelets attach to the protein layer and get activated to form aggregates. The intrinsic

coagulation cascade begins with the zymogen activation step of the factor XII. Factor XII is self-activated by adsorption to form factor XIIa, which converts prekallikrein to kallikrein. Factor XII activation also initiates a cascade of reactions resulting in the generation of thrombin from prothrombin. Thrombin generates fibrin polymers from fibrinogen monomers and further promotes platelet activation. The platelet aggregates get stabilized by the fibrin polymers resulting in the formation of a thrombus. The activation of the complement system by kallikrein, thrombin and other coagulation enzymes results in an inflammatory response in the body of the patient [1, 23].
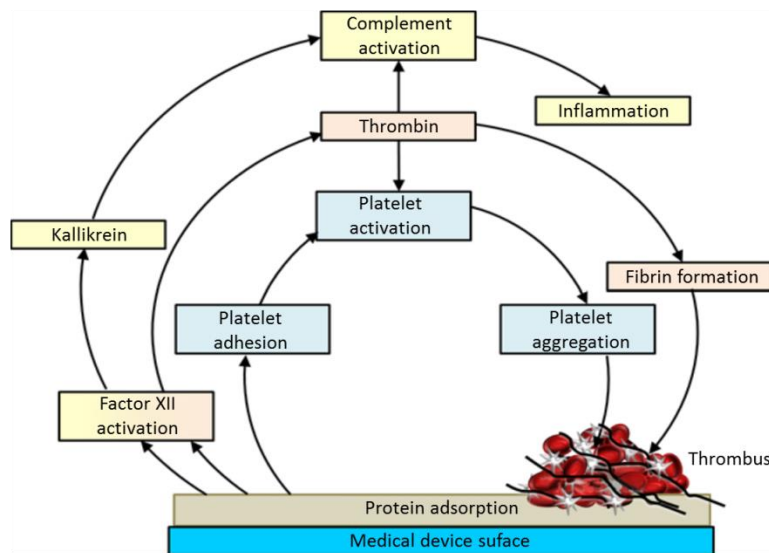
Figure 1-1. Activation of thrombus formation and inflammation via medical device surface.
Via protein adsorption on the medical device surface several cascades are activated simultaneously. The protein adsorption activates the platelet adhesion, followed by the platelet activation and aggregation. The factor XII gets auto-activated to factor XIIa by adsorption, whereby factor XIIa converts prekallikrein to kallikrein. This initiates coagulation and thrombin generation. Thrombin leads to fibrin formation and promotes platelet activation. The platelet aggregates get stabilized by fibrin resulting in the formation of a thrombus. The activation of the complement system by kallikrein, thrombin and other coagulation enzymes induce an inflammatory response in the patient (modified from [23]).

1.2.4 The role of leukocytes during inflammation and neutrophil physiology

The circulating leukocytes comprise neutrophils, monocytes, lymphocytes, basophils and eosinophils. In the application of blood-contacting medical devices, especially cardiovascular devices, neutrophils play the major role in inflammatory response [25].

In healthy humans, the release of mature neutrophils from the bone marrow is a highly regulated process, whereby chemokines control the neutrophils in circulation. This process leads to a pool of neutrophils is always ready for release in case of an infection [26].
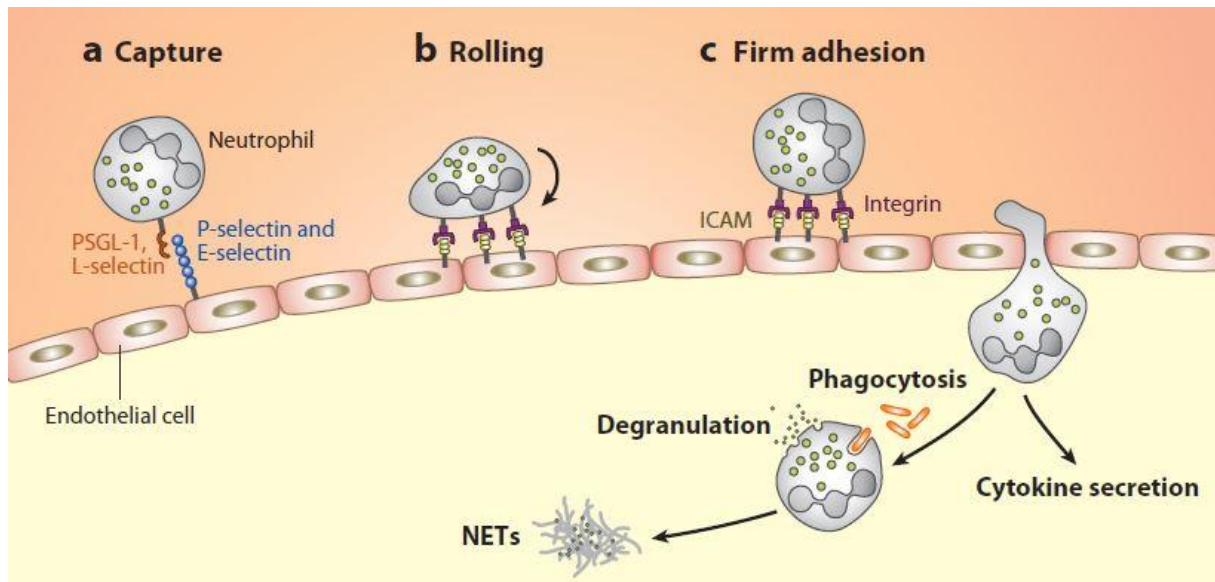
Figure 1-2. Neutrophil recruitment.
When circulating neutrophils recognize signs of inflammation, first they get captured by stimulated endothelial cells, which expose P- and E-selectins on which the exposed L-selectin of the neutrophils can bind. Further, the neutrophils roll along the endothelial cells mediated by expressed selectins until integrins lead to a tight adhesion. Then, the neutrophil passes through the endothelium and arrives at the site of inflammation. There, the neutrophil releases cytokines for recruiting other immune cells, start with engulfment of microbes via receptor-mediated phagocytosis, the release of granular antimicrobial molecules by degranulation and the formation of neutrophil extracellular traps (NETs) [26].

The common opinion is that neutrophils have a short half-live of about 8 hours *in vivo* [27, 28], whereby the lifespan is decreased to < 24 h *ex vivo* [29]. By infection, several disorders, and some diseases the amount of neutrophils and their lifespan is increased after migration into tissue for up to several days [5]. Controversially, Pillay et al. (2010) followed up with the different approaches to investigate the lifespan of neutrophils and found a lot of inconsistent results in neutrophil lifespan depending on *in vivo* or *ex vivo* models. By labelling of neutrophils, he and his colleagues could show an average lifespan of 5.4 days in humans. The at least 10 times longer lifespan than previously reported indicates a novel role of neutrophil functions in health and disease [29].

As neutrophils are essential cells in inflammatory response and during material-mediated immune response, their behavior after and during pro-apoptotic contact is investigated in the work presented in this thesis.

When neutrophils get activated, they migrate to the inflammation site in a process called chemotaxis. Thereby, they roll along the vessels and get attached to endothelial cells. By migration through the tissue they reach the inflammation site, whereby dysfunction during severe inflammation can lead to tissue damage and organ failure [26]. Severe inflammation can be induced by cardiac surgery, trauma, sepsis, reperfusion, organ transplantation or other disorders. By these disorders, dysfunction as the systemic inflammatory immune response syndrome (SIRS) and multiple organ failure are common, whereby highly activated neutrophils may worsen the situation by their prolonged survival and their aggressive immune defense like chemotaxis, the movement of neutrophils to a stimulus, NETosis, a form of cell death by the release of DNA in forms of neutrophil extracellular traps (NETs) or the release of reactive oxygen species (ROS) during respiratory burst [5, 26, 30, 31].

Gorbet et al. (2004) demonstrate in their review the evidence that the normal behavior of circulation neutrophils to roll along endothelium, adhere to stimulated endothelial cell and platelets, may happen as well on biomaterials. However, the mechanism to material-induced leukocyte activation is not fully understood yet. Therefore, a strategy to inhibit the material-induced inflammatory response is a crucial issue for many researchers in the field of material surface coatings.

In conclusion, the excessive immune response due to artificial materials in extracorporeal systems is going along with the activation of neutrophils and other disorders. The high number of activated neutrophils in the blood combined with the ability in inflammatory response enhancement confirms the assumption that inactivation of neutrophils is a central aspect in order to avoid material-mediated inflammation.

1.3 State of the art of material surface coating in the field of medical devices

Previous approaches to address the issue of a material-mediated immune response aim primarily at a passivation of the medical devices by masking their surface. In this part such anti-inflammatory coatings with the function to inhibit instead of to passivate shall be discussed.

1.3.1 Coating of surfaces

In 1916, McLean discovered an anti-thrombin, which is known today as heparin. It is a sulfated glycosaminoglycan, which is naturally produced in mast cells and today is used therapeutically as anticoagulant during surgeries and other medical applications [32, 33]. In nature, heparin is a polymer mix with different chain sizes, whereby the pharmaceutical production offers unfractionated heparin and low-molecular-weight heparin, which was developed in the late 1970s [33].

By its high anionic charge the heparin binds efficiently to the plasma protease inhibitor anti-thrombin III, which further inactivates prothrombin, factor Xa and other proteases by their conformational change induced by heparin binding. This results in an inactivation of fibrin, whereby heparin increases the effect of anti-thrombin III by up to 2000 times [34].

Due to the ability of heparin to anticoagulation, it is used for novel drug treatments for several diseases, including cancer and inflammatory diseases [35]. In the medical device sector heparin is used to mask artificial material and to support the anticoagulation during blood contact [36]. A negative side effect is the heparin-induced thrombocytopenia (HIT), which is a degradation of platelets in the presence of heparin resulting in thrombocytopenia [37].

Another well studied molecule is the human serum albumin, which is known to passivate artificial surfaces mostly by adsorption to the surface and therefore is often used to generate a biocompatible material [38-40].

Using thin biofunctional coatings like polyelectrolyte multilayers in the layer-by-layer method allows new biocompatible materials, which combine the mechanical properties of the classic materials and the new biocompatible property of the coating. These coatings can change the contact from tissue to biomaterial, which can tune the response of the tissue to the contact with the biomaterial. The coatings can consist of Heparin and Collagen or other components depending on their application. The coatings can be used as drug carrier, by loading active

7

substances, or they can specifically respond to the changes in the surrounding [41, 42]. Therefore, biofunctional coating may result in a better application of the biomaterial.

1.3.2 Leucocyte filters

In the 1990s, leukocyte removal filters were developed for incorporation into the cardiopulmonary bypass (CPB) circuit. Some of these filters show efficient depletion of up to 99.5 %, which means almost no cells could be measured post-filtration [43]. However, Boodram and Evans (2008) nicely summarized in their review 40 publications from the past 10 years with the summary that the efficiency of the leukocyte depletion filters is controversial.

On the one hand, some researchers observed positive results for the patient, e.g. they could demonstrate that strategic leukocyte depletion during reperfusion phase reduces myocardial damage when using the filter in arterial line [44]. Other researchers could not find beneficial effects of leukocyte filtration on postoperative myocardial function when using the filter in arterial line [45].

The same controversial findings were summarized by Boodram and Evans (2008) regarding inflammatory mediators using the filter in arterial line. They summarized that the value of the complement component 3 (C3), one important part of the complement system, was significantly lower in the leukocyte filtered group 24 hours postoperatively, but that no impact on the patient recovery was observed [46]. Furthermore, Mair et al. (1999) could show no significant difference in inflammatory parameters measured except for plasma elastase concentrations, which were significantly higher during and immediately after CPB in the leukocyte filtered group compared with controls [47]. They do not support routine use of leukocyte-depleting filters [48]. Summarizing, there is no evidence for the benefit in using leukocyte depletion filters for CPB.

1.3.3 Leucocyte inhibition module (LIM)

A new approach to avoid material-mediated immune responses is the biological modification of the artificial material surfaces to reduce the activity of neutrophils, which are known to trigger further pro-inflammatory immune responses.

In 2000, Cinatl et al. observed a decreased neutrophil adhesion to human cytomegalovirus (HCMV)-infected retinal pigment epithelial (RPE) cells. They recognized that this phenomenon is mediated by an up-regulation of FasL on RPE, which was induced by the virus as a mechanism to escape from immune surveillance. This suggests a novel role for

FasL in the RPE regulation of neutrophil binding [49]. Based on these findings and with the idea to inhibit unwanted material-mediated immune response during CPB, Scholz and colleagues developed a leukocyte inhibition module (LIM) (Figure 1-3): a plastic device containing a polyurethane matrix with covalently bound anti-Fas molecules, the IgM CH11, for extracorporeal immune therapy [5].
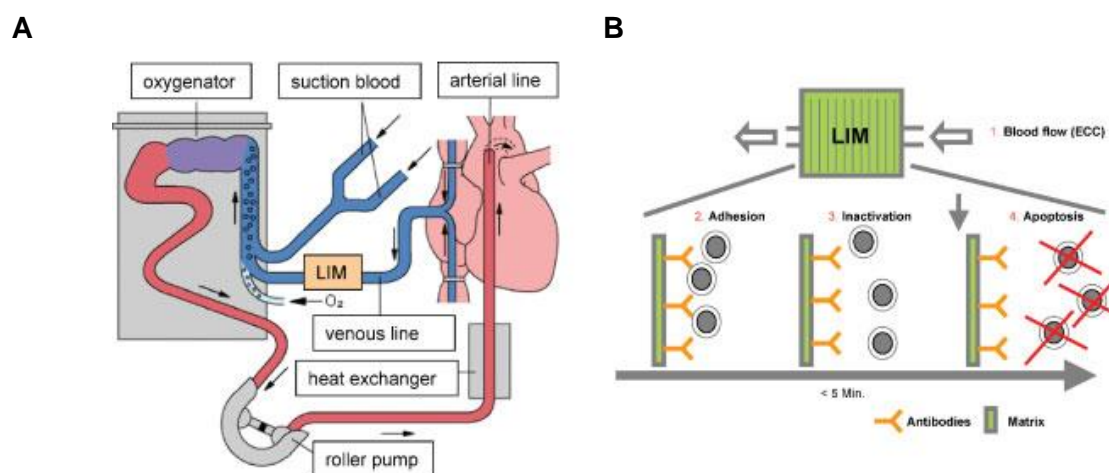
Figure 1-3. Schematic illustration of the leukocyte inhibition module (LIM).
A Localization of the LIM within the venous line of the extracorporeal circulation (ECC) during cardiac surgery. **B** function within the LIM: 1. Blood flow through the LIM, 2. neutrophil adhesion, 3. neutrophil inactivation, and 4. neutrophil apoptosis [5].

The studies show that immobilized anti-Fas molecules, which get in contact with the blood of the patient, are able to prevent excessive neutrophil activity when using extracorporeal blood circuits. The downregulation of the neutrophil activity by Fas/FasL during cardiopulmonary bypass shows the high potential profit in decreasing the material-mediated immune response ([5], [50], [51]).

When LIM was introduced in a porcine model with cardiopulmonary bypass in a heart-lung-machine, they could show reduced inflammatory markers. Furthermore, in the porcine model LIM functionally inhibits leukocyte activation, which limits pathogenic sequelae related to cardiac surgery with CPB. Used LIM in cardiac surgery patients LIM proved to be effective in reducing perioperative inflammation [50]. Furthermore, LIM did overcome apoptosis resistance of highly activated neutrophils in patients and induced anti-inflammatory effects [52-54]. Furthermore, Scholz and colleagues could demonstrate that a proprietary Stabilizing

and Protecting Solution® (SPS®), mainly consisting of amino acids, enables stability of the immobilized anti-Fas IgM molecule CH11 during sterilization [55].

The following chapter describes the extrinsic apoptotic pathway to explain the underlying mechanism of inflammation reduction by the agonistic apoptotic molecules.

1.3.4 Apoptosis as model to study efficacy of anti-Fas molecules

As one possibility to decrease the inflammatory response is the coating of these artificial materials, Scholz and colleagues used immobilized anti-Fas molecules, which get in contact with the blood of the patient, to prevent excessive neutrophil activity when using extracorporeal blood circuits. Thereby, the inactivation of neutrophils is based on the principle that neutrophils express the membrane receptor Fas (also called FasR or CD95) on their cell surface [56]. This receptor plays a crucial role in the process of programmed cell death, also called apoptosis.

The extrinsic death-receptor pathway is activated by members of the death receptor superfamily like the CD95 ligand (FasL) or the tumor necrosis factor receptor I. By the binding of these molecules, e.g. the FasL, the Fas trimerizes, which results in the formation of the death-inducing signaling complex (DISC). The DISC recruits adapter proteins such as the Fas-associated death domain protein (FADD) and the procaspase-8. Multiple procaspase-8 molecules generate the caspase-8 activation through induced proximity. This leads to the activation of the caspase activation cascade. The mechanisms of caspase activation comprise proteolytic cleavage by an upstream caspase, induced proximity and holoenzyme formation. The activated caspases initiate endonucleases and proteases to disrupt the DNA and the cell proteins (e.g. cytoskeletal proteins), which results in cell death (Figure 1-4, left pathway) [57].

The intrinsic apoptosis pathway is induced mostly by DNA damage, but showed to play a role during neutrophil apoptosis as well. In septic patients the antiapoptotic Bcl-2 is downregulated after 5 to 10 days after trauma [58].

Scholz and colleagues could show that stimulation of neutrophil Fas not only stimulates apoptosis but also induces inhibition of neutrophil function [53]. In addition, apoptosis resistance due to high levels of antiapoptotic Mcl-1 and low levels of pro-apoptotic Bax proteins can be overcome by immobilized agonistic anti-Fas [54]. By these findings, they propose the use of Fas for therapeutic strategies to prevent neutrophil hyperactivity, prolonged life-span and sepsis [53].
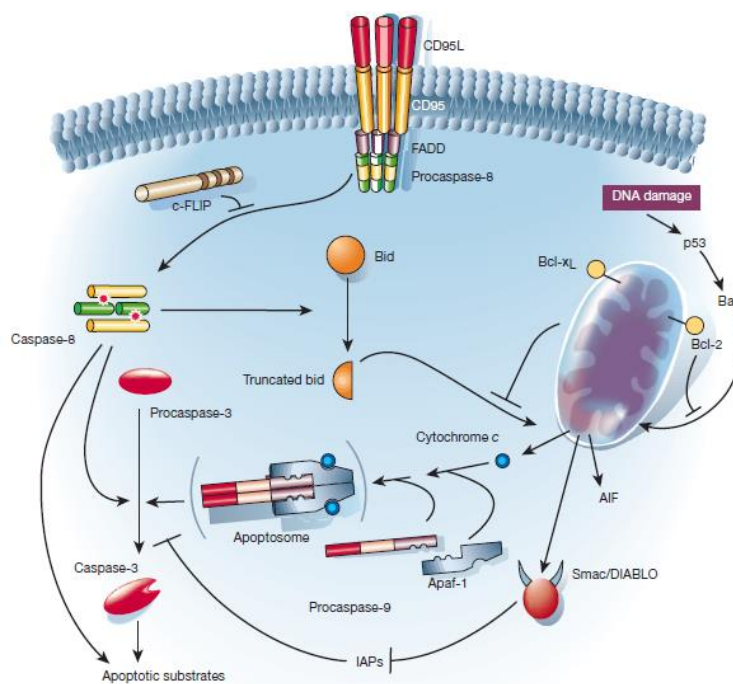
Figure 1-4. Schematic illustration of the apoptosis mechanism.
Extrinsic apoptosis: The binding of CD95L to CD95 leads to the trimerization of the receptor, which allows binding of the FADD (Fas-associated death domain protein). Thus, procaspase-8 activates caspase-8, which results in activation of other caspases that ultimately lead to apoptosis. The intrinsic, mitochondrial apoptosis mechanism is induced by DNA damage [57].

1.4 The innovative anti-inflammatory coating

The design of the innovative anti-inflammatory coating consists of a three step process: first, the selection of the molecule, second, the coupling chemistry and third, the stabilization of the coating.

1.4.1 Selection of the biomolecules

In the scope of this thesis, five anti-Fas molecules, which have optimal binding and trimerization properties to Fas, were pre-selected in this work (Table 1-1): SuperFasL, MegaFasL, Fc-FasL, E09 and CH11. SuperFasL, MegaFasL (two variants), and Fc-FasL are recombinant proteins, which trimerize to homotrimers. Three FasL are located in spatial proximity enabling the induction of apoptosis in Fas positive cells such as activated neutrophils expressing Fas on their surface.

Table 1-1. Overview of pre-selected anti-Fas molecules

Ligand	Structure	Size
SuperFasL	The extracellular domain of human FasL (aa 103-281) is fused at the N-terminus to a linker peptide (26 aa) and a FLAG®-tag.	Monomer 35 kDa glycosylated in SDS-PAGE
MegaFasL, ACRP-FasL [59]	Human FasL (aa 139-281) is fused at the N-terminus to mouse ACRP30 headless (aa 18-111) and a FLAG®-tag. The FasL and the ACRP30 lead to trimerization and disulfide bridges between ACRP30 lead to a stable hexamer.	Monomer 40 kDa glycosylated in SDS-PAGE, Hexamer 192 kDa
APO010, ACRP-FasL [59]	Human FasL (aa 139-281) is fused at the N-terminus to human ACRP30 headless (aa 16-108) and a FLAG®-tag. The FasL and the ACRP30 lead to trimerization and disulfide bridges between ACRP30 lead to a stable hexamer.	Hexamer 192 kDa
Fc-FasL [59]	FasL was fused to C terminus of the dimerization domain of IgG1 (Fc domain), this generates a hexamer structure, and a FLAG®-tag.	Monomer 50 kDa glycosylated in SDS-PAGE
IgG1 E09 [60]	Antibody	150 kDa
IgM CH11	Antibody	900 kDa

This structure makes the proteins extremely efficient because it enables the trimerization of the Fas receptor, which allows the activation of the extrinsic apoptosis pathway. IgG1 E09 and IgM CH11 are monoclonal antibodies (Figure 1-5). E09 has been reported to induce apoptosis in an effective way although the affinity to the Fas receptor is relatively weak [60]. CH11 has been used previously for anti-inflammatory approaches [61] but was shown to be instable over a longer period of storage time. Therefore, CH11 was only used as a control molecule for the assay development.

A

B
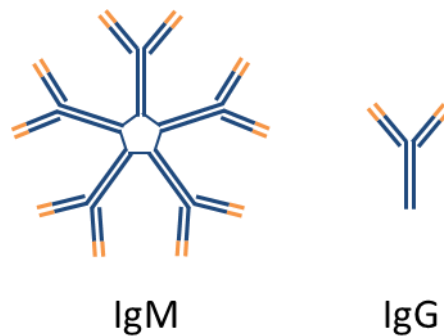
Figure 1-5. Structure of the pre-selected anti-Fas molecules.
A FasL compared to MegaFasL (APO010) and Fc-FasL [59], SuperFasL (not shown) has a similar structure as MegaFasL. **B** schematic structure of IgM and IgG1.

When investigating an anti-inflammatory coating for invasive medical devices several requirements need to be respected. The medical device has to be biocompatible and all components need to be in Good Manufacturing Practice (GMP) quality. A stable coupling of the anti-inflammatory biomolecule is necessary for safety reasons and the functionality during blood contact has to be maintained.

During CPB up to 6 l/min blood are pumped through the medical device, which require high stability of the coating. In addition, the anti-inflammatory coating needs to be haemocompatible, which includes the prevention of clotting and the inhibition of the complement activation. The anti-inflammatory coating should be specific to activated neutrophils, which get in contact with the surface. Thereby, the medical device may not lose its function. As the medical devices have to be sterile, the anti-inflammatory coating has to be resistant to sterilization, e.g. via ethylenoxid (EtO). As well, long term storage for two years at room temperature (RT) is common in medicine and has to be reached.

1.4.2 Stabilization of proteins and biologics by stabilization formulations

Many proteins and biologics are prone to chemical degradation, like oxidation and deamidation, and physical degradation, like aggregation and denaturation. These routes of degradation are dependent on pH changes, reactive oxygen species (ROS), free radicals, e.g. during processing, production, and storage time. Furthermore, increased temperature, freezing and terminal sterilization are crucial issues for biomolecules.

In order to overcome these issues, the formulation development in biotechnology has further advanced over the past decades as shown in many excellent publications, reviews, and books [62-72].

The use of specific formulations is important during the manufacturing of proteins, therapeutic antibodies, recombinant proteins and vaccines. Furthermore formulations for medical devices undergo especially harsh conditions, where they have to enable and protect biofunctional surface coatings for implants, bone cements, extracorporeal blood treatment devices, apheresis columns, wound dressings and patches during terminal sterilization and storage. Insufficient stability during the manufacturing process and long term storage are main issues in the development of pharmaceutical products and may lead to unstable products and low yields [73, 74]. Therefore, it is necessary to adapt the formulation to the desired applications. Formulations mostly consist of small molecules, e.g. sugars or sugar alcohols, in addition with amino acids, salts or other pharmaceutical excipients [63, 65, 69, 71, 75].

Especially the amino acids glycine, alanine or proline, which are called osmolytes have been reported being excellent excipients for protein stability, consistent with the fact that in nature an intracellular high osmolality can protect the organism in high environmental salt concentrations. In addition, these osmolytes do not seem to interfere with enzyme activity or functional structures [65, 75].

The combination of amino acids and sugars effectively stabilizes biologics in dried state as many organisms can survive dehydrated in a process called anhydrobiosis, when they concentrate disaccharides like trehalose intracellular [76, 77]. In dry formulations the excipients replace water and build hydrogen bonds and other non-covalent interaction with the protein [78, 79]. The replacement of water by the formulation excipients prevents oxygen radical formation during increased temperature or irradiation [55]. By choosing optimal excipients and additionally surfactants like Polysorbate 20 or Polysorbate 80, the protein is

thermodynamically stabilized and unfolding and aggregation is prevented [64, 65, 67, 69, 71, 78, 79].

In liquid formulations the excipients are excluded from the hydrated protein in a process called preferential exclusion. In this process, the water-protein interactions are stronger than the excipient-protein interactions. Thereby, the hydration shell is stabilized, which results in a lower free energy and thus increased stability of the protein [64, 65, 71, 78, 79].

In this thesis a stabilization formulation should be added to the anti-inflammatory coating to protect the coating during drying and storage. The formulations will be selected based on the knowledge that amino acids and sugars can stabilize proteins. In nature an intracellular high osmolality can protect the organism during water stress as with high environmental salt concentrations [65, 75].

1.5 Objectives

This work addresses the design of an anti-inflammatory coating to prevent material-mediated neutrophil activity on polymethylpenten (PMP) as a relevant model for a synthetic material used in medical devices.

In the first part (**Chapter 2**) of this work an optional pro-apoptotic anti-Fas molecule should be selected for the purpose to couple it on an artificial surface. Therefore, literature research and analytical assays should be screened.

The next part (**Chapter 3**) deals with the design of the anti-inflammatory coating. The goal of this part is the selection and design of the coupling chemistry and to investigate and characterize the designed coating.

The final anti-inflammatory coating should be investigated by analyzing different aspects of the coating. The coating has to be stable and no leaching is allowed. This should be investigated in a sandwich- Enzyme- linked Immunosorbent Assay (ELISA) called detachment assay. In addition, a reproducible coating process is necessary for an upscaling production. Therefore, the quantitative efficacy of the coating should be determined with an ELISA, which detects the bound anti-Fas molecule, called coating efficacy assay. Finally, the functionality of the coating should be guaranteed by a functionality assay called neutrophil activity assay. The neutrophil activity should be decreased by up to 20 % in solution and >10 % when anti-Fas molecules are immobilized, due to previous investigations with the anti-Fas IgM CH11 in LIM. LIM was incorporated in the circuit of a heart-lung machine and was successfully tested in a clinical study with 150 patients [80].

The characterization of the anti-inflammatory coating should be done by different relevant methods. Due to the shape of the PMP material several known methods cannot be applied. Therefore, the methods have to be selected in regard to the model material.

Chapter 4 deals with the upscaling of the anti-inflammatory coating to the whole medical device and a serial production scale. Therefore, the coating parameters need to be adapted stepwise to the larger scale. Furthermore, stability testings with an accelerated aging protocol need to be performed and analyzed.

SELECTION OF A SUITABLE ANTI-FAS MOLECULE, WHICH CAN BE USED FOR THE ANTI-INFLAMMATORY COATING

2 Introduction

This chapter describes the work which was conducted to define the most efficient anti-Fas molecule that leads to an inactivation of neutrophils. Thereby, a pure and homogenous neutrophil population is needed for proper results. Based on these findings the most suitable anti-Fas molecule will be further used to design an anti-inflammatory coating.

According to the defined requirements in chapter 1 the aim in this chapter is to decrease neutrophil activity for up to >20 % in solution and about >10 %, when anti-Fas molecules are immobilized.

Chapter II: Selection of a suitable anti-Fas molecule, which can be used for the anti-inflammatory coating

2.1 Materials and methods

Table 2-1. Equipment

Name	*Reference*
Analytical balance, AT460 Delta Range	Mettler-Toledo, Columbus, Ohio, USA
Centrifuge Megafuge 1.0R, max. 4000 rpm or 3345 x g	Heraeus, Hanau, Germany
CFX-Connect Real Time PCR-Cycler with C1000 Connect	BioRad, Hercules, California, USA
CO_2 Incubator	BINDER GmbH, Tuttlingen, Germany
CO_2 Incubator	Sanyo Denki K.K, Moriguchi, Japan
Flow cytometer BD Accuri C6	BD Biosciences, San Jose, California, USA
Micro-Centrifuge Galaxy 14 D, max. 13 000 rpm or 14 000 x g	VWR International GmbH, Ismaning, Germany
Micro-Centrifuge Sprout, 2000 x g	Kisker Biotech GmbH & Co. KG, Steinbach, Germany
Microscope Axiovert 40C	Carl Zeiss AG, Oberkochen, Germany
Mini-Shaker PSU-2T	Biosan, Riga, Latvia
Mini-vortexer, Vortex V-1 plus	Kisker Biotech GmbH & Co. KG, Steinbach, Germany
Neubauer counting chamber	Glaswarenfabrik Karl Hecht GmbH & Co K, Sondheim/Rhön, Germany
Sterile bench Biowizard KR 170	Kojair, Vilppula, Finland
Thermo-Shaker TS-1000	Kisker Biotech GmbH & Co. KG, Steinbach, Germany
Water bath	Memmert GmbH + Co.KG, Schwabach, Germany

Table 2-2. Biomolecules

Name	*Reference*
Anti-Adiponectin/Acpr30, 0.2 mg/ml in PBS	R&D Systems, Minneapolis, Minnesota, USA
Anti-Fas IgG1 E09, 2.252 mg/ml in PBS	kindly provided by MedImmune, Gaithersburg, Maryland, USA
Anti-Fas-AK (IgM), clone CH11, 0.5 mg/ml	MBL, Nagoya, Japan
Anti-FasL mouse IgG2B, 0.5 mg/ml in PBS	R&D Systems, Minneapolis, Minnesota, USA
APO010-API, 490 µg/ml in PBS	Oncology Venture, Hoersholm, Denmark

Name	Reference
Bovine Serum Albumin (BSA)	Sigma-Aldrich, St. Louis, Missouri, USA
Fc-APRIL (TNFSF13), 100 ng/ml in PBS	kindly provided from Pascal Schneider, University of Lausanne, Switzerland
Fc-FasL, 100 µg/ml in PBS	kindly provided from Pascal Schneider, University of Lausanne, Switzerland
MegaFasL, 100 µg/ml in PBS (Human FasL (aa 139-281) is fused at the N-terminus to mouse ACRP30 headless (aa 18-111) and a FLAG®-tag)	Adipogen International, San Diego, USA
Mouse anti-Human CD11b/Mac-1, PE-Cy™5 labeled	BD Biosciences, San Jose, USA
Mouse anti-human CD18, FITC labeled	BD Biosciences, San Jose, USA
Mouse anti-human CDI77, FITC labeled	Abcam, Cambridge, United Kingdom
rhIL-8 recombinant human	R&D Systems, Minneapolis, USA
SuperFasLigand, 100 µg/ml in PBS	Enzo Life Sciences, Inc., Farmingdale, NY, USA

Table 2-3. Materials

Name	Reference
Aqua B. Braun, purging solution, sterile and pyrogen-free	B. Braun Melsungen AG, Melsungen, Germany
Ethanol, 70 %	Carl Roth GmbH & Co.KG, Karlsruhe, Germany
Ethanol, absolute	Carl Roth GmbH & Co.KG, Karlsruhe, Germany
Human albumin, 20 %, >95% human albumin	Biotest AG, Dreieich, Germany
Phosphate buffered saline (PBS) w/o Mg^{2+}/ Ca^{2+}	Biochrom GmbH, Berlin, Germany
Polymorphprep™	Axis-Shield, Dundee, Great Britain
Propidium iodide solution (1.0 mg/ml in H_2O)	Sigma-Aldrich, St. Louis, Missouri, USA
RNase A (100 mg/ml, 7000 units/ml, solution)	Qiagen, Hilden, Germany
Sodium citrate tribasic dihydrate, ACS reagent, ≥99.0 %	Sigma-Aldrich, St. Louis, Missouri, USA
SYPRO Orange, 5000 x stock solution in DMSO	Sigma-Aldrich, St. Louis, Missouri, USA
Triton X-100 for molecular biology	Sigma-Aldrich, St. Louis, Missouri, USA
Trypanblue, 0.4 %	Sigma-Aldrich, St. Louis, Missouri, USA

Table 2-4. Media and solutions

Name	*Reference*
Dulbecco´s Modified Eagle Medium (DMEM) w 3.7 g/l NaHCO3, w 4.5 g/l D-Glucose, w Na-Pyruvate, w/o L-Glutamine	Biochrom GmbH, Berlin, Germany
Fetal bovine serum (FBS) Superior	Biochrom GmbH, Berlin, Germany
L-Alanyl-L-Glutamine, 200 mM	Biochrom GmbH, Berlin, Germany
Penicillin / Streptomycin, 10.000 U/ml / 10.000 µg/ml	Biochrom GmbH, Berlin, Germany
RPMI 1640 (Roswell Park Memorial Institute) Medium w 2 g/l $NaHCO_3$, w/o L-Glutamine	Biochrom GmbH, Berlin, Germany
RPMI 1640 Medium w 20 mM HEPES, w/o NaHCO3, w/o L-Glutamine	Biochrom GmbH, Berlin, Germany
Trypsin/Ethylenediaminetetraacetic acid (EDTA) (0.05/0.02%) in PBS w/o Ca^{2+}, Mg^{2+}	Biochrom GmbH, Berlin, Germany

Table 2-5. Kits

Name	*Reference*
Annexin V FITC Apoptosis Detection Kit I:	BD Biosciences, San Jose, California, USA
Annexin V, FITC labeled	
Propidium Iodide (PI)	
Binding Buffer	
Pappenheim-Staining Kit	MORPHISTO GmbH, Frankfurt a. Main, Germany
Giemsa stock solution	
May-Grünwald-Eosin	
Weise buffer pH 7.0, (10x)	

Table 2-6. Cell lines

Name	*Reference*	*Cell type characteristics*
Jurkat DD3	[81, 82]	Suspension cell line: DD3 was designed by a chemical mutagenesis and subsequent selection with the anti-Fas mAb CH11 (Peterson, 1998). DD3 has a deficient in Fas-mediated signaling secondary to a

Name	Reference	Cell type characteristics
Jurkat wild type (wt)	[83]	mutational loss in the cytoplasmic death domain of Fas and is resistant to Fas-mediated apoptosis, kindly provided by Prof. Martin Zörnig, Georg-Speyer-Haus Frankfurt
		Suspension cell line:
		Established from the peripheral blood of a 14-year-old boy with acute lymphoblastic leukemia at first relapse in 1976, **#** ACC 282 from DSMZ
Human blood		Different healthy donors

2.1.1   Cell cultivation

Suspension cell lines

The suspension cell lines Jurkat DD3 and Jurkat wt were cultivated at 37°C and 5 % CO_2-atmosphere. The cells were split at a confluent state. Cell concentration was determined by Trypanblue method: 35 µl of the cell suspension was added to 35 µl Trypanblue to stain dead cells. 10 µl of the mixture was transferred to the counting chamber and the cells were counted in the Neubauer counting chamber (Hecht Assistant) according to the manufacturer data via light microscopy (Axiovert 40C microscope, Zeiss). To maintain the cell line the cells were distributed to cell culture flasks according to Table 2-7.

Table 2-7. Split mode of cell lines

Name	Split mode/week	Cells/cm² flask
Jurkat DD3	3 times	133,000
Jurkat wt	3 times	133,000

Solutions used:

Cultivation medium: **Jurkat DD3:** RPMI 1640, 10 % FBS, 4 mM L-Alanyl-L-Glutamine, 100 U/ml Penicillin/Streptomycin
Jurkat wt: RPMI 1640, 10 % FBS, 4 mM L-Alanyl-L-Glutamine, 100 U/ml Penicillin/Streptomycin

2.1.2 Isolation of neutrophils

The neutrophil granulocyte isolation was established with Polymorphprep™ solution (Axis-Shield), which first was established by Boyum (1968). Boyum developed a one-step centrifugal technique for the isolation of mononuclear cells where polymorphonuclear cells are centrifuged to the bottom of the tube together with the erythrocytes [84]. Polymorphprep™ was further developed to separate erythrocytes from mononuclear cells (Figure 2-1): Polymorphprep™ is a mixture of Sodium Metrizoate and Ficoll. The high osmolality of Polymorphprep™ causes erythrocytes to lose water and shrink, thus increasing their effective buoyant densities. This enables rapid sedimentation of erythrocytes through the dense medium. It is crucial to keep the temperature of samples between 18 °C to 22 °C to obtain optimum results, as changes in temperature effect the density and viscosity of the Polymorphprep™.

The isolation of the neutrophils was carried out according to the manufacturer. Therefore, human blood was collected from healthy donors in lithium heparin S-monovettes (Sarstedt, 16 U/ml). The time from blood sampling to performance of the following tests was about the same in all experiments (2 h). In a 15 ml Falcon tubes 7 ml Polymorphprep™ were filled and layered with up to 7 ml of whole blood. To separate the blood components the falcon tubes were centrifuged for 45 min at 470 x g at 20 °C. The rotor brake have to be turned off in order to avoid mixing of the gradient.

By centrifugation the whole blood was separated by the difference in density of its components in two leukocyte bands, the mononuclear and polymorphonuclear white blood cells (Figure 2-1). To obtain the polymorphonuclear leukocytes (neutrophils), the band was removed with a disposable pasteur pipette. To remove the excess of Polymorphprep™ in the sample, the isolated neutrophils were washed with 20 ml PBS (10 min at 400 x g). The supernatant was discarded. The pellet was resuspended in 2 ml cell culture medium with 20 mM HEPES. The buffering of the cell culture medium with HEPES allows the use of an incubator without CO_2 supply.

To determine the neutrophil concentration 100 µl of the sample was diluted in a ratio of 1:5 in cell culture medium, whereby 5 µl of the diluted cell suspension is measured five times with the BD Accuri C6 flow cytometer (BD Biosciences). By setting a gate for the neutrophil population the number of cells can be calculated through the sample volume and the event number.
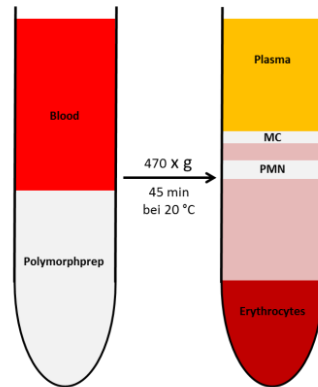
Figure 2-1. Schematic representation of isolation of neutrophils by Polymorphprep™.
Blood is layered on Polymorphprep[TM]. Centrifugation at 470 x g for 45 min at 20 °C leads to separation of blood components. The erythrocytes are located at the bottom, followed by a reddish layer of Polymorphprep[TM], which is contaminated with erythrocytes, then a whitish layer of polymorphonuclear neutrophils (PMN) and a whitish layer of monocytes (MC) are present. The top layer in yellow consists of plasma.

2.1.3 Staining of blood cells

The Pappenheim staining was developed in 1912 by Artur Pappenheim and is nowadays the standard method for staining of blood smear. This method is based on the staining of May-Grünwald and Giemsa [85, 86]. By combining the dye mixtures May-Grünwald [87] and Giemsa [88] it is possible to visualize nuclei and cytoplasm with depiction of their granules [85].

The appearance of hemocytes after performing a Pappenheim staining is different for nuclei, cytoplasm and granules. For example the cytoplasm of erythrocytes appears reddish, the granules of basophils appear blue-violet, the granules of eosinophils appear dark, the granules of neutrophils appear light violet, the nuclei of leukocytes appears blue-violet, platelets appear violet, the cytoplasm of the lymphocytes appears blue and the cytoplasm of the monocytes appear grey-blue [89].

To generate a blood smear 20 µl human blood was placed on a glass slide and was distributed by a second slide. The blood smear was incubated for drying for up to 20 min at RT.

For the staining, the dried blood smear was dipped in three different composite solutions of the Pappenheim-Staining Kit. The procedure was carried out according to the manufacturer.

First, the smear was incubated in a 50 ml Falcon tube with May-Grünwald solution for 2-3 minutes to fix the cells. The excess solution was removed by washing with water (B. Braun). Second, the slide was dipped for 2-3 min in a 50 ml Falcon tube, which contains a mixture of May-Grünwald solution and Weise-buffer (ratio 1:1). Then, the slide was washed with water (B. Braun). Subsequently, the blood smear was incubated for 12 min incubation in a 50 ml Falcon tube, which contains a mixture of Giemsa and Weise-buffer (ratio 1:10). Finally, the slide was washed and dried at RT. The staining was visualized via light microscope (Axiovert 40C microscope, Zeiss) and a camera.

2.1.4 Specific staining of neutrophils

Neutrophils and monocytes have similar properties with respect to their morphology, size and density. This makes a pure isolation of neutrophils of whole blood difficult [90]. The nature and composition of surface molecules of neutrophils and monocytes is similar as well, both cell types have, for example, the receptors CD11b and CD18 in common [91]. However, only neutrophils express the surface receptor CD177 [92].

In order to define a pure population of neutrophils, different surface markers were investigated and analyzed by flow cytometry.

Therefore, first 100 µl of isolated neutrophils (see 2.1.2) at a concentration between 1.0×10^5 to 1.0×10^6 cells/ml were washed with 400 µl PBS/2 % FBS and centrifuged at 400 x g for 5 min. The supernatant was discarded. Second, the samples were blocked with 500 µl PBS/5 % FBS solution for 15 min. Afterwards, the cells were washed as above. Third, the samples were stained with fluorescence labeled surface markers (FITC Mouse Anti-Human CD18, PE-Cy™ 5 Mouse anti-human CD11b / Mac-1 and FITC anti-CD177). Therefore, 20 µl of the antibodies were added for 45 min in the dark at 4 °C. Finally, the cells were washed again and the cell pellet was resuspended in 500 µl PBS/10% FBS and analyzed by flow cytometry. In addition, an isotype control was analyzed to define a proper gate.

By flow cytometry, 10 000 events were analyzed in an BD Accuri C6 flow cytometer (BD Biosciences) using the FL-1 (for FITC detection) and the FL-3 (for PE) detector filters.

2.1.5 Apoptosis assay

During the establishment of an optimal apoptosis assay different assays were tested: first the Nicoletti assay was tested [93, 94], second a method was tested designated Annexin V apoptosis assay.

2.1.5.1 The Nicoletti assay

The Nicoletti assay is based on the detection of DNA laddering as it occurs at the late stage of apoptosis. DNA laddering can be detected by the fluorescent dye propidium iodide (PI), which intercalates into DNA. Flow cytometry allows the quantification of cells undergoing late stage apoptosis. The Nicoletti assay was carried out based on the assay described by Riccardi and Nicoletti [94].

The Fas sensitive cell line Jurkat was used for the apoptosis assay. Jurkat cells are robust suspension cells that are sensitive to Fas signalling and are widely used to quantify FasL-mediated apoptosis. As negative control a Fas deficient cell line Jurkat DD3 was used [81, 82]. As well freshly isolated neutrophils were tested.

500 µl of Jurkat cells or neutrophils, in a concentration of 2×10^6 cells/ml in cell culture medium (RPMI 1640 20 mM HEPES, 10 % FBS, 4 mM L-Alanyl-L-Glutamin, 1 % Penicillin/Streptomycin) were transferred into a 96-well microtiter plate (MTP). In case that wells were previously coated with the anti-FasL molecules cell culture medium was added. In the other case soluble anti-FasL molecules were dissolved in cell culture medium. The samples were incubated for 16-24 h in an incubator at 37 °C. The samples were tested in duplicates.

When anti-FasL molecules were coated to 96-well MTP, 100 µl (1 µg/ml in PBS) were coated for 4 h at RT. After incubation, the wells were washed three times with 300 µl PBS. Then, unspecific binding sites were blocked with 5 % HSA (Biotest) in PBS for 1 h at RT. After incubation, the wells were washed three times with 300 µl PBS. Then, the wells were incubated with 250 µl cells (c_{End}= 1×10^6 cells/ml) for 16-24 h at 37 °C.

When soluble anti-Fas molecules were used, 250 µl cells (c_{End}= 1×10^6 cells/ml) were incubated with 250 µl anti-Fas molecules at different concentrations for 16-24 h at 37 °C.

After the incubation, the cells were transferred to 5 ml FACS-tubes. The cells were centrifuged for 5 min at 209 x g at RT and the supernatant was discarded. Cells were washed in 500 µl ice-cold PBS and centrifuged (209 x g, 5 min, RT). Cells were fixed dropwise with 500 µl ice -cold ethanol (70 %) and incubated for 15 min on ice. Then the ethanol was removed completely by centrifugation (409 x g, 5 min, RT). Cells were washed twice in 500 µl ice-cold PBS and centrifuged (209 x g, 5 min, RT). The pellet was resuspended in 200 µl ice-cold Nicoletti-Staining solution (50 µg/ml propidium iodide, 0.1 % Triton X-100, 5 µg/ml RNase A in 38 mM sodium citrate) and incubated for 2 h on ice for staining the cells. Then, 300 µl PBS was added and the samples were vortexed for 5 s. The samples were analyzed via BD Accuri C6 flow cytometer (BD Biosciences), whereby PI was determined with a 585 nm filter. 10 000 events with a medium flow rate for the Jurkat cells and 5000 events for neutrophils were analyzed in a defined gate in the forward site scatter. All samples were normalized to the untreated negative control.
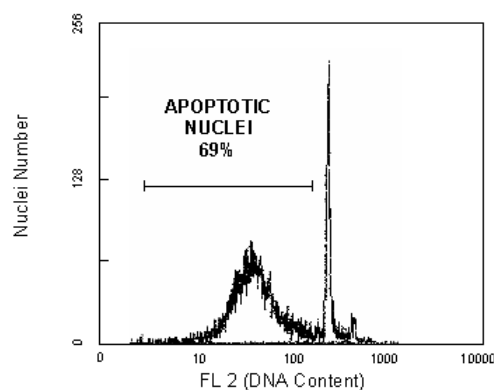
Figure 2-2. Example of flow cytometric analysis of apoptotic cells stained with PI.
The G_1 population or the diploid nuclear fragments (2n) show a stronger PI signal than the sub-G_1 peak, which includes the apoptotic hypodiploid nuclear fragments (< 2n, see gate). The percentage of hypodiploid nuclear fragments is evaluated by gating.

2.1.5.2 The Annexin V assay

The Annexin V assay is based on the phenomenon that cells undergoing apoptosis in the early phase exhibit modifications in their cell membrane. This modification can be detected by fluorescently labeled Annexin V. The addition of PI allows the differentiation between early and late stage apoptosis. In the late stage apoptosis, the cell membrane becomes porous and the cell can be identified by Annexin V and PI in the flow cytometer.

In apoptotic cells the phospholipid phosphatidylserine (PS) is translocated from the inner to the outer leaflet of the plasma membrane. Annexin V is a 35-36 kDa calcium-dependent phospholipid-binding protein and has a high affinity to PS. Therefore, it binds to cells with PS on the outside of the plasma membrane. When Annexin V is conjugated to fluorochromes such as Fluorescein isothiocyanate (FITC), it can be detected via flow cytometry [95].
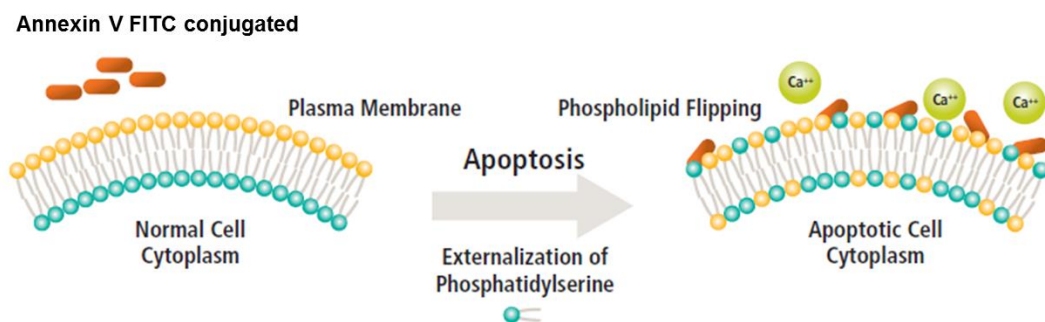
Figure 2-3. Schematic illustration of the externalization of phosphatidylserine.
By induction of apoptosis, the phospholipid phosphatidylserine (PS) is flipped from the inner to the outer leaflet of the plasma membrane. Annexin V, a calcium-dependent phospholipid-binding protein, has a high affinity to PS and can bind to PS on the outside of the plasma membrane. When Annexin V is conjugated to fluorochromes such as FITC it can be detected via flow cytometry (modified by [95]).

After the overnight incubation, the samples were transferred from the MTP to 1.5 ml Eppendorf tubes and centrifuged (300 x g, 5 min, RT). The supernatant was discarded and cells were washed with 0.5 ml ice-cold PBS, centrifuged again (300 x g, 5 min, RT) and the supernatant was discarded. This washing step was performed again to completely remove the cell culture medium. During the washing process the cells were kept on ice.

To analyze the samples by flow cytometry, the cells were stained via the Annexin V FITC Apoptosis Detection Kit (BD Biosciences) according to the manufacturer instructions. For this purpose, the pellet was resuspended in 100 µl of binding buffer (1x) and 5 µl of Annexin V and 5 µl of PI. Then, the samples were incubated for 15 min on ice in the dark. In order to compensate the two different fluorochromes four untreated controls were stained as followed: one was not stained, one was stained with Annexin V, one was stained with PI and one was stained with Annexin V and PI. By these controls a compensation factor for the fluorescence channels 1 and 2 of the fluorescent dyes FITC and PI was determined. 10 000 events with a medium flow rate for the Jurkat cells and 5000 events for neutrophils were

analyzed in a defined gate in the forward site scatter with the BD Accuri C6 flow cytometer (BD Biosciences). All samples were normalized to the untreated negative control.

2.1.6 Chemotaxis assay

The chemotaxis assay is based on the migration activity of neutrophils and represents an early event in neutrophil activation. Chemotactic activity is important for the transepithelial or transendothelial migration from the blood into solid tissue. When the chemotactic activity is reduced by any intrinsic or extrinsic factor, the pro-inflammatory response is largely limited. Therefore, it is an important assay in this work.

Indeed, agonistic anti-Fas CH11 impaired spontaneous or interleukin-8 (IL-8) mediated chemotaxis of neutrophils as reported previously [5, 53]. The experimental set-up is shown schematically in Figure 2-4. Transwell chambers are used that allow the spatial segregation of cell culture medium with IL-8 in the lower compartment and the neutrophils in medium without IL-8 in the upper compartment. The bottom of the transwell inserts is porous with a pore size of 3 µm diameter. Neutrophils are attracted by the IL-8 gradient and start to migrate within minutes through the pores of the transwells towards the higher IL-8 concentration. After one hour, the neutrophils in the lower compartment can be quantified and the number of cells is a measure for the activity of a given neutrophil population by flow cytometry.
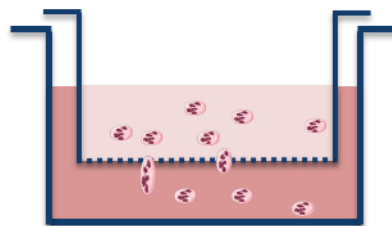
Figure 2-4. Schematic representation of the chemotaxis chamber.
The chamber is divided into two compartments: the upper compartment contains the neutrophil suspension, the lower compartment contains cell culture medium (negative control) or cell culture medium with the chemoattractant IL-8. Between the two compartments there is a porous membrane with a pore size of 3 µm. The neutrophils can actively migrate through the pores and after 1 h incubation the neutrophil suspension in the lower compartment is analyzed by flow cytometry.

In this setting, the anti-Fas molecules were incubated with the neutrophils before the chemotaxis assay was performed. For this purpose, 600 µl of the isolated neutrophils (1 - 1.5 × 10^6 cells/ml) were mixed with 600 µl of anti-Fas molecules in several concentrations (4 ng/ml - 40 ng/ml). In the controls, cell culture medium is used instead of cell suspension. The samples were incubated from 0.5 h to o/n at 37 °C depending on the experimental setup. The 1:1 mixture halves the end concentration of the cell suspension and the anti-Fas molecule solution.

When using coupled anti-Fas molecules, the anti-FasL molecules were coupled as described in 2.2.6. 500 µl of cell suspension (1 × 1.5 × 10^6 cells/ml) were added to each coated well. To bring the cells into the spatial proximity of the coupled molecules, the MTPs were centrifuged for 5 min at 300 x g and incubated from 0.5 h to o/n at 37 °C.

After incubation, the cell suspensions were transferred to FACS tubes and the cell count is determined. 100 µl of the samples were diluted 1:5 with cell culture medium and 5 µl of the sample were analyzed by flow cytometer to calculate the cell concentration.

To test the vitality of the samples, PI was mixed to the cell suspension. 200 µl of the cell suspension used for the cell number determination was mixed 1:1 with PI solution (50 µg/ml) (0.1 - 0.15 × 10^6 cells/ml). The cell number determination and the vitality test before the addition of the cell suspension to the chemotaxis chamber is necessary to ensure that sufficient cells are present for the following cell number determination (> 0.5 × 10^6 cells/ml) and are also vital (> 60 % cell viability).

Then, 1 ml of pure cell culture medium or medium with IL-8 additive (25 ng/ml) were added into the lower compartment of the chemotaxis chamber, 500 µl of cell suspension with different pre-incubation with anti-Fas molecules were added to the upper compartment. Then the samples were incubated for 1 h at 37 °C.

Finally, the contents of the lower compartments were transferred to a FACS tube and 25 µl of the samples were measured with the BD Accuri C6 flow cytometer (BD Biosciences). The number of events in the previously determined gate was counted. A vitality test was carried out after the chemotaxis incubation as well. All samples were normalized to the untreated negative control for each group (with and without IL-8), respectively.

2.1.7   Differential scanning fluorimetry (DSF)

Differential scanning fluorimetry (DSF) is an assay to monitor melting profiles of proteins via the fluorescent dye SYPRO Orange. In an aqueous environment of a correctly folded protein, the signal of SYPRO Orange is attenuated, by thermal unfolding of the protein, the dye can interact with the hydrophobic sides of the unfolded protein, which results in an enhancement of the fluorescent signal of the dye. Further unfolding results in protein aggregation, thus the dye dissociates from the protein and the fluorescence signal decreased [96].

The resulting melting curve delivers the melting temperature (T_m) of the protein, which can be calculated using a sigmoidal Boltzmann equation.

The anti-Fas molecules were diluted in a 1:100 dilution of SYPRO Orange (5000 x stock solution) in PBS to different concentrations (18.75 µg/ml to 90 µg/ml) depending on the availability of each protein.

For each sample 20 µl solution was added to a 96 well q-PCR plate (BioRad) and centrifuged briefly for 1 min at 500 rpm at 4 °C (Megafuge 1R, Heraeus). The samples were analyzed according to the parameters in Table 2-8 in the real-time Polymerase Chain Reaction (q-PCR)-Cycler (BioRad).

Table 2-8. Settings of DSF measurement

Settings	
Repeats	141
Start temperature	25 °C
Interval duration	10 s
Temperature increase	0.5 °C
Final temperature	95 °C
Measuring time in total	55 min

2.2 Results

The selection of a suitable anti-Fas molecule is the crucial issue of this chapter. Not only the functionality of the molecule is important for the design of an anti-inflammatory coating, but as well the stability and the availability in GMP quality of the molecule is very important. To reach these goals, different assays were established. The purity of isolated neutrophils was investigated to ensure reproducible results. Neutrophils were used in a chemotaxis assay to investigate the influence of the anti-Fas molecules to the neutrophils. To demonstrate the efficiency of the molecules an apoptosis assay was developed with the Jurkat cell line and neutrophils. The thermal stability of each molecule was determined as well.

2.2.1   Purity of isolated neutrophils

Neutrophils are sensitive cells and always have to be isolated freshly from human blood. Therefore, it is important to guarantee a consistent quality. Before neutrophil isolation, fresh blood sampling from healthy donors was performed. Thereby, EDTA, citrate and heparin are mostly used to inhibit blood clotting after blood sampling for clinical analysis *in vitro*. But it is known that blood cells behave different by using different anticoagulants during collection.

Thus, before the selection of the anticoagulant a literature research was performed and the findings may be summarized as follows: as EDTA is a chelating agent for Ca^{2+} and other bivalent cations and citrate as well interferes with Ca^{2+} levels, these anticoagulants affect the respiratory burst of neutrophils, which is associated with intracellular Ca^{2+} concentrations. Freitas et al. (2008) investigated the influence of EDTA, citrate and heparin with the result that by use of EDTA the highest yield of isolated neutrophils could be observed, whereby the isolation by citrate and heparin was lower.

On the other hand the respiratory burst induced by phorbol myristate acetate (PMA) was drastically reduced by EDTA, whereby citrate and heparin were twice as high. The intracellular Ca^{2+} concentration was highest in the heparin pre-treated sample [97]. Each anticoagulant has advantages and disadvantages, e.g. heparin leads to more aggregation and the layer during density centrifugation is more difficult to separate [97]. But in this work heparin was chosen as the best option. In the following chapters the heparin concentration during blood sampling was decreased as far as possible from 16 U/ml to 5 U/ml to decrease unwanted side-effects.

In the first step, the neutrophils were isolated via Polymorphprep™ and stained via Pappenheim staining. Figure 2-5 shows the characteristic morphology of hemocytes, whereby erythrocytes appear reddish without nuclei, the cytoplasm of the monocyte appears grey-blue, the granules of neutrophils appear light violet and the polymorph nucleus appears blue-violet. In Figure 2-5 A blood smear of whole blood is shown, with many erythrocytes, one monocyte and two neutrophils. After isolation of neutrophils a pure population of isolated neutrophils with their characteristic polymorph nuclei was shown in Figure 2-5 B.

A

B
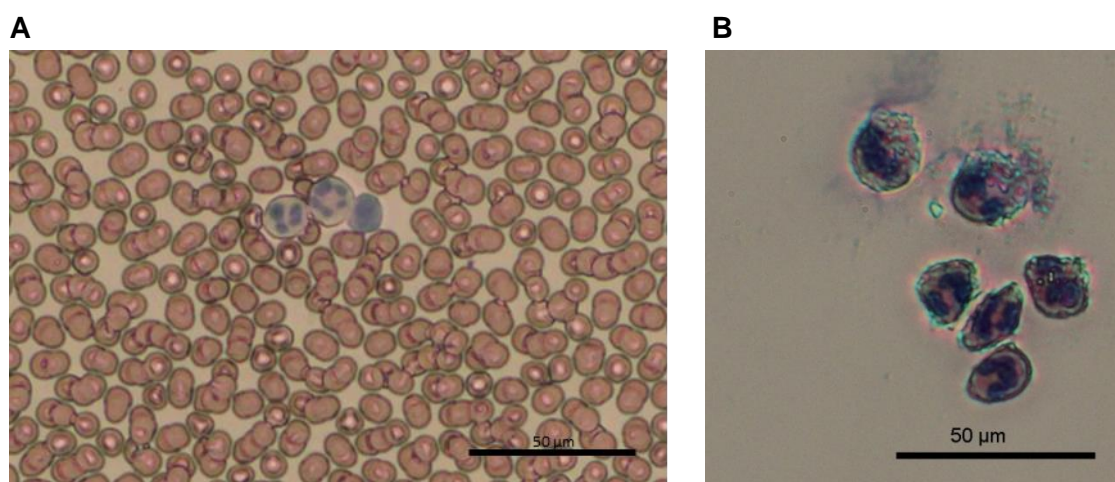
Figure 2-5. Images of blood smear stained via Pappenheim staining.
A Image of blood smear of whole blood stained with Pappenheim staining kit. **B** Image of blood smear of isolated neutrophils stained with Pappenheim staining kit to confirm the high purity of the population used in the functional experiments.

Neutrophils and monocytes have a similar cell shape, why the separation via Polymorphprep™ is not entirely pure. To obtain a pure neutrophil population analysis via flow cytometry were carried out. The neutrophil population was identified via fluorescence-labeled antibodies analyzed by flow cytometry. Three different surface markers were identified, which are common on neutrophils: the cluster of differentiation (CD) 11b, CD18 and CD177.

CD11b, an adhesion glycoprotein, interacts with CD18 (integrin β2), which results in the CD11b/CD18 complex. CD11b is expressed on activated lymphocytes, monocytes, granulocytes and a subset of natural killer cells, whereby CD18 is expressed on lymphocytes, monocytes and more weakly on granulocytes. The complex is important to form cell-cell contacts e.g. during inflammation and is known to be highly expressed during neutrophil activation [98]. Another surface protein which is specific for neutrophils is the

CD177, a glycosyl-phosphatidylinositol-anchored receptor, which is expressed on circulating neutrophils in healthy humans [92, 99, 100].

Neutrophil cell surface staining with markers detecting CD11b, CD18, and CD177 was done to confirm the neutrophil population by flow cytometry (Figure 2-6). In the dot plots (Figure 2-6 B) the samples show two point clouds, which show the neutrophil population and a mixed population of erythrocytes and monocytes, respectively.

Figure 2-6 A shows that CD177 is a suitable marker to specifically detect neutrophils (green dots), whereas CD11b (red dots) and CD18 (orange dots) are expressed on granulocytes and also on some monocytes, respectively. The black dots in the dot plots indicate residual erythrocytes. The neutrophil point clouds were gated in the dot plots, which results in a pure neutrophil population for further analysis.
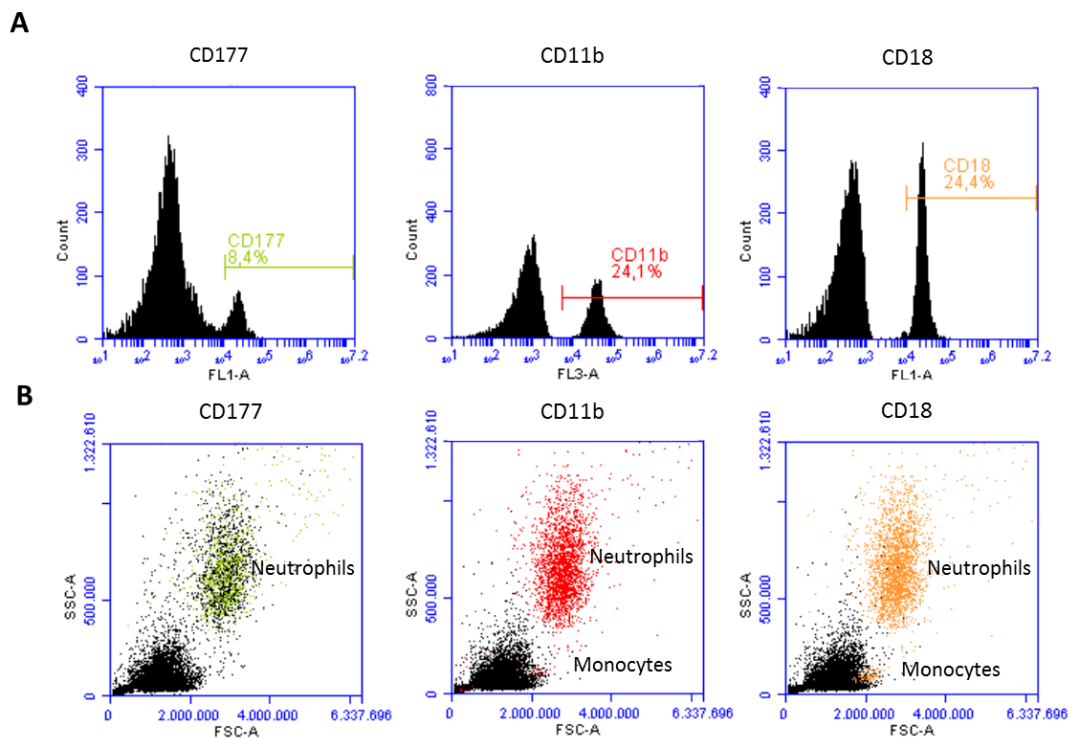
Figure 2-6. Flow cytometry analysis histograms and dot plots.
Neutrophils were isolated via Polymorphprep™ and afterwards labeled with specific surface markers CD177 in green, CD11b in red and CD18 in orange. In **A** the histograms and in **B** the dot plots are shown. All dot plots show a specific labeled neutrophil population with some residual monocytes (labeled as well with the surface markers) and a big population of residual erythrocytes in black. The histograms show the percentage labeled cells for the whole sample.

2.2.2   Results of Nicoletti assay in solution with Jurkat cells

As the Nicoletti assay is based on the detection of DNA laddering as it occurs at the late stage of apoptosis, DNA laddering can be detected by the fluorescent dye propidium iodide (PI), which intercalates into DNA. As DNA laddering is the last step in apoptotic cells, flow cytometry allows only the quantification of cells undergoing the late stage of apoptosis.

To establish the Nicoletti assay only two model anti-Fas molecules were tested in Jurkat wild type (wt) and Fas deficient DD3 cell lines. The result is shown in Figure 2-7. The Jurkat DD3 cells show low kill-rates < 5 %, whereas the wild type cells shows concentration dependent kill-rates, whereby 10 ng/ml SuperFasL indicates medium kill-rates of 36.6 ± 20.1 % and 10 ng/ml CH11 only 13.3 ± 2.2 %. The concentrations were determined due to earlier experiments and due to manufacturer information.
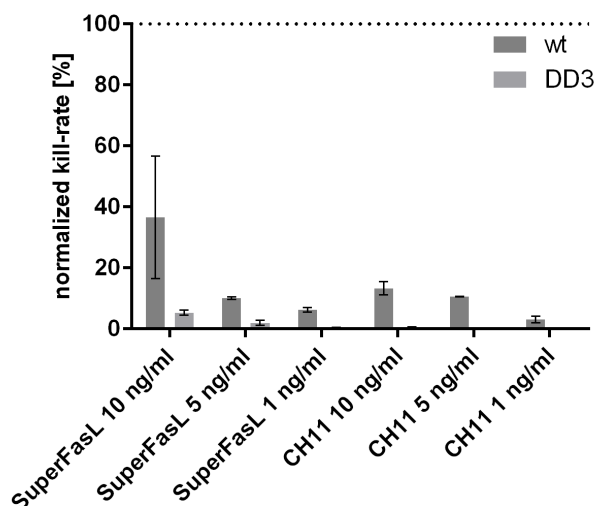
Figure 2-7. Results of Nicoletti assay with Jurkat cells.
Apoptosis was induced by incubation of Jurkat cells o/n with different concentrations of SuperFasL and CH11 in Jurkat wt and Jurkat DD3. The kill-rate was normalized to untreated sample (Mean ± SD from n=2).
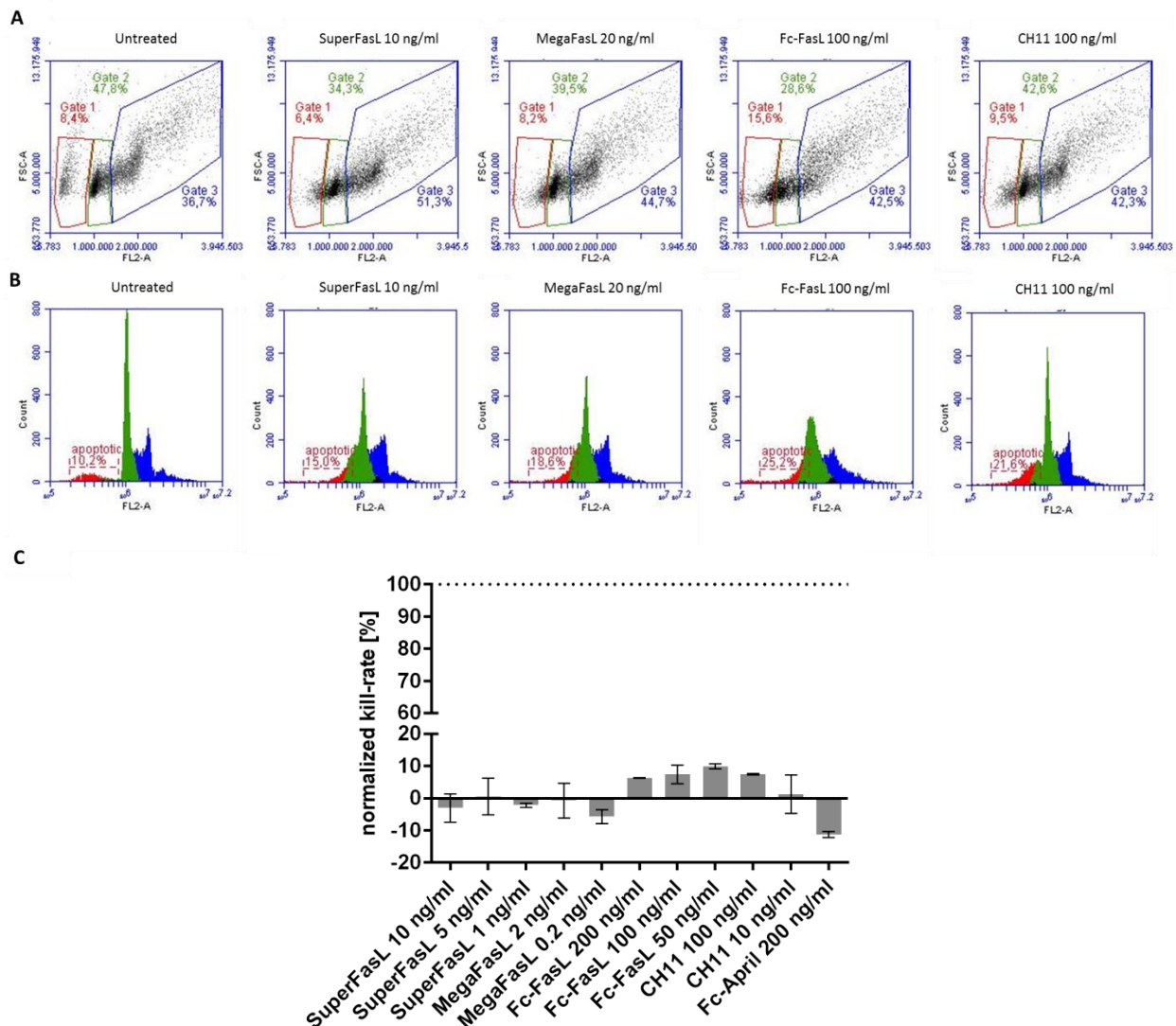
Figure 2-8. Flow cytometric dot plot and histogram of Nicoletti assay.
A Dot plots (FSC-A/FL1-A) of different treated Jurkat cells stained with PI. The three gates indicate three populations in different cell cycle stages. **B** Histograms of different treated Jurkat cells stained with PI. The gate indicates the apoptotic nuclei. **C** Apoptosis was induced by incubation of Jurkat cells o/n with different concentrations of SuperFasL, MegaFasL, Fc-FasL, CH11 and Fc-April (negative control, TNFSF13). The kill-rate was normalized to untreated sample (Mean ± SD from n=2).

In Figure 2-8 the results of all pre-selected anti-Fas molecules, except the E09, are shown, whereby in the dot plots the different gates define the different stages of cell cycle with different DNA content. Gate 1 defines the apoptotic cells with a DNA content < 2n, whereby gate 2 defines the normal cells with a DNA content of 2n. The gate 3 shows normal cells with higher DNA content due to the different cell cycle phases. In the histograms the cell count is plotted to fluorescent intensity and shows the different DNA content of the cells. It is divided

from left to right in the sub-G_1 apoptotic peak (hypo diploid DNA < 2n), the G_0/G_1 phase peak with normal diploid DNA content, the S phase peak (> 2n) and the G_2/M phase peak (4n) followed by peaks with cells with higher DNA content than 4n [93, 94]. The effect of the pro-apoptotic anti-Fas molecules as shown in the previous experiment is not shown here. All anti-Fas molecules induce low apoptosis rates in a concentration independent manner to Jurkat cells as shown in Figure 2-8 C.

Due to these inconsistent results of the Nicoletti apoptosis assay, the next experiments were carried out with the Annexin V apoptosis assay as described in the next section.

2.2.3   Results of Annexin V assay in solution with Jurkat cells

Figure 2-9 shows the results of the Annexin V assay carried out with all pre-selected anti-Fas molecules in Jurkat wt. By plotting the fluorescence channels of FITC (FL1) and PI (FL2) against to each other, the different cell stages are located in the different quadrants: quadrant 1 low left (Q1-LL) shows the living cells, Q1 upper left (Q1-UL) shows the cells undergoing necrosis, Q1 upper right (Q1-UR) shows late apoptotic cells and Q1 lower right (Q1-LR) shows early apoptotic cells. The incubation of anti-Fas molecules induces apoptosis in Jurkat cells and leads to a shift from Q1-LL to Q1-LR and Q1-UR (Figure 2-9 B). After an overnight incubation of untreated Jurkat cells 14.4 % cells died. Thus, this number changes slightly, all results in his work were normalized to the negative control for comparison of different experiments.

To investigate the efficiency of the pre-selected effector molecules the Annexin V assay was chosen to determine the optimum concentration of each molecule to induce apoptosis in Jurkat cells. As depicted in Figure 2-9 C, the molecules SuperFasL, Fc-FasL, MegaFasL and CH11 induced apoptosis in a concentration dependent way. Therefore, the well reported feature of the SuperFasL, Fc-FasL and MegaFasL to induce apoptosis via Fas signalling was demonstrated. Interestingly, MegaFasL was highly efficient at 2 ng/ml whereas the other molecules required more than 5-fold concentrations. The Fc-FasL molecule showed the highest apoptosis induction, but at these high concentrations the Fas deficient cell line Jurkat DD3 shows high apoptosis rates as well (data not shown). This unspecific apoptosis induction is generally not appreciated, but Fc-FasL is known to kill highly efficient at high concentrations.
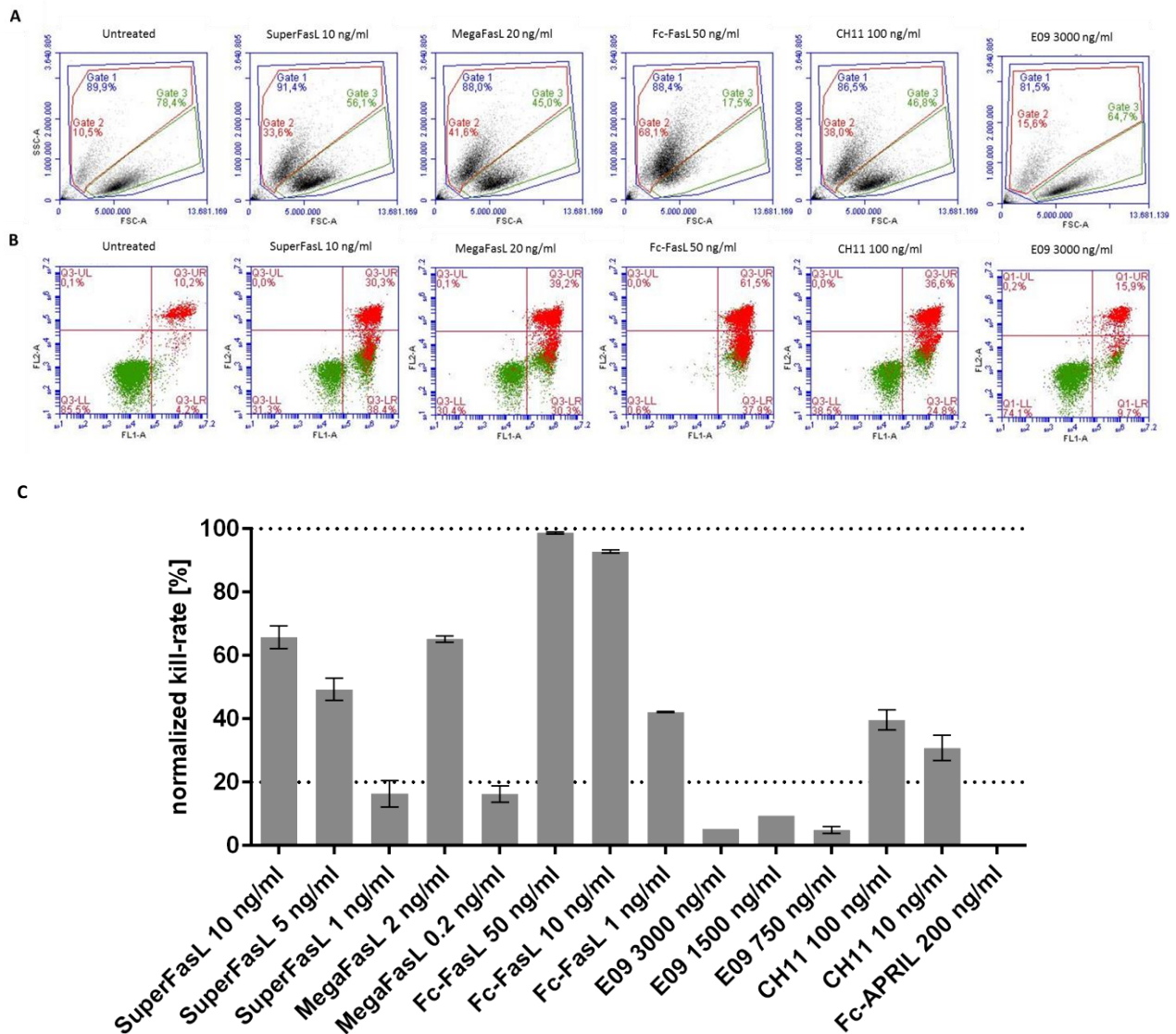
Figure 2-9. Flow cytometric dot plots and histograms of Annexin V assay.
A Dot plots (SSC-A/FSC-A) of different treated Jurkat cells stained with Annexin V / PI. The three gates indicate three populations in different cell cycle stages. **B** Histograms of different treated Jurkat cells stained with Annexin V / PI and gated with Gate 1. **C** Apoptosis was induced by incubation of Jurkat cells o/n with different concentrations of SuperFasL, MegaFasL, Fc-FasL, IgG E09, IgM CH11 and Fc-April (negative control, TNFSF13). The kill-rate was normalized to untreated sample (Mean ± SD from n=2).

The goal was to reach more than 20 % of apoptotic cells after o/n incubation with the soluble effector molecules. This could be reached with all effector molecules (Figure 2-9 A), except the IgG1 E09 for unknown reasons (Figure 2-9 B).

Although the IgG E09 has been reported to efficiently induce apoptosis [60], we were not able to confirm this finding even by using high concentrations. Thus, the IgG E09 failed to induce strong apoptosis and therefore was not further evaluated.

2.2.4 Results of Annexin V assay with soluble and immobilized effector molecules with neutrophils

In another set of experiments, the two variants of the MegaFasL (MegaFasL and APO010) were compared in their efficacy to induce apoptosis in human neutrophil suspensions. The molecular structure of MegaFasL and APO010 is similar, but the MegaFasL has a human FasL (aa 139-281) which is fused at the N-terminus to mouse ACRP30 headless (aa 18-111) and a FLAG®-tag and it is available for *in vitro* use only. To use it in clinical studies the APO010 was designed with a human sequence instead of the mouse sequence and the FLAG®-tag was removed. Figure 2-10 A depicts the results of the Annexin V apoptosis assay after neutrophil incubation with soluble MegaFasL and APO010. Interestingly, the efficacy of 2 ng/ml of APO010 was comparable with 20 ng/ml of MegaFasL.

A   **B**
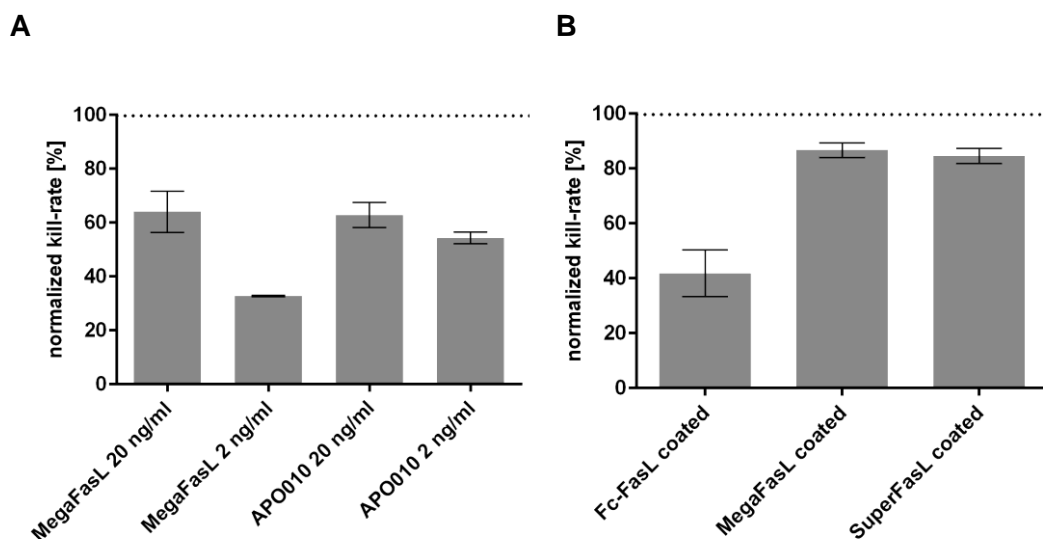
Figure 2-10. Results of Annexin V Apoptosis assay with neutrophils.
A Apoptosis was induced by incubation of neutrophils with different concentrations of MegaFasL and APO010 in solution. The kill-rate normalized with untreated sample is shown (n=3). **B** Apoptosis was induced by incubation of neutrophils with (1 μg/ml in PBS) Fc-FasL, MegaFasL and SuperFasL coated to a MaxiSorp plate for 4 h at RT. The kill-rate was normalized to untreated sample (Mean ± SD from n=3).

In the experiments with immobilized anti-FasL molecules, the effector molecules were coated on MaxiSorp plates in saturation and the coupling efficiency was detected by ELISA. As shown in Figure 2-10 B, all coupled test molecules were able to induce apoptosis in neutrophils. The kill-rates were around 80 % to 90 % for SuperFasL and MegaFasL and about 40 % for Fc-FasL (Figure 2-10 B). However, it shall be noted here, that the immobilization of the anti-Fas molecules is not covalent. This means, some of the attached anti-Fas molecules can be detached from the MaxiSorp plate during the incubation with the cells. Therefore, this approach allows only to determine a trend. As a conclusion, MegaFasL and SuperFasL were superior in eliciting functional apoptosis and seem to be more suitable for the coating than Fc-FasL.

In summary, the apoptosis assay was established successfully and the goal to induce apoptosis in more than 20 % of target cells was reached for the recombinant proteins Fc-FasL, MegaFasL/APO010 and SuperFasL and for the IgM CH11. The IgG E09 failed to efficiently induce apoptosis and therefore was not further considered in this work. The CH11 served as control to compare the efficacy of the molecules in the apoptosis assays and was not evaluated further.

2.2.5   Results of chemotaxis assay with anti-Fas molecules in solution

For the chemotaxis assay, neutrophils were incubated with anti-Fas agonistic molecules for different times.

Figure 2-11 A compares the different inactivation efficacies in chemotaxis between Fc-FasL, SuperFasL and MegaFasL after normalization to the negative control. A control group without IL-8 was included to differentiate between spontaneous and stimulated chemotaxis. To compare the different neutrophil activities with each other, both groups were normalized to the untreated negative control, respectively.

The group without IL-8 showed lower neutrophil activities than with IL-8, but the tendency that incubation with the anti-Fas molecules reduces neutrophil activity was demonstrated in both groups. Thus, the MegaFasL and Fc-FasL (20 ng/ml) efficiently inactivated the neutrophil chemotaxis (> 90 %), whereby SuperFasL even at high concentration (20 ng/ml) inactivated the neutrophil chemotactic activity by approximately 50 % in the group with IL-8. The largest inactivation effects were obtained with MegaFasL with almost 100 % inactivation with the highest (20 ng/ml) and medium (10 ng/ml) concentration. With the lowest

concentration of MegaFasL (2 ng/ml) the chemotactic activity was reduced approximately 2.5 fold.

In addition, the two MegaFasL variants were compared in their efficacy with each other to reduce chemotactic activity in neutrophils (Figure 2-11 B). Here again, it becomes apparent that even the 2 ng/ml APO010 could inhibit chemotactic activity by approximately 90 %. In these experiments 20 ng/ml MegaFasL was used as a benchmark (99 % reduction of neutrophil chemotaxis).
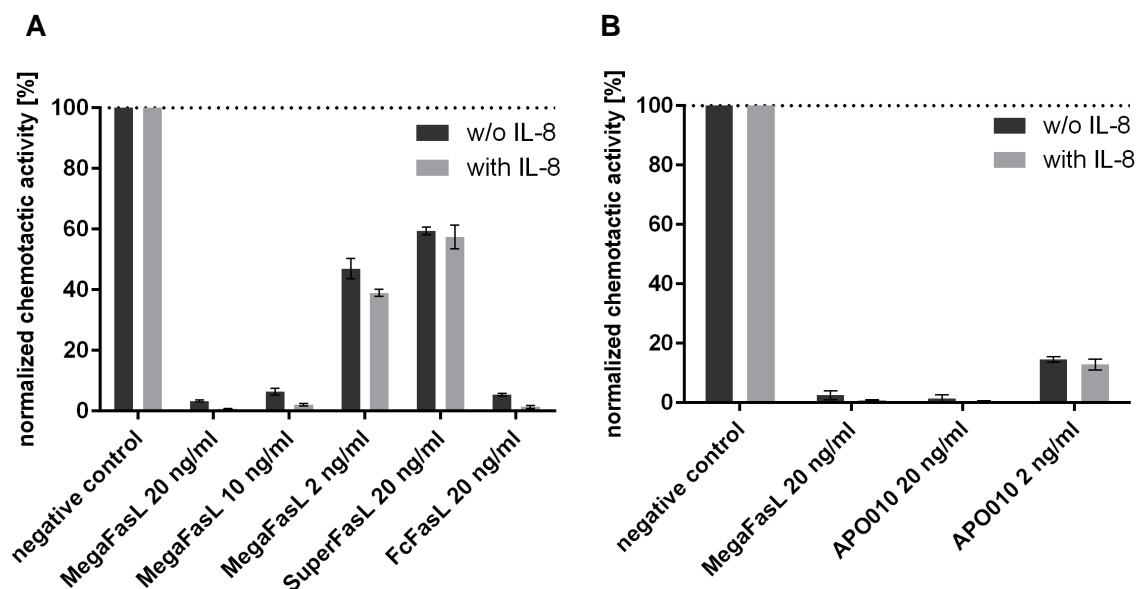
Figure 2-11. Results of chemotaxis assay.
A Neutrophils were incubated o/n with Fc-FasL (20 ng/ml) SuperFasL (20 ng/ml) and MegaFasL (20 ng/ml, 10 ng/ml and 2 ng/ml) in solution. Afterwards, neutrophils were transferred to chemotaxis inserts and incubated
B Neutrophils were incubated o/n with MegaFasL (20 ng/ml) and APO010 (20 ng/ml, 2 ng/ml). Afterwards, neutrophils were transferred to chemotaxis inserts and incubated for 1 h. Analysis was carried out by flow cytometry. The kill-rate was normalized to untreated sample (Mean ± SD from n=2).

2.2.6 Results of neutrophil inactivation by immobilized anti-Fas molecules

Similar to the experiments described for soluble incubation of neutrophils with the anti-Fas molecules, experiments were done with neutrophils and immobilized agonistic molecules on MaxiSorp cell culture plates. The concentrations of the effector molecules were defined to be 10-fold higher compared with the concentrations used in liquids, because only approximately 10 % of the soluble effector molecules may be stably coupled to the MaxiSorp plate. This

means, 200 ng/ml coating solution refers to 20 ng/ml coupled effector molecules to MaxiSorp plate. After incubation for different time intervals, neutrophils were transferred to the transwell chambers. For each time point, a separate negative control was included, including neutrophils incubated in the same plate, but without immobilized agonistic molecules. To compare the different neutrophil activities with each other, the samples were normalized to the untreated negative control, respectively.

In Figure 2-12, the chemotactic activity of neutrophils, which were incubated for up to 9 h, with MegaFasL is depicted. It shows that after 1 h incubation the chemotactic activity decreases by 40 %, whereas MegaFasL reduces neutrophil activity after 6 h by 64 % and after 9 h by 79 %. Therefore, the immobilized MegaFasL can efficiently reduce neutrophil activity. However, there is a huge variation from 20 % to 80 % in reduction of chemotactic activity due to the very sensitive neutrophils used in this model and two different donors. Samples from 1 h to 2 h were from the same donor, whereas the samples 6 h to 9 h were from another donor (see Figure 2-12).
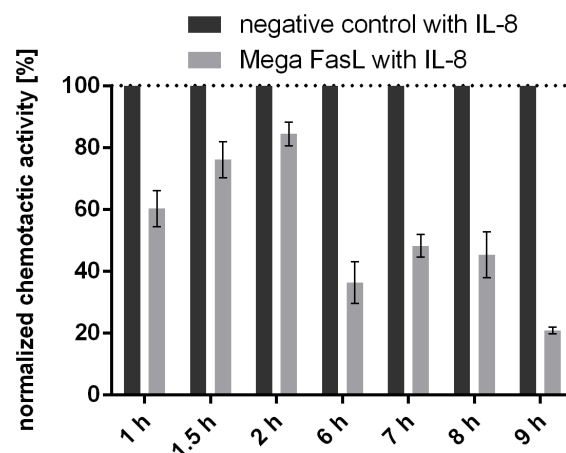
Figure 2-12. Results of chemotaxis assay with coated MegaFasL.
Neutrophils were incubated for different times with coated (200 ng/ml coating solution refers to 20 ng/ml coupled effector molecules to MaxiSorp plate) MegaFasL. Neutrophils were transferred to chemotaxis inserts and incubated for 1 h. Analysis was carried out by flow cytometry. Samples from 1 h to 2 h were from the same donor, whereas the samples 6 h to 9 h were from another donor. The kill-rate was normalized to untreated sample (Mean ± SD from n=2).

2.2.7 Evaluation of molecular stability

The thermal stability of each test molecule was systematically analyzed by differential scanning fluorometry (DSF). This is an important criterion for the determination of stability during storage at elevated temperatures and terminal gas sterilization with EtO at elevated temperatures. In general, antibodies, like IgG, have two melting points: one for the temperature sensitive Fab-region (T_{m1}) and one for the more pH sensitive Fc-region (T_{m2}) [101]. Monomeric proteins regularly have one melting point.
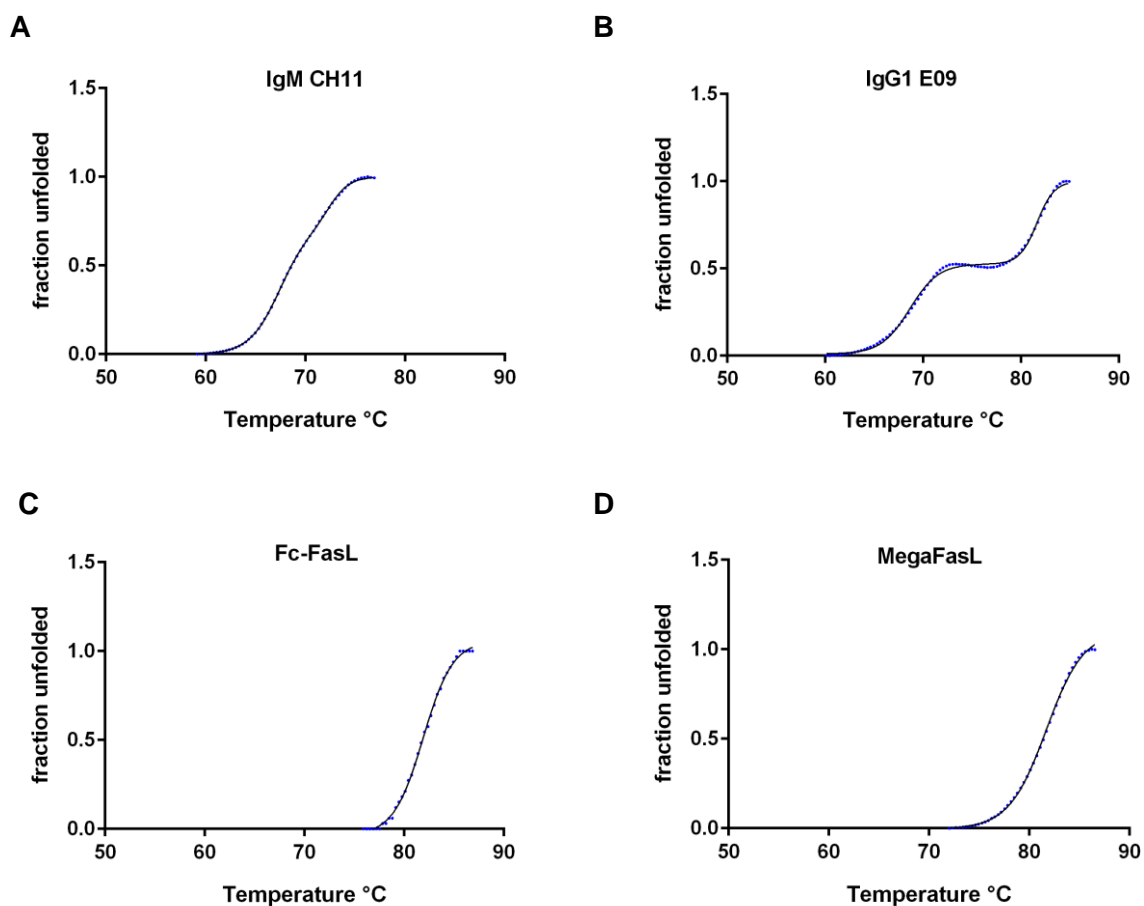
Figure 2-13. Stability tests by differential scanning fluorimetry (DSF).
Normalized melting point curves of anti-Fas molecules at different concentrations are shown. **A** IgM CH11 (0.09 mg/ml in PBS), **B** IgG$_1$ E09 (0.09 mg/ml in PBS), **C** Fc-FasL (0.075 mg/ml in PBS), **D** MegaFasL (0.0375 mg/ml). Different concentrations were used due to material availability (n=3).

In Figure 2-13 the melting curves are shown. The CH11 IgM and the E09 IgG1 antibodies exhibit two mean points of thermal degradation, whereby E09 IgG_1 is more stable than CH11. The Fc-FasL curve is similar to IgG antibodies because of its fused Fc-domain. The second melting point of Fc-FasL is missing due to the missing Fab domain. The T_{m1} of Fc-FasL is similar to the T_{m1} of E09. The melting point of MegaFasL was the highest with 81.74 °C and thus, MegaFasL is extremely stable at elevated temperatures. SuperFasL could not be analyzed due to low quantities tested. In Table 2-9 the melting points are summarized.

Table 2-9. Overview of mean melting points of FasL molecules

FasL molecule	Concentration [µg/ml]		Melting point [°C]
IgM CH11	90	T_{m1}	67.39
	90	T_{m2}	72.42
IgG_1 E09	90	T_{m1}	68.56
	90	T_{m2}	81.65
Fc-FasL	75	T_{m1}	68.62
	75	T_{m2}	82.10
MegaFasL	37.5	T_m	81.56
SuperFasL	18.75	T_m	-

An advantage for the monomeric protein MegaFasL is the high thermal resistance. In contrast, the tested molecules with Fab- and Fc-domains (CH11, E09, Fc-FasL) showed thermal instability due to the more instable Fab-region in case of the CH11 and the E09. The Fc-FasL is more instable due to the fusion of the two protein sequences.

In conclusion, regarding thermal stability, the MegaFasL proved to be the most suitable molecule for the use in anti-inflammatory coating in medical devices undergoing terminal sterilization at elevated temperatures as it is the case in EtO sterilization procedures.

2.2.8 Summary

The goals of the first part of this project can be summarized as follows: the read out models for apoptosis and neutrophil activity have been established. Soluble and immobilized effector molecules were systematically evaluated on their potential to induce apoptosis and to reduce neutrophil activity. Except the E09 antibody, each anti-Fas molecule induced apoptosis in > 20 % of target cells and impaired neutrophil activity in > 10 % of target cells. Therefore, the goals defined in Chapter 1 were reached. The APO010 is the most suitable molecule due to the availability and already existing Good Manufacturing Practice (GMP) quality. In addition, clinical safety data for systemic application are available [102, 103].

2.3 Discussion

The selection of the most efficient anti-Fas molecule was the prerequisite for the further design of the anti-inflammatory coating. Thereby, an assay had to be chosen and adapted to evaluate these molecules.

As neutrophils and monocytes express a low level of Fas on their cell surface [56] the specific inactivation of neutrophils due to anti-Fas molecules is characterized by the fact that neutrophils roll along the endothelial cells. This is mediated by expressed selectins until integrins lead to a tight adhesion [26]. Monocytes do not have this behavior and therefore are not the main targets for material-mediated immune responses.

Therefore, in the first step, a neutrophil isolation method was chosen and the purity of the cells was analyzed. It was possible to define a pure neutrophil population by flow cytometry after defined gating via different neutrophil specific surface markers. These findings were confirmed by the characteristic cell staining by Pappenheim, which leads to a polymorphonuclear staining of the neutrophils.

Before neutrophil isolation, fresh blood sampling from healthy donors was performed. To inhibit blood coagulation heparin was selected as the most suitable anticoagulant with the lowest influence in neutrophil behavior. The separation during neutrophil isolation is more difficult with heparin or citrate than with EDTA [97], but the presence of erythrocytes and monocytes is acceptable due to the flow cytometry method, which can gate the specific neutrophil population. An additional hemolysis step is undesirable, because it may lead to an activation of neutrophils.

The efficiency of the anti-Fas molecules to induce apoptosis in the model cells lines Jurkat wt and Jurkat DD3 was successful for the so called Annexin V assay. The Nicoletti assay shows more variations in the results when using incubations times shorter than 24 h. The DNA laddering in the Nicoletti assay needs probably the full 24 h, therefore the defined incubation range of 16 h to 24 h was set too wide. Usually an incubation time of 18 h was applied. The incubation time for the Nicoletti assay was not optimized, because of the successful results of the Annexin V assay. In addition, the Annexin V assay provides more information due to the application of two markers for early and late apoptosis and it delivers more reproducible results. Therefore, only the Annexin V assay was further used in this work.

All pre-selected anti-FasL molecules resulted in apoptosis rates higher than the untreated sample. However, the IgG E09 showed very similar results compared to the untreated sample independent of the concentration used. The molecules SuperFasL, Fc-FasL, and MegaFasL induced apoptosis in a concentration dependent way. They demonstrated efficiently apoptosis rates in low concentration for up to 93 % for Fc-FasL (10 ng/ml), followed by SuperFasL (66 %, 10 ng/ml), MegaFasL (65 %, 2 ng/ml) and CH11 (31 %, 10 ng/ml). Thus, the MegaFasL was the most efficient anti-FasL molecule at low concentrations of 2 ng/ml, whereas the other molecules required more then 5-fold concentrations. Also Fc-FasL was very effective in Jurkat wt and was able to induce even in the Fas sensitive Jurkat DD3 an apoptosis signal. Fc-FasL needs to be applied in higher concentrations than MegaFasL, which results in higher costs. On the other hand, Fc-FasL is easier to produce than the hexamer MegaFasL [59].

The IgG E09 was reported from Chodorge and his colleagues (2012) as to be comparably effective as the natural FasL. Here, it demonstrated low apoptosis rates of less than 10 %. They predict E09 as an antibody with partially fast dissociation from Fas and therefore the possibility to recruit with the free Fab arm new Fas monomers to create an active signaling complex [60]. It is likely that E09 has to be cross-linked in this approach in order to elicit its activity to trimerize the Fas receptor. Only trimerization of the Fas receptor leads to an intracellular apoptosis signal and therefore is necessary in this approach. Since cross-linking as an additional coating step is not appreciated, E09 did not reach sufficient priority to be further evaluated.

The MegaFasL was one of the most efficient molecules and has already been further developed for anti-tumor treatment in humans [102, 103]. This adapted molecule is called APO010 and is available in GMP quality. It was already investigated in non-clinical and clinical research. Therefore, APO010 would be the optimal molecule for the design of an anti-inflammatory coating for medical devices. The direct comparison between MegaFasL and APO010 showed that apoptosis in neutrophils was induced by both molecules, whereby APO10 needed lower concentrations for the same result (2 ng/ml APO010 compared to 20 ng/ml MegaFasL). Therefore, APO010 can be used instead of MegaFasL.

When using immobilized anti-Fas molecules the kill-rates in neutrophils were around 80 - 90 % for SuperFasL and MegaFasL and about 40 % for Fc-FasL (Figure 2-10). This shows that MegaFasL is one of the best molecules similar to SuperFasL. However, it is not

clear how meaningful these results are due to the non-covalent coupling of the molecules to the MaxiSorp plates. Some of the molecules may be detached from the surface and subsequently are more effective in solution than immobilized. Further approaches to define the coupling stability were investigated in chapter 3 via ELISA to quantify detached molecules.

As a conclusion, MegaFasL and SuperFasL were superior in eliciting functional apoptosis and seem to be more suitable for the coating than Fc-FasL.

In further experiments to investigate the ability of the anti-Fas molecules to inhibit neutrophil activity, chemotaxis assays were carried out. All anti-Fas molecules, the MegaFasL, Fc-FasL, SuperFasL and APO010, were able to efficiently inactivate the neutrophil chemotaxis (> 90 %) in solution, whereby the largest inactivation effects were obtained with MegaFasL and APO010. Interestingly, the spontaneous migration of neutrophils in the control group without IL-8 was reduced by incubation of the anti-Fas molecules similarly as in the group with IL-8. This means, that the anti-Fas molecules induce apoptosis in the neutrophils, which leads to an immediate inactivation of neutrophils migration. This inactivation of neutrophil migration indicates the ability for the anti-inflammatory effect of the novel coating on the medical device. By an immediate inactivation of the highly activated neutrophils, the preapoptotic neutrophils are detached and phagocytized by monocytes or macrophages and eliminated in the spleen [51]. Thus, the anti-Fas molecules inhibit tissue damage and inflammation in the patient.

When MegaFasL was immobilized to a MaxiSorp plate it was able to decrease chemotactic activity of neutrophils after 1 h by 40 %, but the chemotactic activity was further decreased after 9 h by 79 %. Therefore, the immobilized MegaFasL can efficiently reduce neutrophil activity after a short time span. This makes it interesting for short time applications as needed in CPBs and for long time applications in oxygenators. The huge oscillation from 1 h up to 9 h incubation is due to two different neutrophil donors (1 to 2 h one donor, 6 to 9 h other donor) and due to the sensitive neutrophils, which have to be handled with care through the whole experiment.

Thermal stability of the anti-Fas molecule is an important property for a suitable molecule, which can be used in an anti-inflammatory coating. During the production of a medical device the molecule has to go through many harsh conditions, ending in a sterilization process, which mostly means EtO sterilization. Here temperatures of about 50 °C are occurring.

All molecules show high thermal stability and therefore can be used for the further development of an anti-inflammatory coating. MegaFasL has the highest T_m value and thus is the most stable protein here.

Table 2-10. Scoring of selection criteria

Value (V): 1-5, Fulfillment (F): 1-10

| | SuperFasL | | MegaFasL | | | | Fc-FasL | | E09 IgG$_1$ | | CH11 IgM | |
| | | | APO010 | | *Mega*FasL | | | | | | | |
	F	F x V	F	F x V	F	F x V	F	F x V	F	F x V	F	F x V
Apoptosis induction: V2	10	20	10	20	10	20	10	20	5	10	10	20
Neutrophil inactivation: V5	3	15	8	40	8	40	5	25	0	0	10	50
Specificity: V3	8	24	8	24	8	24	8	24	0	0	8	24
Stability: V5	8	40	10	50	10	50	8	40	5	25	3	15
Availability: V5	8	40	10	50	8	40	8	40	8	40	5	25
Clinical safety data available: V5	0	0	10	50	0	0	0	0	0	0	10	50
GMP quality: V5	0	0	10	50	0	0	0	0	0	0	0	0
Total		**139**		**299**		**174**		**149**		**75**		**184**

All technical, functional, economical, and regulatory aspects relevant for the anti-inflammatory coating using for a medical device are summarized in Table 2-10, scoring each criterion with different values (1-5), according to their importance and their fulfilments (1-10), according to the obtained results with a maximum possible value of 300.

The apoptosis induction has a value of 2 and neutrophil inactivation has the highest value of 5, because the inactivation is more important for the anti-inflammatory coating than the apoptosis itself. The specificity of the anti-Fas molecule has a value of 3, because all cells with Fas receptors should be inactivated by the anti-inflammatory coating. The stability, which was investigated in this part as thermal stability has a value of 5, but should be investigated further with different methods. The availability, clinical safety data availability and GMP quality have a value of 5, because these aspects enable a faster and more convenient development process.

All effector molecules (CH11, SuperFasL, Fc-FasL, and MegaFasL) except the E09 were shown to induce sufficient apoptosis rates in Jurkat wt cells and in neutrophils. The trimerization of the Fas receptor on the cells is the crucial step for inducing apoptosis and inactivation and therefore is highly efficient. In general, CH11 was only used as a control because it was not the intention to select an IgM antibody for the coating. However, CH11 has been extensively studied during the past years and thus was an ideal benchmark in the establishment of different experiments. The values in the scoring table are partly based on previous unpublished studies. The anti-Fas molecules SuperFasL, Fc-FasL, and MegaFasL (Table 1-1, Figure 1-5) are based on the work of Pascal Schneider and his colleagues and therefore have comparable structures [59]. All three molecules proved to induce apoptosis in neutrophils and also reduced neutrophil activity, when cells were challenged in solution and with immobilized molecules. MegaFasL is the only effector molecule, which has been evaluated in clinical studies and is available in GMP quality [103].

Essentially, the GMP quality variant of MegaFasL, the APO010, reached the highest score with 299 of 300 maximum possible points, largely resulting from the criteria "GMP quality available" and "Clinical safety data available". The use of APO010 in the anti-inflammatory coating is therefore the best option and will be further used in this work.

CHAPTER III

DESIGN OF AN ANTI-INFLAMMATORY COATING

3 Introduction

In addition to the right selection of an anti-inflammatory molecule, its covalent coupling chemistry is one of the most important parts in the design of an anti-inflammatory coating.

The direct linkage of proteins enables the most efficient strategy, however this method is difficult to achieve. Recombinantly produced proteins can be designed according to the coupling requirements. It enables a direct linkage via click chemistry or via maleimide linker. For example Simon et al. (2012) developed a "clickable" protein, which can be clicked to polyethylene glycol (PEG) using copper free click chemistry at the N-terminus. The C-terminal cysteine can be tagged with a fluorescent dye (Alexa-488) via maleimide linker or can be added to an activated surface via the maleimide linker [104]. The maximum functionality is expected when the protein is coupled to the surface in a way that the antigen specific paratope remains free to bind to the epitope. When using an unspecific coupling strategy, for example via the 1-ethyl-3-(3-dimethylaminopropyl)carbodiimide hydrochloride (EDC) chemistry, all free amino groups of the protein to couple can undergo a covalent binding.

However, before choosing a coupling chemistry, it is crucial to think about the properties of the surface material. For example it is important to know, if the material has to be porous or non-porous and if the surface material is durable in the used solvents, like acids, bases, high salt or organic solvents. Most surface materials need to be activated first to generate a covalent binding with the biomolecule. When using inorganic materials like ceramics or

glasses, silanization is one of the best options. It is one of the most used techniques to couple biomolecules to inorganic materials [105].

When using polyurethane (PU), poly(hydroxyethylmethacrylate) (pHEMA) is a good choice as coupling reagent. It is easy to polymerize and possesses hydroxyl groups that can be used for the immobilization of the biomolecules [106]. In addition, it serves as blocking layer, which is used in several medical devices such as contact lenses and is known to be biocompatible. PU is often used for medical devices due to its good physical and chemical properties. It shows higher reactivity with primary amine groups than with secondary amine, hydroxyl, acid, anhydride or epoxide groups [107, 108]. Therefore, as well polyethyleneimine (PEI), with its high number of primary amine groups, is a polymer, which can react with PU.

Another method to couple protein to a surface is the thiol chemistry, which enables site-specific reaction using recombinant proteins with a single C-terminal cysteine. To modulate the distance and therefore optimize the functional action of the biomolecule, cross-linkers with different spacer arms can be used.

When using an inert material like the Polymethylpentene (PMP) or Poly(4-methyl-1-pentene), which is used in this work as the relevant material for the functionalization of membrane ventilators, it is difficult to generate a covalent coupling due to missing functional groups. Therefore, plasma activation can be used to modify the surface by generating functional groups. The modification of the material via the plasma is based on physical and chemical processes carried out by neutrons, electrons, positively charged ions, radicals and UV radiation [109].

By using different types of gas the modification of the material can be selected. Generally, O_2, N_2, H_2O or noble gases are used. O_2 generates mostly aldehyde groups, which oxidize to carboxyl groups. H_2O generates hydroxyl, aldehyde and carboxyl groups. When noble gases are used, the plasma generates no oxidation processes, but cross-linking of polymer structures [109].

This chapter focusses on the finding of the right coupling strategy for the anti-inflammatory coating and the investigation of its functionality.

3.1 Materials and methods

Table 3-1. Equipment

Name	Reference
Analytical balance, AT460 Delta Range	Mettler-Toledo, Columbus, Ohio, USA
Bruker Tensor 27 FTIR and thermostat DC30-K20	Bruker Optics, Ettlingen, Germany Thermo Haake GmbH, Karlsruhe, Germany
Centrifuge Biofuge fresco, max.13 000 rpm or 16 060 x g	Heraeus, Hanau, Germany
Centrifuge Megafuge 1.0R, max. 4000 rpm or 3345 x g	Heraeus, Hanau, Germany
CO_2 incubator	Sanyo Denki K.K, Moriguchi, Japan
Filter holder device (diameter 25 mm, PSU)	Whatmann, Maidstone, United Kingdom
Filter holder device (diameter 50 mm, PC)	Sartorius, Göttingen, Germany
Flexible-tube pump MCP	IDEX Health&Science (ISMATEC), Wertheim, Germany
Flow cytometer BD Accuri C6	BD Biosciences, San Jose, California, USAGermany
Fusion photometer	PerkinElmer, Inc., Waltham, Massachusetts, USA
Incubator	BINDER GmbH, Tuttlingen, Germany
Jeol JSM-6500 F	Jeol, Tokyao, Japan
Kruess Drop Shape Analyzer DSA25E	Kruess GmbH, Hamburg, Germany
Leica DMi8	Leica Microsystems, Wetzlar, Germany
Micro-Centrifuge Galaxy 14 D, max. 13 000 rpm or 14 000 x g	VWR International GmbH, Ismaning, Germany
Micro-Centrifuge Sprout, 2000 x g	Kisker Biotech GmbH & Co. KG, Steinbach, Germany
Microscope Axiovert 40C	Carl Zeiss AG, Oberkochen, Germany
Mini-Shaker PSU-2T	Biosan, Riga, Latvia
Mini-vortexer, Vortex V-1 plus	Kisker Biotech GmbH & Co. KG, Steinbach, Germany
Nanophotometer 7122 V2.3.1	Implen GmbH, Munich, Germany
Neubauer counting chamber	Glaswarenfabrik Karl Hecht GmbH & Co K, Sondheim/Rhön, Germany
Novex-Mini-Cell	Invitrogen AG, Carslbad, California, USA
Sterile bench	Kojair, Vilppula, Finland
Thermo-Shaker	Kisker Biotech GmbH & Co. KG, Steinbach, Germany
Water bath	Memmert GmbH + Co.KG, Schwabach, Germany

Table 3-2. Biomolecules and amino acids

Name	*Reference*
Alanine,L- (EP, USP)	AppliChem GmbH, Darmstadt, Germany
Anti-Adiponectin/Acpr30, 0.2 mg/ml in PBS (binds polyclonal to aa 19-244)	R&D Systems, Minneapolis, Minnesota, USA
APO010-API, 490 µg/ml in PBS	Oncology Venture, Hoersholm, Denmark
Arginine, L- (USP)	Carl Roth GmbH & Co.KG, Karlsruhe, Germany
Bovine Serum Albumin (BSA)	Sigma-Aldrich, St. Louis, Missouri, USA
EZ-Link®Sulfo-NHS-LC Biotinylation	Thermo Fisher Scientific, Waltham, Massachusetts, USA
Fas-Fc, lyophilized (extracellular part of Fas receptor fused to a Fc-domain)	kindly provided by Prof. Martin Zörnig, Georg-Speyer-Haus, Frankfurt, Germany
Glutamic acid, L- (EP)	Carl Roth GmbH & Co.KG, Karlsruhe, Germany
Glycine (EP, USP, JP)	Carl Roth GmbH & Co.KG, Karlsruhe, Germany
Histidine, L- (EP)	Carl Roth GmbH & Co.KG, Karlsruhe, Germany
Lysine, L-, HCl (EP, USP, JP)	Carl Roth GmbH & Co.KG, Karlsruhe, Germany
Recombumin Alpha 10 % (albumin)	Novozymes A/S, Bagsværd, Denmark
rhIL-8 recombinant human	R&D Systems, Minneapolis, Minnesota, USA
Streptavidin conjugated to horseradish peroxidase (Streptavidin-HRP)	R&D Systems, Minneapolis, Minnesota, USA
Streptavidin-Northernlights-NL 557	R&D Systems, Minneapolis, Minnesota, USA
Tryptophan, L- (EP)	Carl Roth GmbH & Co.KG, Karlsruhe, Germany

Table 3-3. Materials

Name	*Reference*
Aqua B. Braun, purging solution, sterile and pyrogen-free	B. Braun Melsungen AG, Melsungen, Germany
EDC (1-ethyl-3-(3-dimethylaminopropyl)carbodiimide hydrochloride)	Thermo Fisher Scientific, Waltham, Massachusetts, USA
Ethanol, 70 %	Carl Roth GmbH & Co.KG, Karlsruhe, Germany
OXYPLUS®, Polymethylpentene (PMP) hollow fibers for gas excahnge	Membrana, Wuppertal, Germany
PBS w/o Mg^{2+}/ Ca^{2+}	Biochrom GmbH, Berlin, Germany

Name	Reference
Polysorbate 20	Carl Roth GmbH & Co.KG, Karlsruhe, Germany
Skim milk powder	Sigma-Aldrich, St. Louis, Missouri, USA
Sulfuric acid (H_2SO_4), 96 %	Sigma-Aldrich, St. Louis, Missouri, USA
TMB (3,3',5,5'-Tetramethylbenzidine)	Invitrogen, Carlsbad, California, USA
Trypanblue, 0.4 %	Sigma-Aldrich, St. Louis, Missouri, USA

Table 3-4. Media and solution

Name	Reference
DMEM w/o phenol red, w/ 3.7 g/l $NaHCO_3$, w/ 4.5 g/l glucose, w/o L-Glutamine	Biochrom GmbH, Berlin, Germany
DMEM w/ 3.7 g/l $NaHCO_3$, w/ 4.5 g/l D-Glucose, w/ Na-Pyruvate, w/o L-Glutamine	Biochrom GmbH, Berlin, Germany
Penicillin/Streptomycin, 10.000 U/ml/ 10.000 µg/ml	Biochrom GmbH, Berlin, Germany
Trypsin/EDTA (0.05/0.02 %) in PBS w/o Ca^{2+}, Mg^{2+}	Biochrom GmbH, Berlin, Germany

Table 3-5. Kits

Name	Reference
Pierce® Biotin Quantitation Kit	Thermo Fisher Scientific, Waltham, Massachusetts, USA
Biotinylation kit Affinity Purified Avidin BupH™ Phosphate Buffered Saline Pack EZ-Link Sulfo-NHS-Biotin HABA Zeba™ Spin Desalting Column, 5mL	Thermo Fisher Scientific, Waltham, Massachusetts, USA
XTT (tetrazolium salt) Kit	F. Hoffmann-La Roche AG, Basel, Switzerland

Table 3-6. Cell lines

Name	Reference	Cell type characteristics
L-929	[110, 111]	Murine connective tissue fibroblast cell line, which was established from the normal subcutaneous areolar and adipose tissue of a male C3H/An mouse; used as target in TNF detection assays
Human blood		Different healthy donors

3.1.1 Cell cultivation

Adherent cell line

The adherent cell line was cultivated at 37 °C and 5 % CO_2-atmosphere. The cells were split at a confluent state. The old medium was removed and the cells stuck to the flask were washed once with 5 ml PBS. Then 2.5 ml trypsin/EDTA was added and incubated for 5 min in the incubator at 37 °C to detach the cells from the bottom of the flask. Afterwards, the trypsin reaction was stopped by adding 7.5 ml medium. Cell concentration was determined by Trypanblue method: 35 µl of the cell suspension was added to 35 µl Trypanblue to stain dead cells. 10 µl of the mixture was transferred to the counting chamber and the cells were counted in the Neubauer counting chamber (Hecht Assistant) according to the manufacturer data via light microscopy (Axiovert 40C microscope, Zeiss). To maintain the cell line the cells were distributed to cell culture flasks according to Table 3-7.

Table 3-7. Split mode of cell line

Name	Split mode / week	Cells/cm^2 flask
L-929	3 times	40,000

Solutions used:

Cultivation medium: **L-929:** DMEM, 10 % FBS, 2 mM L-Alanyl-L-Glutamine, 100 U/ml Penicillin/Streptomycin

3.1.2 Isolation of neutrophils

Neutrophils were isolated as described in 2.1.2. Human blood was collected from healthy donors in neutral S-monovettes (Sarstedt) spiked with 5 U/ml Na-Heparin instead of previously used lithium heparin S-monovettes (Sarstedt, 16 U/ml lithium heparin).

3.1.3   Apoptosis assay

The apoptosis assay was carried out as described in 2.1.5.

3.1.4   Chemotaxis assay

The chemotaxis assay was carried out as described in 2.1.6.

3.1.5   Anti-inflammatory coating

The anti-inflammatory coating consists of the polymethylpentene (PMP) hollow fibers as artificial material, EDC as cross-linker reagent, APO010 as anti-inflammatory molecule and recombinant albumin to passivate the surface. To stabilize the biomolecule during drying, sterilization and storage an amino acid (aa)-based stabilizing formulation (Table 3-8) was added as shown in Figure 3-1.

Table 3-8. AA-based stabilization formulation

AA-based stabilization formulation	Content
F1 (aa-based formulation with 7 aa)	Ala, Arg, Glu, Gly, His, Lys-HCl, Trp pH 6.5 in H_2O
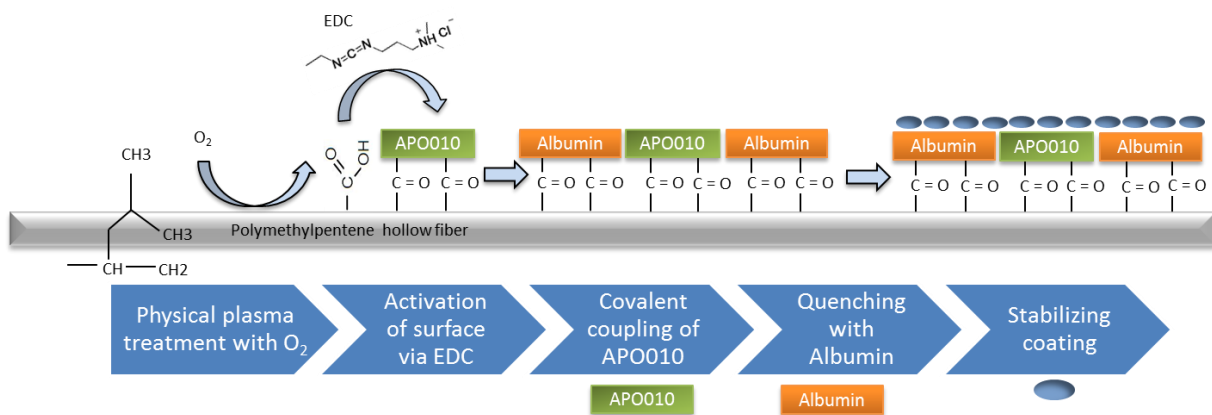
Figure 3-1. Scheme of the coupling chemistry for an anti-inflammatory coating.
For the anti-inflammatory coating, first, the polymethylpentene (PMP) hollow fiber was plasma activated with O_2. Second, the plasma activated PMP, which has now carboxyl groups, reacts with EDC. The activated PMP can react in a third step with APO010, which results in a stable amid bond. Afterwards, the reaction is quenched with a recombinant albumin, which results in covalent coupling of APO010 and albumin to the PMP. Albumin interacts as blocking reagent with free PMP groups and avoids unwanted binding of blood components. In the last step an amino acid-based stabilizing formulation is added to the coating and will protect the coating during drying, sterilization, and storage.

3.1.5.1 The polymethylpentene hollow fibers

The PMP hollow fibers (OXYPLUS®, Membrana) are woven to PMP mats (14 cm × 10 cm) by a polyester weaving thread, whereby 120 to 220 mats are rolled on a coil. These coils are then plasma activated as depicted in

Table 3-9 with O_2 to generate functional carboxyl groups on the inert PMP material. The carboxyl groups can be used for crosslinking and can be formed by oxidation of aldehyde, keto and hydroxyl groups. The OXYPLUS® PMP hollow fibers have a dense outer skin, which prevents liquid entry into the fiber and a diffusion membrane for gas exchange of oxygen and carbon dioxide. Therefore, this material is used in oxygenators for gas exchange.
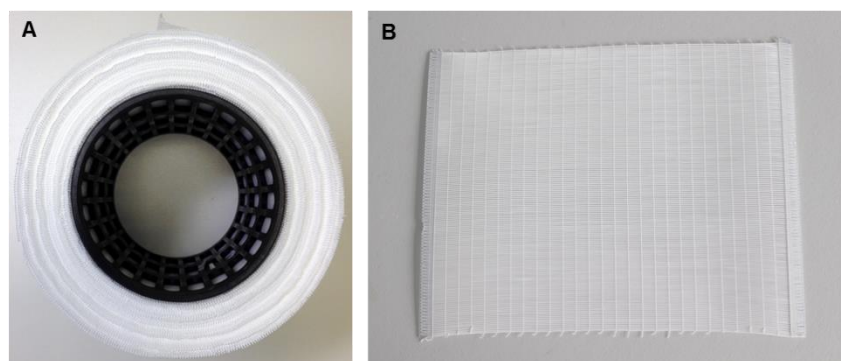
Figure 3-2. Illustration of the PMP.
A PMP mats on a coil, B one PMP hollow fiber mat.

Table 3-9. Parameter of plasma activation

Plasma activation	
Generator power	750 W
Vacuum end pressure	1-2 Pa
Gas	O_2
Gas flow	300 ml/min
Rotating time	6 U/min
Warm-up	15 min
Activation time	90 sec
Duration	30 min
Capacity	4 coils with up to 220 mats

3.1.5.2 The coupling strategy

The coupling strategy was stepwise evaluated in the bench setting and in the rotating setting. The information obtained in these settings was transferred to the circuit setting to simulate circulating characteristics for further upscaling approaches.

3.1.5.2.1 The bench setting

PMP was cut in 1 cm^2 slides, whereby three slides were put in a 5 ml PP-tube with a silicone slice on top to fix the PMP within the fluid (Figure 3-3). The 600 µl of EDC solution (0.5 mM in H$_2$O) were incubated with three slides PMP in one 5 ml tube for 15 min at RT on a shaker. Then, the EDC solution was removed and the slides were washed once with 1 ml H$_2$O. Subsequently, 600 µl of the APO010 solution (from 20 ng/ml to 1 µg/ml in PBS) were added to the slides and incubated for 1 h at RT on a shaker. The solution was removed and washed 5 times with 1 ml H$_2$O for 1 min. Afterwards, the reaction was quenched by adding 1 ml 1 % albumin (in H$_2$O) for 15 min at RT on a shaker. The solution was removed and the slides were washed 5 times with 1 ml H$_2$O.
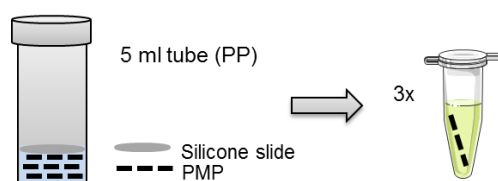
Figure 3-3. Schematic illustration of coupling approach in bench setting with ELISA as read-out.
Three PMP slides were coupled to APO010 in one 5 ml PP tube (left) and were incubated on a shaker. After the coupling, each PMP slide was transferred to 1.5 ml tube (right) in which the ELISA was carried out.

3.1.5.2.2 The rotating setting and the circuit setting

PMP was cut in round slides (50 mm or 20 mm diameter) and placed in a 5 ml tube, respectively. The 2.5 ml (for 50 mm holder device) or 1 ml (for 20 mm holder device) EDC (0.5 mM in H$_2$O) was incubated with the PMP for 15 min at RT on a rotating wheel (Figure 3-4 A). Then, the EDC solution was removed and the PMP was washed 3 times with 2.5 ml or 1 ml H$_2$O.

Subsequently, 2.5 ml or 1 ml of the APO010 solution (20 ng/ml to 1 µg/ml in PBS) was added to the slide and incubated for 1 h at RT on a rotating wheel. The solution was removed and the mat was washed 3 times with 2.5 ml or 1 ml H_2O on a rotating wheel for 5 min. Afterwards, the reaction was quenched by adding 2.5 ml or 1 ml 1 % albumin (in H_2O) for 15 min at RT on the rotating wheel. The solution was removed and the mat was washed 5 times with 2.5 ml or 1 ml H_2O. Afterwards, the PMP was transferred in the circuit setting (Figure 3-4 B) for functionality approaches and the whole circuit was flushed with washing solutions. The read-out was an Apoptosis Assay or a Chemotaxis Assay to investigate the functionality with neutrophils and Jurkat cells or a Sandwich ELISA to investigate detached APO010.
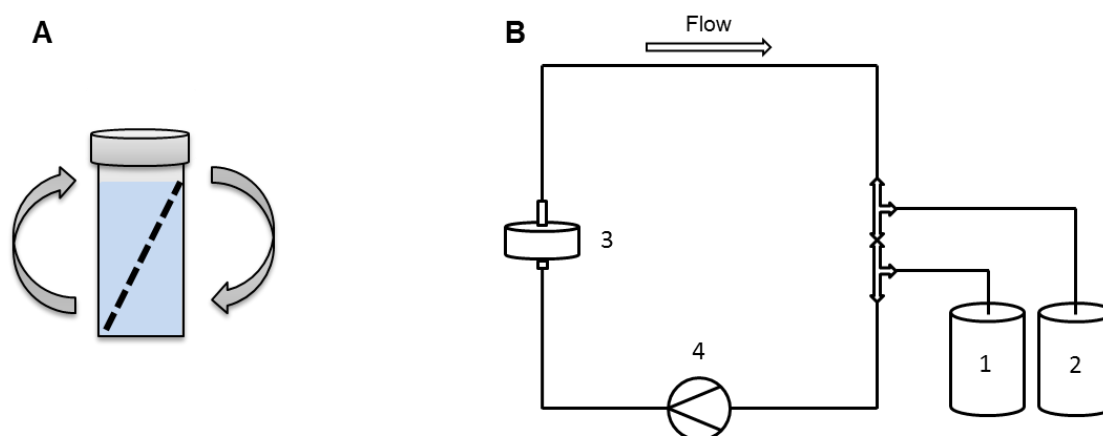
Figure 3-4. Schematic illustration of coupling approach in rotating and circuit setting.
A Rotating setting: The coupling chemistry was carried out in 5 ml PP tubes and the incubation times were carried out on a rotating wheel.
B Circuit setting: After the coupling in the rotating wheel, the PMP was transferred to a mini circuit with flexible-tube pump (4). Round PMP slides with 50 mm or 20 mm diameter are fixed in the corresponding holder device (3) in the circuit. The circuit has a total volume of 28 ml (50 mm holder device) or 8 ml (20mm holder device) and the coating solution (1) is pumped through the circuit via a flexible-tube pump into a collecting container (2).

3.1.6 Washing of the anti-inflammatory coating

In order to wash non-covalently bound proteins off the PMP mats, the mats were coated and washed in the circuit setting (according to Figure 3-4 B). Three mats (circle with diameter 20 mm) were placed into a holder device (diameter 20 mm) to simulate layers as in the medical device. The circuit setting was flushed with 8 ml of the respective washing solution. The mats were rinsed with a flow rate of 31.4 ml/min, which corresponds to 100 ml/min as used in the medical device for washing.

The flow rate for the circuit setting can be calculated as follows:

$$v = \frac{Q}{A} \quad (1)$$

with: v = flow velocity, Q = flow rate, A = flow area

$$v_{medical\ device} = v_{circuit\ setting} \quad (2)$$

$$Q_{circuit\ setting} = Q_{medical\ device} * \frac{A_{circuit\ setting}}{A_{medical\ device}} = 1\frac{l}{min} * \frac{3,14\ cm^2}{100\ cm^2} = 31,4\ \frac{ml}{min} \quad (3)$$

3.1.7 Functional Enzyme-linked Immunosorbent Assay (ELISA)

A functional ELISA was developed and used for the detection of functionally bound APO010 on the PMP. This method is based on a color reaction, which can be measured photometrically. The color intensity corresponds to the coupled amount of APO010 to the PMP mat.

As APO010 consists partly of a Fas ligand, it can bind to the extracellular part of Fas. This Fas is cloned to a Fc part of an antibody. It was biotinylated (Fas-Fc-biotin) according to the manufacturer (Pierce) and the amount of biotin coupled to the Fas-Fc was measured by the Biotin Quantitation Kit (Pierce). The binding efficiency of Fas-Fc to anti-Fas was analyzed in an ELISA.

Initially, the PMP mats were coupled with the anti-inflammatory molecule, APO010, via the EDC chemistry according to the coupling protocol in 3.1.5. Afterwards, the PMP mats were transferred into 1.5 ml Eppendorf tubes and incubated with 500 µl blocking solution (5 % skim milk in washing buffer) for 1 h, respectively. After each ELISA step, the solution was aspirated via a vacuum pump followed by three washing steps with 500 µl washing buffer (PBS + 0.05 % Polysorbate 20). After three times of washing, 200 µl of a Fas-Fc biotin solution (194 ng/ml in PBS) was added to each sample and incubated for 1 h and washed

afterwards three times. Then, 200 µl streptavidin-HRP solution (1:200 in 1 % BSA/PBS) was added for 1 h. After three washing steps, 200 µl TMB solution (1: 1 in water) was added and incubated for 30 min. By addition of 50 µl H_2SO_4 (3.6 M in water) the reaction was stopped. 125 µl of each sample was transferred into an MTP and measured at 450 nm in the photometer. The reference was measured at 550 nm.
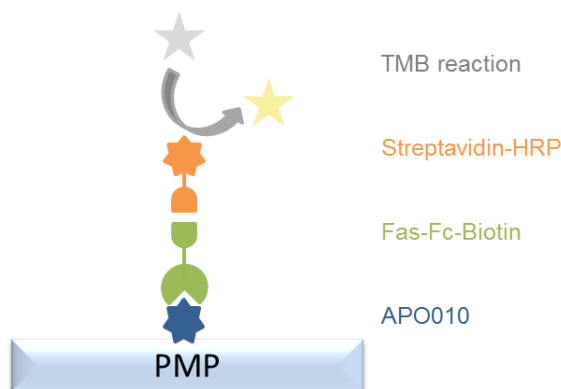
Figure 3-5. Schematic illustration of functional ELISA.
The functional ELISA is carried out in a MTP to detect coupled APO010 on PMP. The Fas-Fc-Biotin binds to the functional FasL domain of the APO010. By biotinylation of the Fas-Fc the Streptavidin-horseradish peroxidase (HRP) can bind to Biotin. By adding the TMB substrate to the HRP, TMB is oxidized which results in a color change from colorless to blue (absorption maximum at 650 nm). The reaction is stopped by adding H_2SO_4 and the solution turns yellow. This shifts the absorption maximum to 450 nm [112]. The solution is transferred to a MTP and can be measured photometrically at 450 nm, whereby a reference is measured at 550 nm.

3.1.8 Non-functional ELISA

A non-functional ELISA was used for the detection of total bound APO010 on the PMP. This method is based on a color reaction, which can be measured photometrical. The color intensity corresponds to the coupled amount of APO010 to the PMP mat.

Initially, the PMP mats were coupled with the anti-inflammatory molecule, APO010, via the EDC chemistry according to the coupling protocol in 3.1.5. Afterwards, the PMP mats were transferred into 1.5 ml Eppendorf tubes and incubated with 500 µl blocking solution (5 % skim milk in washing buffer) for 1 h, respectively. After each ELISA step, the solution was aspirated via a vacuum pump followed by three washing steps with 500 µl washing buffer (PBS + 0.05 % Polysorbate 20). After three times of washing, 200 µl anti-Adiponectin-Biotin (50 ng/ml in PBS) was added to each sample and incubated for 1 h and washed afterwards

three times. Then, 200 µl streptavidin-HRP solution (1:200 in 1 % BSA/PBS) was added for 1 h. After three washing steps, 200 µl TMB solution (1:1 in water) was added and incubated for 30 min. By addition of 50 µl H_2SO_4 (3.6 M in water) the reaction was stopped. 125 µl of each sample was transferred into an MTP and measured at 450 nm in the photometer. The reference was measured at 550 nm.
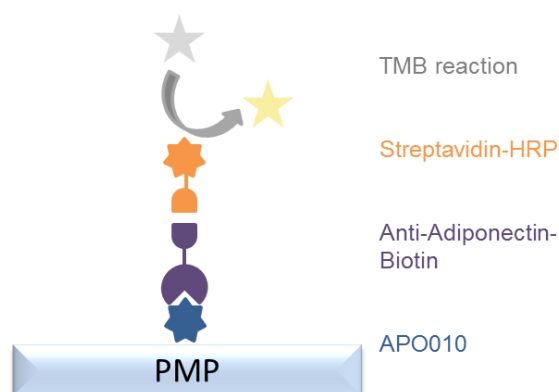
Figure 3-6. Schematic illustration of non-functional ELISA.
The non-functional ELISA is carried out in a MTP to detect coupled APO010 on PMP. The anti-Adiponectin-Biotin binds to the Adiponectin domain of the APO010 not being related to FasL function. Streptavidin-HRP binds to anti-Adiponectin-Biotin. By adding of the TMB substrate the color is changed and the reaction is stopped by adding H_2SO_4. The solution is transferred to a MTP and can be measured photometrically at 450 nm, whereby a reference is measured at 550 nm.

3.1.9 Detachment assay

In order to detect detached or soluble APO010 molecules, a sandwich ELISA was performed. By immobilization of a capture antibody the soluble APO010 can be bound and can be detected specifically of the antigen. The quantification is carried out via an enzymatic color reaction. The sandwich ELISA binds the APO010 molecules in solution, which results in a highly sensitive detection method to detect low amounts of APO010.

First, 100 µl anti-FasL IgG2B (0.1 µg/ml in PBS) was incubated in a MTP for 17 h at 5 °C. Unbound antibody was washed away with 300 µl washing buffer (PBS + 0.05 % Polysorbate 20) for three times. Second, the wells were blocked for unspecific binding with blocking buffer (5 % skim milk in washing buffer) for 1 h. Three washings steps as above mentioned were carried out. Third, 100 µl of the washing solution, after washing of the anti-inflammatory coating as described in 3.1.6, was added and incubated for 2 h. Fourth, after three times of washing, 100 µl anti-Adiponectin-Biotin (400 ng/ml in PBS) was added for detection and

incubated for 1 h followed by three washing steps. Fifth, 100 µl of streptavidin-HRP solution (1:200 in 1 % BSA/PBS) was incubated for 20 min in the dark and washed away three times. Sixth, 100 µl TMB substrate was added and incubated for 30 min at 37 °C. Finally, the reaction was stopped by addition of 50 µl H_2SO_4 (3.6 M in water) and the MTP was measured at 450 nm in the photometer. The reference was measured at 550 nm.

To quantify the soluble APO010, dilution series of APO010 (50 ng/ml to 0 ng/ml) was performed in the same washing medium as the PMP mats were washed.

TMB reaction

Streptavidin-HRP

Anti-Adiponectin-Biotin

APO010
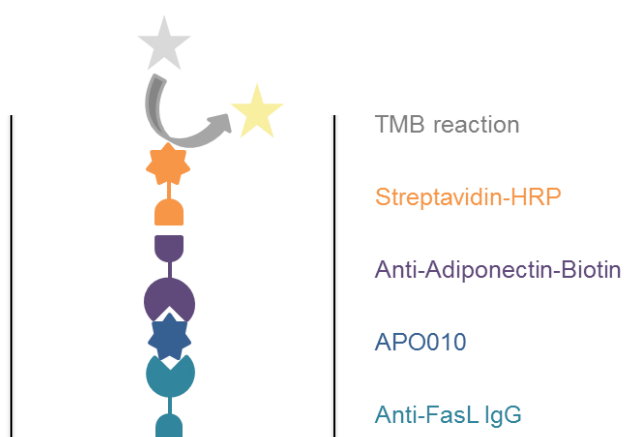
Anti-FasL IgG

Figure 3-7. Schematic illustration of detachment assay.
The detachment assay is carried out in a MTP to detect soluble APO010 in the washing solution of anti-inflammatory coated PMP. The anti-FasL IgG2B is immobilized at the MTP and binds specific to the FasL domain of APO010. To detect the bound APO010 an anti-Adiponectin-Biotin binds to the Adiponectin domain of APO010. Streptavidin-HRP binds to anti-Adiponectin-Biotin. By adding of the TMB substrate the color is changed and the reaction is stopped by adding H_2SO_4. The color can be measured photometrically at 450 nm, whereby a reference is measured at 550 nm.

3.1.10 Cytotoxicity assay / XTT-staining

The cytotoxicity assay using tetrazolium salt (XTT) or so-called XTT-staining is based on the described methods for examination of cytotoxicity of medical devices [113-115]. It describes the investigation of cytotoxicity by XTT-staining, whereby metabolism processes and reproduction of L-929 mouse fibroblasts after incubation with extracts of the test material or chemicals is determined colorimetrically.

The living cells absorb the XTT and convert it to a water-soluble formazan dye via dehydrogenases. The intensity of the coloration change correlates with the cell count and therefore with the mitochondrial activity of the cells. The dehydrogenase activity of the cell

culture serves as a measure for the growth of the L-929 mouse fibroblasts or for growth inhibition in the presence of cytotoxic substances. As a clearly cytotoxic effect the dehydrogenase activity is reduced to less than 30 %, a slight to weak cytotoxic effect decreases dehydrogenase activity to 30 % to 70 %. A dehydrogenase activity over 70 % compared to the solvent control (100 %) corresponds to a negative cytotoxic effect.

L-929 cells were harvested as described in 3.1.1 and 100 µl of 0.1 x 10^6 cells/ml in cell culture medium (DMEM w/o phenol red, 10 % FBS, 2 mM L-Alanyl-L-Glutamine, 100 U/ml Penicillin/Streptomycin) were transferred into a 96 well MTP and incubated for 24 ±2 h at 37 °C / 5 % CO_2.

On day two, the PMP mats were coated according to the coupling protocol on the rotating setting in 3.1.5.2.2 and afterwards the PMP mats were transferred to the circuit setting for washing. There, the settings were flushed 5 times with cell culture medium at a flow rate of 10 ml/min for 5 min. The circuits were then incubated for 1 h with cell culture medium under the same conditions. The respective solutions were sterile filtrated, transferred to a tube, and stored at RT.

To analyze the incubation solutions they were transferred to the L-929 MTP. Therefore, 95 µl of the supernatant of the cells were removed and 100 µl of the washing solution were added. The PMP mats were tested as well by cutting them into small pieces. As positive control a 10 % DMSO solution was used, and cell culture medium was used as negative control. After transfer, a further incubation of the MTP for 24 h at 37 °C / 5 % CO_2 was performed.

On day three, 50 µl of the XTT solution (5 parts reagent 1:0.1 parts reagent 2, Roche) were added and incubated for 2 h to 4 h at 37 °C/ 5 % CO_2. Finally, 100 µl of the supernatant were transferred to a new MTP and measured photometrically at a wavelength of 450 nm and at 630 nm for reference.

3.1.11 Hemocompatibility

Hemocompatibility of the anti-inflammatory coating is important for the approval of the medicinal product. Therefore, whole blood was incubated with coated PMP mats and subsequently the blood was analyzed by an external laboratory for a full blood count. Several controls were included.

For this test, PMP mats were coated in the rotation setting as described in 3.1.5. After the coating, the PMP mats were transferred in the circuit setting for incubation with 0.9 % NaCl solution five times for 5 min at a flow rate of 10 ml/min. Then, the circuit was incubated an additional time with 0.9 % NaCl solution for 1 h at a flow rate of 10 ml/min. Finally, whole blood in heparin (5 U/ml) coated syringes were transferred in the circuit and circulated at a flow rate of 10 ml/min for 2 h. After the incubation period, the whole blood was removed from the respective circulation and 3 ml were filled into an EDTA coated S-monovette K3E (Sarstedt). The samples were analyzed by an external laboratory.

3.1.12 Contact angle measurement

To measure the contact angles of deionized water on untreated and stepwise coated PMP mats the Kruess Drop Shape Analyzer DSA25E was used using the sessile drop method. Therefore, a 2 µl drop of deionized water was placed on the PMP mats under investigation. The mats were fixed on the surface via double-adhesive tape. After adjustment of the manual baseline, contact angles of the drop were fitted by the Tangent-1 method. Three measurements were performed for 10 seconds each after the drop formation with 1 second delay between the measurements. On each sample three different positions were analyzed. The ADVANCE software v1.1.0.2 was used for data evaluation.

3.1.13 Fluorescence spectroscopy

The Leica DMi8 was used to analyze coupled APO010 on the PMP surface by fluorescence labeling. Therefore, the PMP mats were coated in the bench setting according 3.1.5 with 35 ng/ml APO010. The PMP mats were blocked for non-specific staining by adding 400 µl blocking buffer (1 % BSA/PBS) and incubated for 45 min. The blocking buffer was removed and 200 µl anti-Adiponectin-Biotin antibody (200 ng/ml in PBS) was added. Afterwards, the mats were washed two times in 400 µl PBS. 200 µl of the Streptavidin-Northernlights NL557 (1 µg/ml and 5 µg/ml in 1 % BSA/PBS) was added and incubated according to the manufacturer's instructions at RT for 1 h in the dark. After washing with PBS, the samples were transferred to coverslips for analysis.

For Streptavidin-Northernlights NL557 the wavelength 557 nm for absorption and 574 nm for emission were used. Appropriate controls were carried with.

3.1.14 Scanning electron microscope (SEM)

For scanning electron microscopy a Jeol JSM‑6500 F was used at an acceleration voltage of 2.0 kV and different magnifications. The PMP samples were cut in 1.1 x 1.1 cm pieces and were coated according the bench setting described in 3.1.5. Afterwards, they were attached to aluminum blocks with double-adhesive tape. To avoid charging during analyzation the samples were carbon sputtered under vacuum.

3.1.15 Fourier transform infrared spectroscopy (FTIR)

FTIR spectroscopy experiments were performed using the Tensor 27 FTIR spectroscope connected to a thermostat DC30-K20. The sensor was cooled with liquid nitrogen and a constant gaseous nitrogen flow. The samples were analyzed in solution and coupled to the PMP. Therefore, different APO010 concentrations (20 ng/ml to 50 ng/ml) in solution or APO010 coupled to PMP in the bench setting (3.1.5) were used. For each spectrum 100 absorbance scans were measured at a single beam mode and a resolution of 4 cm^{-1}. The spectra were analyzed by the Opus 7.5 (Bruker Optics GmbH) and indicated as vector-normalized second-derivative spectra. The infrared spectra were recorded with a BioATR (Attenuated Total Reflectance) cell at 20 °C and analyzed by Protein Dynamics for Opus 7.5.

3.2 Results

After selection of APO010 as the most suitable effector molecule, the goal in this part of this work was the covalent coupling of the APO010 on PMP as the relevant material for the functionalization of membrane ventilators.

Each development step in this project was chosen in regard to the general regulatory requirements for the approval of medical devices. For the evaluation and selection of the ideal coupling protocol the following issues have been discussed. First, the covalent binding of APO010 on the inert PMP material was achieved by using plasma activation of the PMP material. Second, as coupling strategy the EDC chemistry was chosen due to easy handling and compatibility with the APO010. Third, the stability of the coating was investigated by leaching experiments and the functionality of the coating was investigated by chemotaxis analysis. Fourth, the safety of the coating in blood circulation was analyzed by a hemocompatibilty test and finally, the toxicity of the anti-inflammatory coating was analyzed by a cytotoxicity test. In addition, the anti-inflammatory coating was characterized by different analyzing methods.

PMP is commonly known to be an extremely inert material. Therefore, the major challenge in this project was to define a coupling strategy for the APO010 on PMP, which is in conformity with regulatory requirements. This means that the biomolecule has to be stably bound to the surface even under stress conditions such as thermal stress during sterilization or mechanical stress during blood circulation. Therefore, plasma activation of PMP was chosen to be adequate for covalent coupling of APO010 in conjunction with the crosslinking reagent EDC. The use of albumin as a blocker of uncovered spots of PMP is used to avoid the generation of a biofilm, an adsorption of blood proteins.

3.2.1 Homogeneity of plasma activation

As the homogenous functionalization of the PMP material is important for homogenous covalent coupling of APO010, the plasma activation process was investigated. Therefore, first the PMP mats were rolled on a coil and were plasma activated. Second, the different positions in the coil were analyzed by the functional ELISA after coating the PMP with the anti-inflammatory coating.

The ELISA shows a homogenous distribution from mat #1 to #120 (Figure 3-8 A) and from #1 to #178 (Figure 3-8 B). The mats #180, #220 and #222 show decreased absorption signals but #198, #200 and #218 show similar signals compared to the other mats. The

mean of the absorption signal of Figure 3-8 A with 2.44 ± 0.38 RU and of Figure 3-8 B with 1.26 ± 0.19 RU shows minimal variance in absorption, but it shows as well different absolute values due to different TMB incubation times (15 min and 8 min). Therefore, an absolute comparison of the two graphs is not possible.

However, due to the homogenous distribution of APO010 coupled to the PMP, it can be assumed that the plasma activation on a role was successful and can be continued in this way.
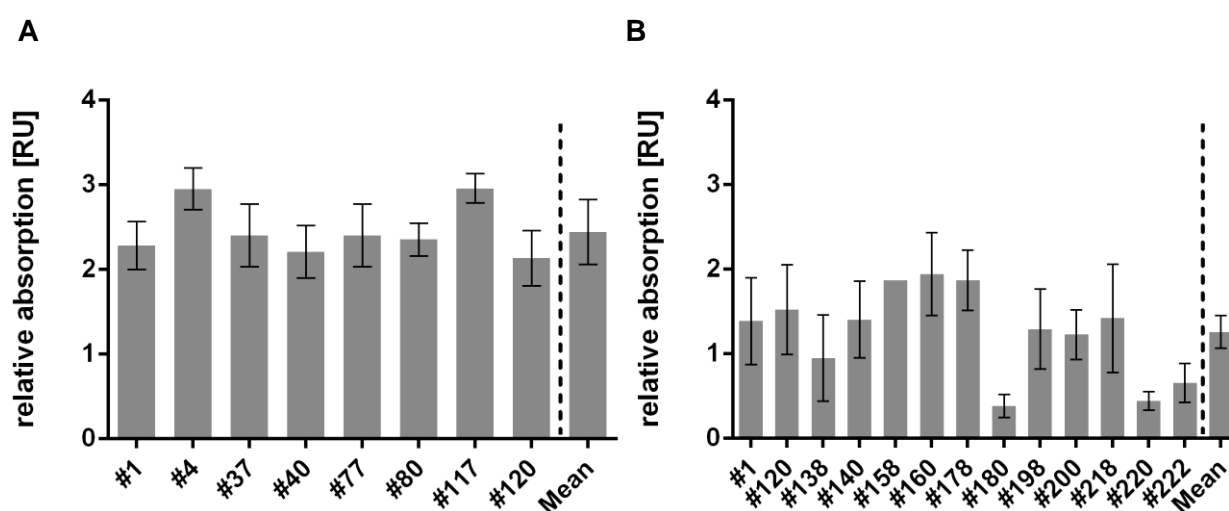
Figure 3-8. Graphical representation of the coupling experiments with different positions of the PMP mats during plasma activation.
120 PMP mats (**A**) or 222 PMP mats (**B**) were rolled on a coil (see Figure 3-2) and were plasma activated. Four mats produce one round. The first and the last mat per round were analyzed. Position one is on the outside and position 222 on the inside of the coil. The coupling of APO010 was carried out via EDC chemistry. The mats were incubated with EDC for 30 min. Then washed and treated with APO010 (1 µg/ml) for 60 min. The reaction was quenched by 5 % albumin (Recombumin alpha, Novozymes) for 15 min. The read-out was performed by a functional ELISA. The TMB reaction was performed for 15 min for A and 8 min for B (Mean ± SD from n=3).

3.2.2   Design of the anti-inflammatory coating

The coupling protocol based on plasma activation of PMP was tested in two different scenarios. The lab scale model referred to as "bench setting" (described in 3.1.5.2.1) was carried out to obtain first evidence for the potential of the functionalized PMP matrix *in vitro*. For testing the functionality of the pre-selected coating under flow conditions the functionalized PMP material was first coupled with APO010 in the rotating setting (described in 3.1.5.2.2) and then inserted into holder devices in mini circuits referred to as "circuit

setting" (described in 3.1.5.2.2). The coupling protocols were in principle identical, but adapted to the different PMP sizes and volumes. Data from these experiments were used to define the final coupling protocol, which is applicable for the serial production. The efficacy of the coupling protocol was verified by the functional ELISA.

3.2.2.1 Crosslinking of APO010 via EDC

The incubation time of the coupling component APO010 and EDC was systematically investigated to get the optimum reaction time. The incubation range was defined according to the manufacturer´s instruction for EDC coupling. The PMP material was coated with anti-inflammatory coating in the bench setting by using the functional ELISA for analysis. Figure 3-9 shows the different approaches, whereby the highest absorption signal was observed with 15 min EDC incubation and 30 min APO010 incubation. The APO010 incubation time seems to be more important than the EDC incubation time, because 5 to 30 min EDC incubation with 60 min APO010 incubation time show the same absorption signal. As optimal incubation time 15-30 min EDC with 60 min APO010 were defined.
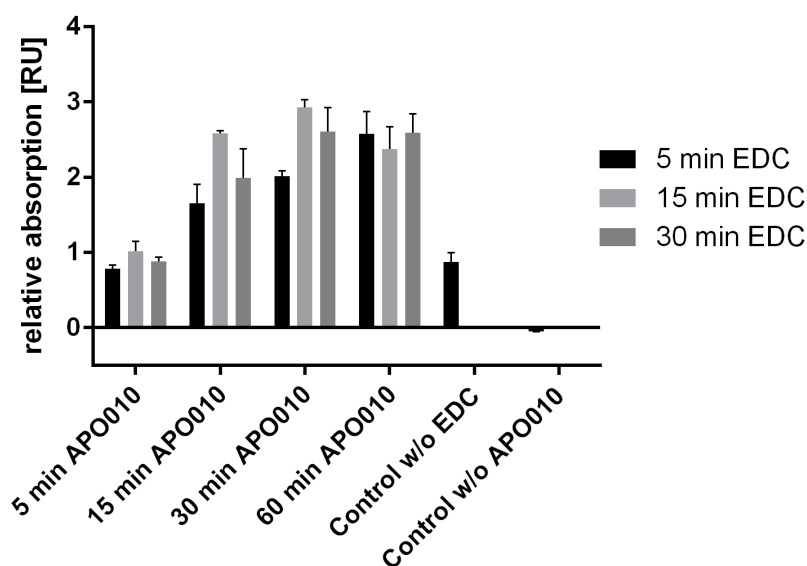
Figure 3-9. Different incubation times to couple APO010 to PMP in the bench setting.
APO010 was coupled (1 µg/ml) via EDC (0.5 mM) to PMP in the bench setting with different incubation times. The reaction was quenched with 5 % albumin. The coating success was analyzed via the functional ELISA. The column chart shows the relative absorbance $_{450-550\ nm}$ in relative units [RU], whereby the relative absorbance is proportional to the amount of bound APO010 (Mean ± SD from n=3).

In the next step, the concentrations of the crosslinker EDC and the concentration of APO010 were systematically varied to identify the optimum combination for the anti-inflammatory coating. The combination of 0.5 mM EDC and 1 µg/ml APO010 is most efficient in the *in vitro* experiments and will be used in the following experiments (Figure 3-10). The first column shows the highest relative absorbance due to unappreciated non-covalently bound APO010 which will be easily washed off, as is shown in the leaching experiments in the next part.
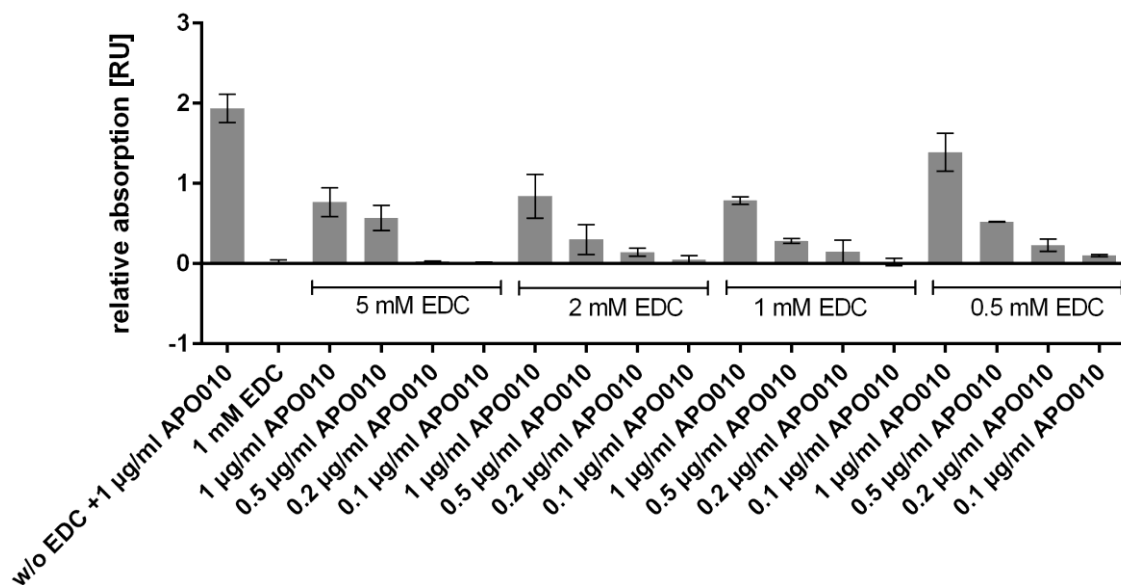
Figure 3-10. Different coating concentrations to couple APO010 to PMP in the bench setting. APO010 was coupled in different concentrations (0.1 µg/ml, 0.2 µg/ml, 0.5 µg/ml, 1 µg/ml) via EDC (0.5 mM, 1 mM, 2 mM, 5 mM) to PMP in the bench setting. The reaction was quenched with 5 % albumin. The coating success was analyzed via the functional ELISA. The column chart shows the relative absorbance $_{450\text{-}550\ nm}$ in relative units [RU], whereby the relative absorbance is proportional to the amount of bound APO010 (Mean ± SD from n=6 from two experiments).

APO010 is a highly functional protein available in GMP-quality, but at a high price. To keep the production costs as low as possible a recycling step of the remaining APO010, which had not reacted with the EDC crosslinking, was preferable. Therefore, the APO010 solution was used for three coatings in a series, whereby all coatings were analyzed by the functional ELISA. In Figure 3-11 A it becomes clear that a recycling step is not possible. Already after the first recycling step no APO010 was bound to the PMP mats. Therefore, it is necessary to use fresh APO010 solutions.

The amount of bound APO010 was analyzed indirectly by unbound APO010 in solution. Therefore, the APO010 solution was analyzed before and after the coating process via the

detachment assay. About 17.95 ng/ml of APO010 was detected before coating, whereas 1.45 ng/ml was left after coating. Therefore, almost 100 % of APO010 was bound to PMP (Figure 3-11 B). To quantify the APO010 indirectly, a dilution series of APO010 was carried out. The resulting standard curve and the residuals from the non-linear regression fit show optimal results and minimal deviation (Figure 3-11 C, D).

A

B

C

D
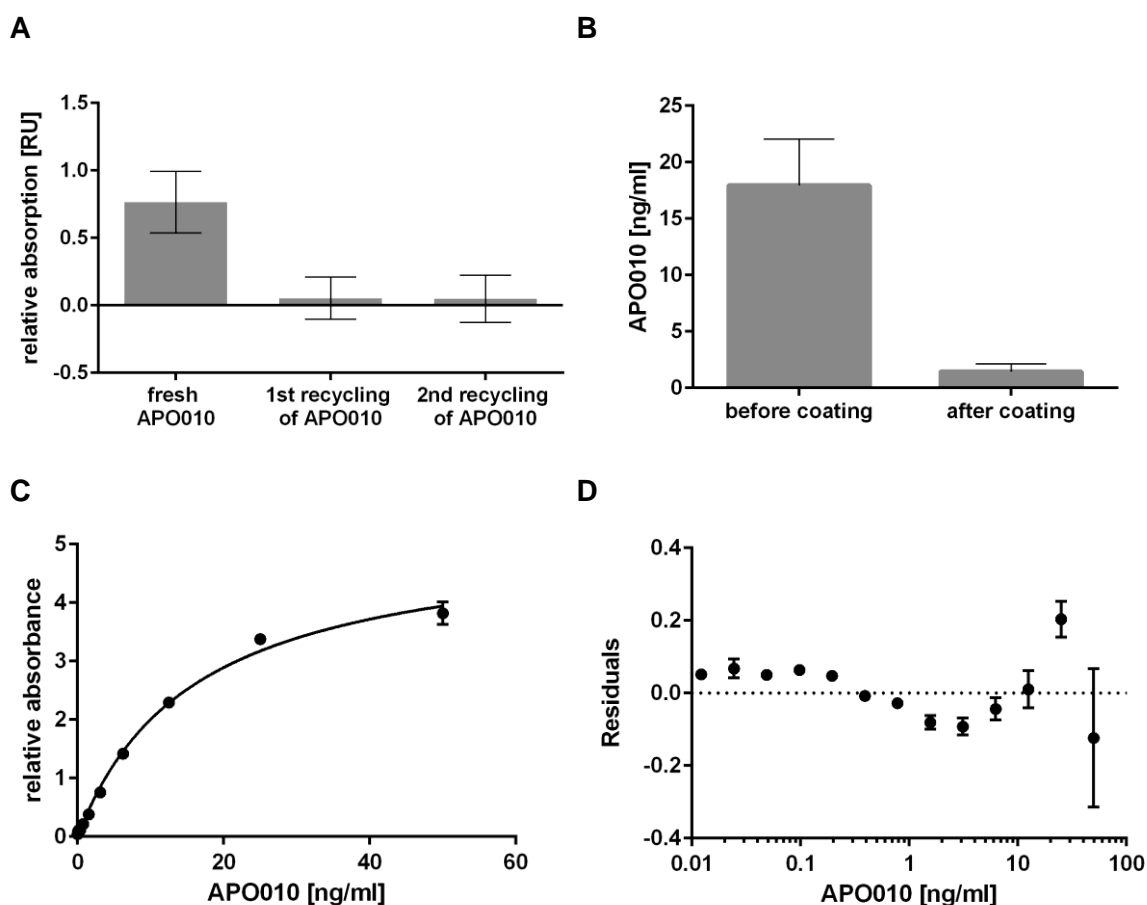
Figure 3-11. Detection of bound and soluble APO010 coupled to PMP in the bench setting.
A Functional ELISA to detect APO010 coupled to PMP after bench setting: APO010 was coupled (1 µg/ml, 60 min) via EDC (0.5 mM, 30 min) to PMP in the bench setting. The reaction was quenched with 5 % albumin. The column chart shows the relative absorbance $_{450-550\ nm}$ in relative units [RU], whereby the relative absorbance is proportional to the amount of bound APO010 (Mean ± SD from n=6). **B** Sandwich ELISA to determine APO010 concentration before and after coating with 20 ng/ml in the bench setting (Mean ± SD from n=9). **C** The concentration was determined by APO010 dilution series from 0 to 50 ng/ml. **D** Residuals from non-linear regression fit performed by PRISM. The residuals are the difference between the actual Y value and the Y value predicted by the model.

3.2.2.2 Leaching experiments

In order to determine the necessary washing steps after the coating procedure and to document the stability of the coupled APO010 on PMP, the material was washed using defined washing protocols. For this approach, the rotating setting was used in order to analyze the total washing volume, which was 500 µl in this case.

The detached APO010 molecules were detected by the highly sensitive Annexin V assay with Jurkat cells that undergo apoptosis after contact with agonistic Fas molecules as APO010. The kill-rate, which is measured in the washing solutions, is an indicator for the detached APO010 from the anti-inflammatory coating. After five washing steps with cell culture medium, no detectable amounts of APO010 molecules were detached from the surface in the sample, which was coated with EDC. The five washing solutions from the sample without EDC show high apoptosis rates (mean = 98.38 ± 0.32 %) (Figure 3-12 A) even after the fifth washing step.
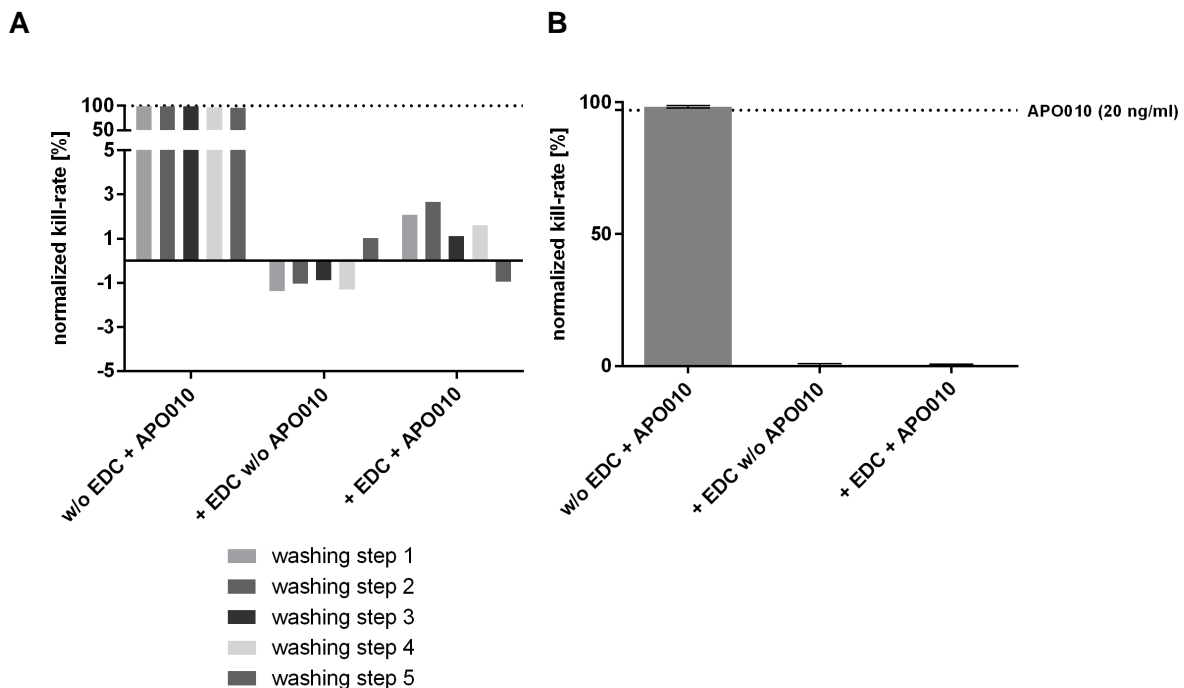
Figure 3-12. Washing solutions from the rotating setting were analyzed in the Annexin V Assay.
A Washing solutions were analyzed by apoptosis assay to detect detached APO010 molecules from the PMP surface after 5 washing steps with 500 µl cell culture medium in the rotating setting for 1 min. **B** Washing solutions were analyzed by apoptosis assay to detect detached APO010 molecules from the PMP surface after an additional washing step of 1 h with 500 µl cell culture medium in the rotating setting. Before, the PMP was coupled to APO010 (1 µg/ml) in the rotating setting (Mean ± SD from n=3).

Afterwards, the PMP samples, which were washed five times, were washed for an additional hour. The washing solutions were analyzed by the apoptosis assay as well, whereby the detachment was clearly observed in the samples with non-covalently coupled APO010 (98.28 ± 0.49 %), but not with covalently coupled APO010 (0.26 ± 0.50 %) (Figure 3-12 B). In conclusion to these results, five washing steps after the APO010 coupling step were included in the anti-inflammatory coating process.

In order to correlate the kill-rate caused by detached APO010, with the amount of molecules given as the concentration, APO010 was serially diluted from 20 ng/ml to 0.078 ng/ml and evaluated in the same apoptosis assay for read-out. The results indicate that the amount of detached APO010 after five times of washing and subsequent washing for 1 h is below the limit of detection. The limit of detection was defined as a kill-rate of 1.39 % (Figure 3-13), which corresponds to an APO010 concentration of 0.078 ng/ml. After subsequent washing a kill-rate of 0.26 ± 0.50 % was measured.
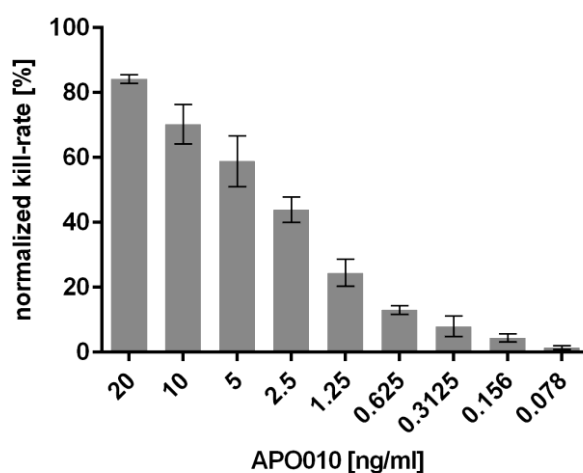
Figure 3-13. Serial dilution of APO010 in solution detected via the Annexin V assay.
Apoptosis was induced by incubation of Jurkat cells with different concentrations of APO010: the kill-rate was normalized with untreated sample is shown (Mean ± SD from n=2).

To simulate the stress conditions of the anti-inflammatory coating during flow conditions the rotating setting was used. The approach **A** represents the anti-inflammatory coating, whereby approach **B** illustrates the coating without EDC and **C** demonstrates the negative control without APO010. The PMP mats were coupled in the bench setting and were washed eight times in the rotating setting with 0.5 ml, respectively. In Figure 3-14 all approaches with APO010 show high kill-rates with the first washing solution, whereby approach **A** shows a

kill-rate of 38.71 ± 23.85 % and approach **B** 81.11 ± 11.01 %. With the third washing solution the kill-rate decreases drastically to 8.40 ± 2.30 % for approach **A**, and 6.89 ± 7.35 % for approach **B**. The fifth washing solution shows no kill-rate for approach **A** and **B**, whereby the values decreases slightly in the eighth washing solutions. Interestingly, the first washing solution from approach **B** is the highest due to non-covalently bound APO010. The control group **C** without APO010 shows no kill-rate as expected.
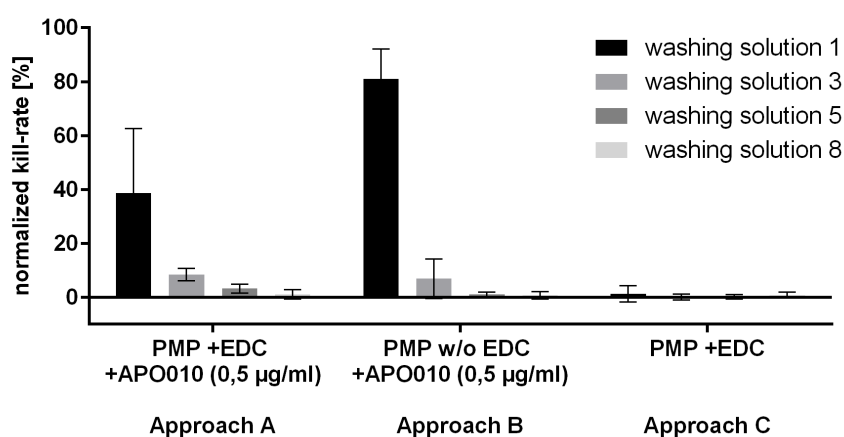
Figure 3-14. Washing solutions from the rotating setting were analyzed by Annexin V Assay.
Washing solutions were analyzed by apoptosis assay to detect detached APO010 molecules from the PMP surface after 8 washing steps with 0.5 ml washing buffer (0.02 % Polysorbate 20 in PBS) in the rotating setting for 30 min, respectively. Before, APO010 (0.5 µg/ml) was coupled to PMP in the bench setting: approach A, without EDC in approach B and without APO010 in approach C (Mean ± SD from n=3).

3.2.2.3 Stability of the anti-inflammatory coating after incubation with blood

In order to show that the anti-inflammatory coating comprising APO010 is bound stably during contact with blood, the detachment assay was conducted with anti-inflammatory-coated PMP samples. PMP mats were washed for 1 h with blood or PBS in the circuit setting. To compare the signals of the relative absorbance for every experiment defined APO010 concentrations were diluted in blood or PBS, respectively (Figure 3-15).

Table 3-10. Results of detachment assay in ng/ml after washing of anti-inflammatory coating with blood and PBS

	Approach	Washing solution in blood		Washing solution in PBS	
		Mean [ng/ml]	SD [ng/ml]	Mean [ng/ml]	SD [ng/ml]
A	PMP + EDC + APO010 (0,1 µg/ml)	0.59	0.23	1.01	1.13
B	PMP w/o EDC + APO010 (0,1 µg/ml)	1.61	0.31	4.12	5.23
C	PMP w/o EDC w/o APO010	0.035	0.10	0.20	0.39
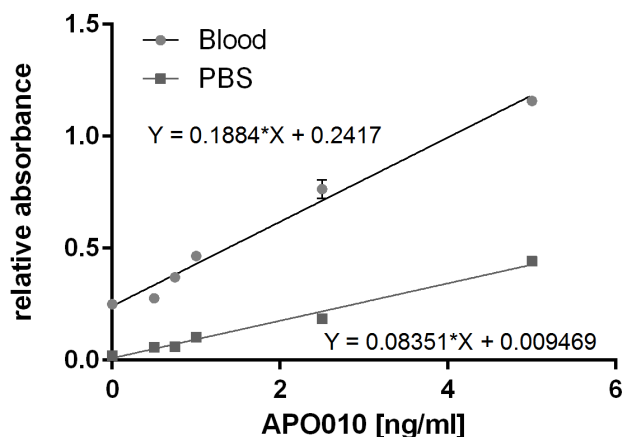
Figure 3-15. Detection of washing solutions of circuit setting analyzed by detachment assay.
To determine the APO010 amount in solution defined APO010 concentrations (0 ng/ml, 0.5 ng/ml, 0.75 ng/ml, 1.0 ng/ml, 2.5 ng/ml, 5.0 ng/ml), diluted in blood (R= 0.9846) or PBS (R=0.9847), were carried out.

The results of the washing experiments are depicted in Table 3-10. The highest absorbance was measured in samples with non-covalently coupled APO010 (approach B, w/o EDC + APO010). This confirms that adhesive coupling of APO010 is not recommended in order to avoid safety issues. By contrast, the samples with EDC and APO010 (approach A, covalent coupling) show low amounts of detached APO010 in blood (0.59 ± 0.23 ng/ml) and PBS (1.01 ± 1.13 ng/ml).

3.2.3 Verification of anti-inflammatory functionality in neutrophil activity assays

After confirming the functionality and stability of the anti-inflammatory coating on the apoptosis induction features as outlined above, chemotaxis experiments with activated neutrophils were carried out to confirm the immunomodulatory efficacy. The ability of neutrophils to migrate through a porous membrane towards a gradient of the cytokine IL-8 within a two chamber model is a measure of activity.
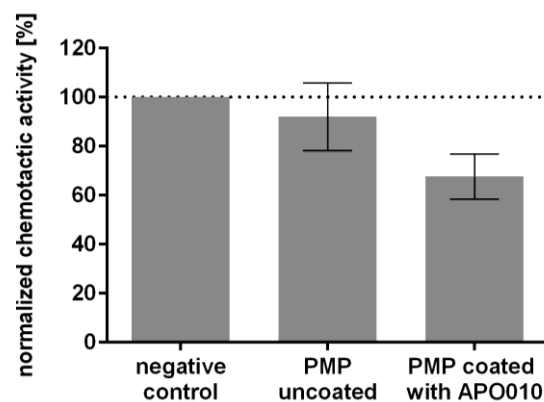
Figure 3-16. Neutrophil chemotaxis assay after circuit setting.
PMP, which was untreated or coupled with APO010 (1 µg/ml) via EDC, was transferred into the circuit setting (50 mm diameter device holder) and incubated for 2 h at RT with a flow rate of 10 ml/min. Afterwards, neutrophils were harvested from circuits and transferred to chemotaxis chambers, where the samples were incubated for 1 h at 37 °C. Analysis of the migrated cells, which were migrated to the IL-8 gradient in the lower compartment, was carried out by flow cytometry (the kill-rate was normalized to untreated sample (Mean ± SD from n=4).

The goal in this approach was that neutrophils, that were in contact with the anti-inflammatory coating, reduce their chemotactic activity compared with neutrophils without previous contact to this coating. The results show that IL-8 induced neutrophil chemotactic activity is indeed reduced by 33 % after incubation of the coating in the circuit setting (Figure 3-16). In this experiment a concentration of 1 µg/ml APO010, coupled to PMP, was sufficient to reduce chemotactic activity in neutrophils by more than 20 %. Therefore, the goal was reached. In comparison to the untreated PMP the anti-inflammatory coating reduced chemotactic activity in neutrophils by 24 % (Figure 3-16).

3.2.3.1 Hemocompatibility

In order to confirm the hemocompatibility of the anti-inflammatory coating, the circuit setting (50 mm holder device) was filled with fresh human blood. The blood was heparinized and circulated for two hours via the circuit setting with or without PMP material, with and without APO010. At the end of the circulation, blood samples were harvested and analyzed. As shown in Table 3-11 no evidence of blood incompatibilities was found on the basis of the obtained hemograms in comparison to the control groups at RT and 5 °C.

Table 3-11. Results of blood analysis

	Unit	Untreated PMP	Coated PMP	w/o PMP	Control at RT	Control at 5 °C
Leucocytes	Tsd/µl	6.63	6.67	6.67	8.32	7.18
Erythrocytes	Mio/µl	4.51	4.47	4.47	6.27	4.71
Hemoglobin	g/dl	13.9	13.8	13.7	18.9	14.5
Hematocrit	%	39.4	39.2	39.2	53.5	41.3
Mean corpuscular volume (MCV)	fl	87.4	87.7	87.7	85.3	87.7
Mean corpuscular hemoglobin (MCH)	pg	30.8	30.9	30.6	30.1	30.8
Mean corpuscular hemoglobin concentration (MCHC)	g/dl	35.3	35.2	34.9	35.3	35.1
Thrombocytes	Tsd/µl	285	293	290	171	267
Neutrophils	%	61.3	63.1	62.4	62.5	62.8
Neutrophilic granulocytes	/µl	4070	4210	4160	5210	4510
Lymphocytes	%	30.8	30	29.7	29.6	29.4
Lymphocytes abs.	/µl	2040	2000	1980	2460	2110
Monocytes	%	6.3	5.7	6.7	6.6	6.7
Monocytes abs.	/µl	420	380	450	550	480
Eosinophils	%	1.1	0.9	0.9	0.7	0.7
Eosinophilic granulocytes abs.	/µl	70	60	60	60	50
Basophil	%	0.5	0.3	0.3	0.5	0.4
Basophilic granulocytes abs.	/µl	30	20	20	40	30

3.2.3.2 Cytotoxicity

In addition to the hemocompatibility approach, the samples harvested from the rotating setting were analyzed for non-cytotoxicity of the fluids incubated with the anti-inflammatory coating. For this purpose, a standard XTT-assay was carried out. Therefore, the mouse fibroblasts L-929 were incubated with fluids, which were incubated previously with the anti-inflammatory coating. The mitochondrial activity is measured by means of an enzyme assay, whereby a low enzyme reaction indicates a reduced mitochondrial activity and viability of the cells. The anti-inflammatory coating and the uncoated PMP show no evidence for any cytotoxic effect elicited by the harvested fluid samples (Figure 3-17).
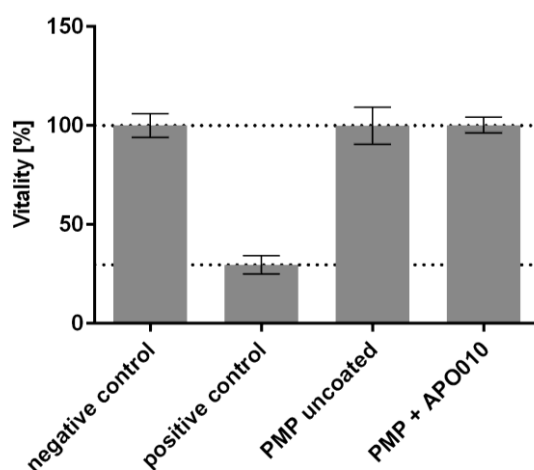
Figure 3-17. Results of cytotoxicity assay/ XTT-staining.
PMP, which was untreated or coupled with APO010 (1 µg/ml, 30 min) via EDC (0.5 mM, 15 min), was transferred into 5 ml tubes and incubated with 3 ml cell culture medium for 1 h at 37 °C on the rotating setting (Mean ± SD from n=3). Afterwards, the medium was transferred to 96-well MTP with L-929 mouse fibroblasts. After an incubation of 24 h a XTT-staining was performed and after 2 h incubation the samples were analyzed photometrically at 450 nm and 630 nm. Negative control contains medium and L-929, positive control includes medium + 10 % DMSO and L-929.

3.2.4 Characterization of the anti-inflammatory coating surface

The characterization of the anti-inflammatory coating by visual and analytical methods is another approach to determine the quality of the designed coating. In the following section the coating was analyzed using SEM, contact angle analyzation, fluorescent labelling and FTIR spectroscopy.

3.2.4.1 Characterization via SEM

The PMP fibers are woven together by a polyester weaving thread. To analyze the whole anti-inflammatory coating on the artificial material, the coating was analyzed by SEM after each coating step. In Figure 3-18 A and B the mats were analyzed untreated by SEM in different magnifications. The surface of the uncoated PMP appears smooth with slight scratches through handling with the tweezers.
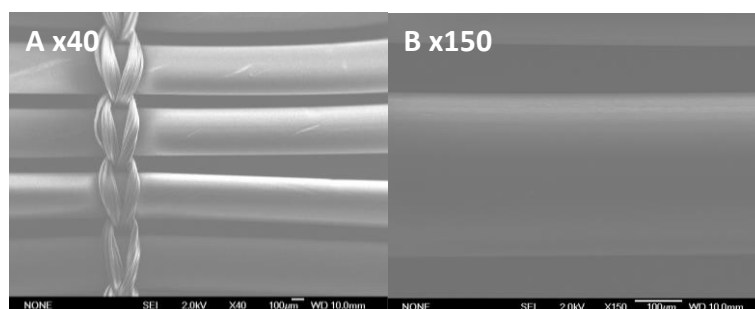
Figure 3-18. The untreated PMP hollow fibers analyzed by SEM.
A (x40 magnification) to **B** (x150 magnification) show the untreated PMP hollow fibers.

When PMP was treated with EDC as shown in Figure 3-19, the surface of the mat with EDC appears smooth and unchanged compared to the uncoated mat.
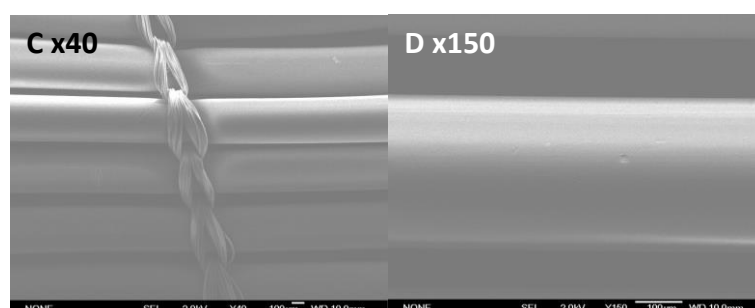
Figure 3-19. The PMP + EDC analyzed by SEM.
C (x40 magnification) to **D** (x150 magnification) show the PMP hollow fiber, which was treated with 0.5 mM EDC for 15 min.

The mat coated with APO010 (Figure 3-20) appears smooth with some small deposits and does not differ from the uncoated mat. The PMP with EDC, APO010 and Albumin shows small deposits and some scratches through the tweezers (Figure 3-21).
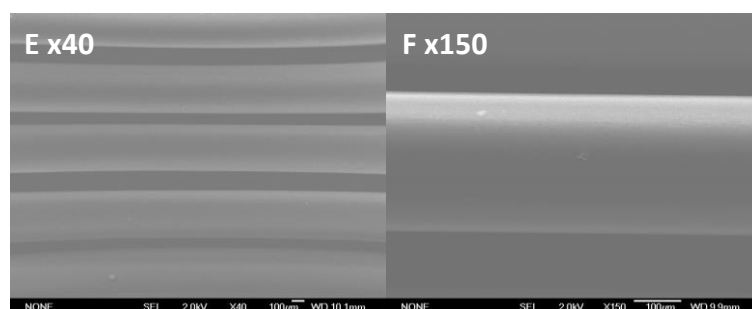
Figure 3-20. The PMP + EDC + APO010 analyzed by SEM.
E (x40 magnification) to **F** (x150 magnification) show the PMP hollow fiber, which was treated with 0.5 mM EDC for 15 min and 20 ng/ml APO010 for 1 h.
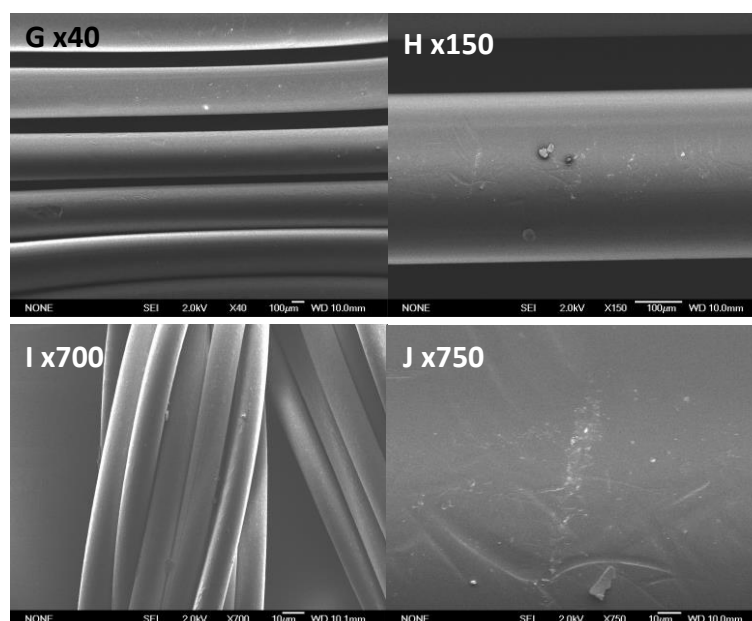
Figure 3-21. The PMP + EDC + APO010 + Albumin analyzed by SEM.
G (x40 magnification), **H** (x150 magnification) and **J** (x750 magnification) show the PMP hollow fiber, which was treated with 0.5 mM EDC for 15 min and 20 ng/ml APO010 for 1 h and EDC reaction was quenched with Albumin for 15 min. **I** (x700 magnification) shows the woven thread, which holds together the single hollow fibers.

The mats, which are coated with the stabilizing formulation F1, show deposits of F1 and are inhomogeneous skin-dried (Figure 3-22). In the images K (x40 magnification), L (x150 magnification), M (x350 magnification) and N (x700 magnification) the PMP hollow fiber was analyzed from the bottom. They show the deposits between and on the bottom of the PMP

hollow fiber. There it becomes visible that the protection layer carried out by the dried stabilizing formulation covers the entire fiber as expected. At 150-fold magnification, sharp-edged deposits are shown, which were probably formed during the drying process.
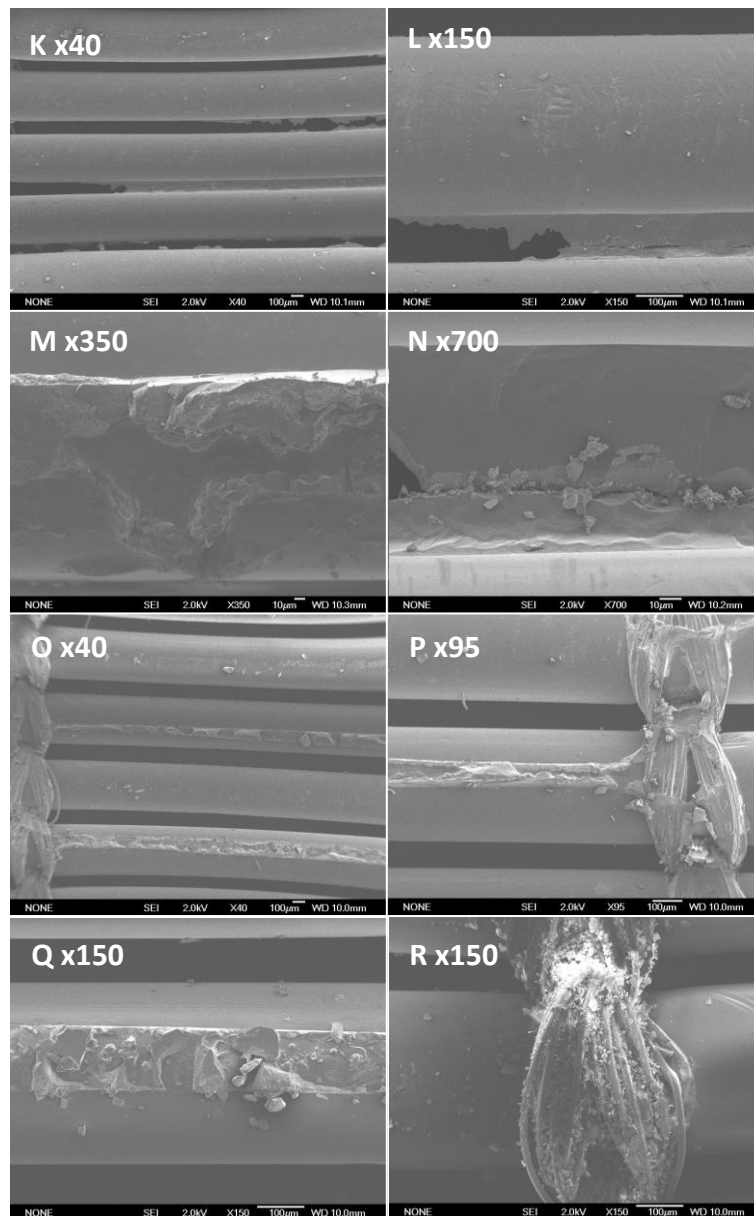
Figure 3-22. The PMP + EDC + APO010 + Albumin + stabilizing formulation analyzed by SEM.
K (x40 magnification), **L** (x150 magnification), **M** (x350 magnification) and **N** (x700 magnification) show the PMP hollow fiber from the bottom, which was treated with 0.5 mM EDC for 15 min and 20 ng/ml APO010 for 1 h and EDC reaction was quenched with Albumin for 15 min. The stabilizing formulation F1 was added and the samples were dried in a cell culture plate at 50 °C. In **O** (x40 magnification) **to R** (x150 magnification) the weaving thread and the PMP hollow fibers are shown in detail.

The mats were individually air-dried in cell culture wells and attached to the bottom of the well. Therefore, the drying process is an important step in building the homogeneous protection layer. In image O (40-fold magnification) through R (150-fold magnification) the weaving thread and the PMP hollow fibers are shown in detail. The images show that the protecting layer is visible on the fibers and in the weaving thread. In image P the stabilizing formulation is coated like a film on the thread, whereby in image R the dried stabilizing formulation indicates crystalline structures located in the thread. Here, the layer appears to be more crystalline than on the PMP fiber. Also the sharp-edged deposits formed by the drying model are visible.

In summary, the analyzation of the anti-inflammatory coating gives insights to the dried layer of the formulation, but not on the other components.

3.2.4.2 Characterization via contact angle

The contact angle shows the physical property of surfaces. The drop shape analysis obtained for water with stepwise coated PMP mats is shown in Figure 3-23. The corresponding contact angles are summarized in Table 3-12. The stepwise coated PMP samples with EDC, APO010 and Albumin exhibited high water contact angles of 121° to 127°. When the stabilizing formulation F1 was added to the coating the contact angle decreases to 89°. This means, that the anti-inflammatory coating does not change the physical property of the artificial material PMP.
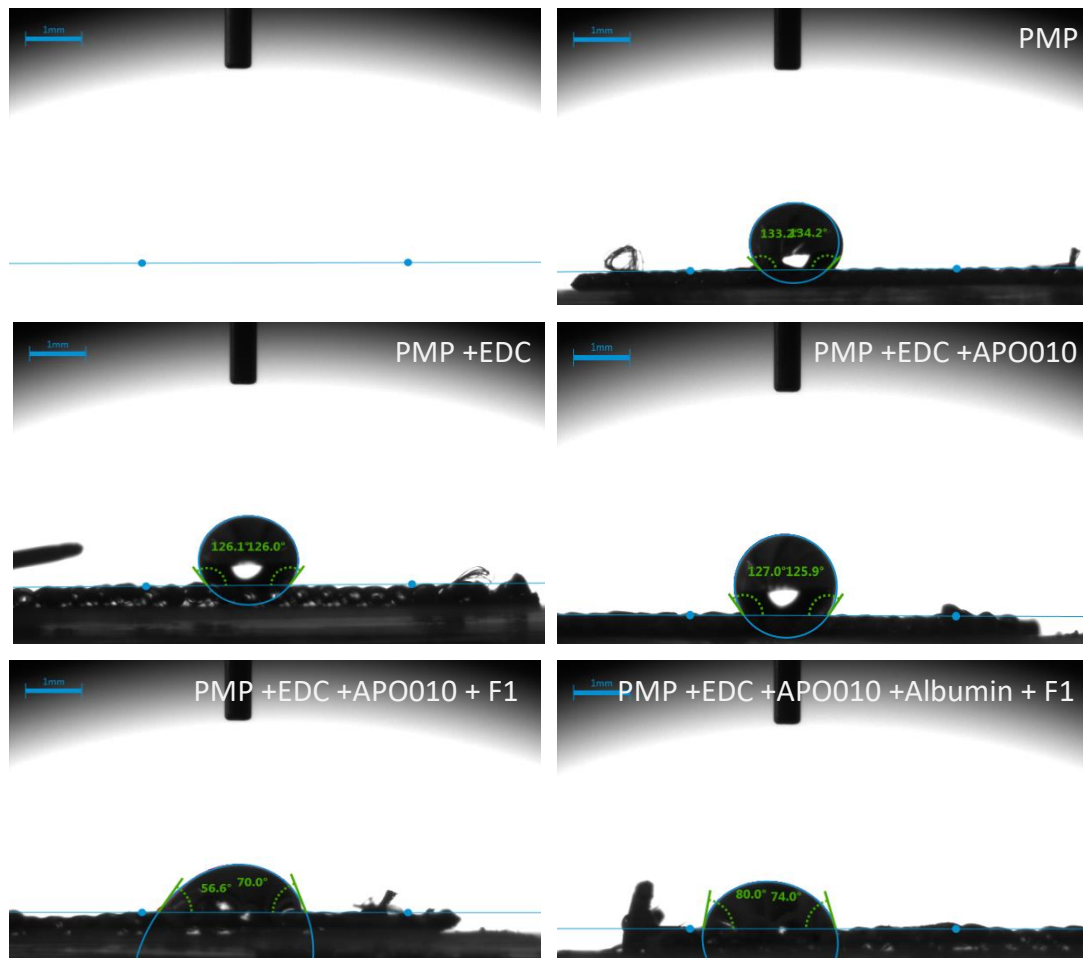
Figure 3-23. The contact angle analyzation of anti-inflammatory coated PMP.
The contact angle of the anti-inflammatory coating was analyzed stepwise as indicated in the picture.

Table 3-12. Contact angles with water of coated PMP, n=3 with 3 sub-measurements each

untreated	PMP +EDC	PMP +EDC +APO010	PMP +EDC +APO010 +Albumin	PMP +EDC +APO010 +Albumin +F1
122.87 ± 8.41 °	126.53 ± 8.14 °	124.64 ± 4.54 °	120.75 ± 9.14 °	89.33 ± 18.25 °

3.2.4.3 Characterization via fluorescent labelling

The anti-inflammatory coating was labelled as described in 3.1.13 with specific anti-APO010 antibodies. By analysing the samples no fluorescent signal from the bound APO010 to the PMP mats could be observed due to too low concentration of APO010.

3.2.4.4 Characterization via FTIR

The anti-inflammatory coating was analyzed at several positions with the IR microscope. As well soluble APO010, at low concentrations of 20 ng/ml and 50 ng/ml, was analyzed by the FTIR spectrometer. With both methods (solid and in solution) no difference compared to the negative control could be observed. Furthermore, no characteristic IR bands for proteins, like N-H, C-H or O-H, could be observed. Therefore, the method is not able to show APO010 coupled to the PMP mats.

3.2.5 Summary

The anti-inflammatory coupling protocol to covalently bind APO010 to PMP comprises recombinant human albumin, recombinant human APO010 and an aa-based stabilization formulation. Each compound has been already approved to be safe for clinical applications. Covalent and stable binding of APO010 to PMP was shown in leaching experiments. Five washing steps are recommended after crosslinking APO010 with EDC for removing residual non-covalently bound APO010 from PMP. Functionality was shown by reduced chemotactic activity of neutrophils after challenging with the anti-inflammatory coating. Hemocompatibility of PMP coated with the anti-inflammatory coating was shown in the circuit setting with whole blood. Moreover, no cytotoxic effects of fluid samples harvested from circuits with the anti-inflammatory coating could be observed. The characterization of the anti-inflammatory coating was investigated via SEM, FTIR, and contact angle. These methods were not able to detect APO010 on the PMP mats. However, the functional ELISA and the Apoptosis assay could prove the presence of APO010 on the PMP mats. The assays for characterization need higher protein concentrations than used in this work.

3.3 Discussion

This chapter deals with the design of the anti-inflammatory coating. Therefore, several investigations were carried out to define the optimal coating parameters like concentration and incubation time. The parameters for the anti-inflammatory coating are summarized in Table 3-13 and will be adapted in the last part to the serial production scale. There, the concentrations of the components and the incubation times have to be adapted in regard to economic efficiency.

Table 3-13. The anti-inflammatory coating parameters

Step	Process parameter
1	Plasma activation of PMP with O_2
2	Activation of the PMP surface with EDC (0.5 mM) for 15 to 30 min
3	Coupling of APO010 (20 to 1000 ng/ml) for 60 min
4	Quenching of the reaction with albumin (1 %) for 15 min
5	5 times washing with H_2O
6	Adding of an aa-based coating solution for 1 h and then air-drying

APO010 was coupled via EDC and the plasma activation to the inert PMP hollow fibers. The functional ELISA served as analytical method to investigate the concentration of EDC and APO010 and to determine the incubation time of both. As the functional ELISA only detects functional active bound APO010, it must be assumed that a higher amount of APO010 was bound to the PMP mats. In this regard a specific coupling of APO010 would lead to a higher economic efficiency, but is not possible for the APO010 molecule. One possibility to generate a specific binding site is to generate a single C-terminal Cysteine to couple it via thiol chemistry as done for several proteins like the DARPins [104, 116-118]. Thereby, no additional Cysteines can be present in the protein sequence. In this case, APO010 needs its Cysteines to form disulfide bridges between the monomers to generate a stable hexamer. This stable hexamer leads to the high efficiency of APO010 and therefore needs to be maintained. The adiponectin domain is fused to the FasL domain of APO010 and has the function to strengthen hexamer formation by its stalk domain. This stalk domain has no strong influence to the EDC crosslinking compared to the functional active FasL domain.

Therefore, it was assumed that all adiponectin domains could be detected by the antibody and can be correlated with all APO010 bound to the PMP mats.

Stepwise, the anti-inflammatory coating was investigated, initiating with the plasma activation. The successful plasma activation was indirectly proven by the detection of APO010 with the result that APO010 is coupled consistently over the whole mat. As there were some outliers at mat position 180, 200 and 222 and no one up to position 120s, optimal results will be generated when at least 120 mats will be plasma activated on a coil. Different labeling of activated functional groups on the PMP mat can strengthen this outcome, but were not tested in this work.

The investigations of incubation time and concentrations of EDC and APO010 indicate that the incubation time and concentration of EDC are more variable than those of APO010. The used APO010 concentration was varied in this chapter between 20 ng/ml and 1 µg/ml depending on the read-out methods and the questions to be addressed.

To analyze the bound amount of APO010, indirect methods as the sandwich ELISA were used. By using 20 ng/ml APO010, it becomes clear that almost the whole amount of APO010 was coupled to the PMP mats. In addition, it was investigated if APO010 can be recycled when using higher concentrations of 1 µg/ml. It shows clearly that no recycling of APO010 is possible in this setting. This means that the low protein concentration needs to be prepared freshly for optimal crosslinking results. One reason could be the low protein concentration in PBS without stabilizer, another reason could be that APO010 reacts completely with the activated PMP mat. Other labeling methods, like radioactive labeling or immunogold labeling, which directly detect APO010 on the PMP mats, were not carried out. The PMP hollow fibers limit the analyzing methods due to the irregular surface.

After finishing the coating process, unbound APO010 has to be washed away. To analyze this procedure a sensitive apoptosis assay was carried out. After five washing steps, no apoptosis was induced in Jurkat cells, but when no EDC is present APO010 is attached to the PMP mats, but is washed away during the five washing steps and as well after an additional washing hour. Almost 100 % apoptosis was induced in Jurkat cells during the detachment process. Therefore, it gets clear that EDC leads to a covalent binding of APO010, whereby without EDC APO010 is attached tight and gets detached by washing solutions, as cell culture medium. To increase the stress conditions to the anti-inflammatory coating, the PMP mats were transferred to a rotating setting and were washed for 30 min

eight times with PBS and only low Tween-20 concentrations (0.02 %) as not to stress the Jurkat cells by the detergent. As expected, the samples without EDC show high apoptosis rates in the first washing solution, but interestingly from the third washing solution the apoptosis rate decreases to the same as for the sample with EDC. This means that both samples showed similar results in the washing solutions, but the kill-rates for the samples with EDC were much lower.

As the anti-inflammatory coating shall be used in a medical device with blood contact, it is important to understand the behavior of the anti-inflammatory coating during usage. Therefore, the coating was incubated with blood and the blood was analyzed for APO010 content. Small amount of APO010 were detected in the blood sample with and without EDC. But functionality of anti-inflammatory coating with neutrophils showed the expected results and the analyzed blood samples showed no transition in the full blood count. In addition, no cytotoxicity was found in mouse fibroblasts.

Summing up, the assays performed with blood suggest that no relevant detectable amounts of APO010 have detached from the surface even after washing with blood or PBS. Thus, the results indicate that the anti-inflammatory coating is stable and functional even after contact with blood.

Thus, more detailed results of the blood compositions would be interesting. Therefore, chemotaxis assays with full blood cultures would be of great interest, but are difficult to handle due to the huge amount of different components in the blood.

In this part an aa-based stabilizing formulation with only seven amino acids at pH 6.5 was used as last coating step. As the formulation was only added to analyze the coating via SEM no stability tests were performed. In the next chapter three different formulations will be investigated to analyze the stability effect of the formulations. By the characterization of the anti-inflammatory coating via SEM, it could be shown that the stabilizing formulation was dried skin-shaped and irregular with sharp-edged deposits on the bottom. As the shape of the stabilizing formulation has no high impact on the stability, this was not further investigated. However, to avoid inhomogeneous results due to the drying process in lab scale, in the next chapter in the upscaling whole medical devices were used. In this setting defined contact points should generate reproducible drying results.

The characterization of the surface in general was not possible due to the low APO010 concentrations. Most characterization methods as FTIR need smooth surfaces and high

protein concentrations of at least 1 mg/ml. The contact angle method to differ the surface properties before and after coating of the anti-inflammatory coating showed only differences by adding the stabilization formulation.

Anti-inflammatory coatings are used for implants or prostheses [119, 120], hernia repair [121], disorders [122] or are used in general to differentiate monocytes into macrophages [123]. This anti-inflammatory coating is an innovative approach for a medical device with blood contact, with high requirements in stability and functionality. Thus, it can possibly show the way for new biofunctional coatings in the medical device sector.

UPSCALING OF THE COUPLING PROTOCOL TO SERIAL
PRODUCTION SCALE

4   Introduction

This chapter describes the upscaling of the anti-inflammatory coating to a serial production scale. The anti-inflammatory coating had to be upscaled stepwise in order to generate a homogenous distribution on the PMP hollow fibers. In the previous chapters the anti-inflammatory molecule was selected, the coating was developed in a lab scale model and in a circuit setting to investigate the flow behavior of the solutions in the coating procedure.

In the final lab scale model a very low concentration of 20 ng/ml of APO010 was determined as functional. This low concentration requires a fast und homogenous binding of the anti-inflammatory molecule APO010 in the EDC crosslinking step, whereby it is crucial to consider this aspect during the development of an upscale process.

In this upscaling process, several intermediate steps were included, whereby the bench setting with three 1.1 x 1.1 cm PMP pieces was first transferred to the circuit setting with three PMP circles with 20 mm diameter. The circuit setting then was upscaled to the coating of one medical device with a PMP surface area of 10 800 cm^2. This was transferred to the coating of 6, then 20 and then 22 medical devices.

One medical device consists of 54 10 x 10 cm PMP mats, which are 90° rotated on top of each other. The surface area was simply calculated for a flat area, whereby the fiber tube structure was disregarded.

Incubation times and concentrations of the coating components will be investigated in this chapter. A stabilization formulation is included in the anti-inflammatory coating to protect the coating during drying, and sterilization via EtO. Three different formulations will be tested in this part. The stabilization formulation F1 has only seven amino acids (aa) [55, 124]. F2 is more complex with 15 aa and 2 dipeptides and F3 consists of 8 aa, one sugar, and Polysorbate.

The formulations were selected based on the knowledge that amino acids can stabilize proteins and on the fact that in nature an intracellular high osmolality can protect the organism during water stress as with high environmental salt concentrations [65, 75]. The combination of amino acids and sugars can effectively stabilize biologics in the dried state as many organisms can survive dehydrated in a process called anhydrobiosis, when they concentrate disaccharides like trehalose intracellularly [76, 77].

The upscaling process is a crucial step in the design of the anti-inflammatory coating, which shall be used for invasive medical devices. Therefore, the three serial production runs were performed in a clean room under terms and conditions of the ISO 11607 [125].

4.1 Materials and methods

Table 4-1. Equipment

Name	Reference
Analytical balance, AT460 Delta Range	Mettler-Toledo, Columbus, Ohio, USA
Balance	KERN & SOHN GmbH, Balingen, Germany
Balance Scout Pro SPU 123	VWR International GmbH, Ismaning, Germany
Centrifuge Biofuge fresco, max.13 000 rpm or 16 060 x g	Heraeus, Hanau, Germany
Centrifuge Megafuge 1.0R, max. 4000 rpm or 3345 x g	Heraeus, Hanau, Germany
CO_2 incubator	Sanyo Denki K.K, Moriguchi, Japan
Filter holder device (diameter 25 mm, PSU)	Whatmann, Maidstone, United Kingdom
Filter holder device (diameter 50 mm, PC)	Sartorius, Göttingen, Germany
Flexible-tube pump MCP	IDEX Health&Science (ISMATEC), Wertheim, Germany
Flow cytometer BD Accuri C6	BD Biosciences, San Jose, Germany
Flowmaster FMT 300	IDEX Health&Science (ISMATEC), Wertheim, Germany
Fusion photometer	PerkinElmer, Inc., Waltham, Massachusetts, USA
Helios Gamma Spectrophotometer	Thermo Fisher Scientific, Waltham, Massachusetts, USA
Incubator	BINDER GmbH, Tuttlingen, Germany
Karl-Fischer-Coulometer KF 831	Metrohm GmbH & Co, Filderstadt, Germany
Micro-Centrifuge Galaxy 14 D, max. 13 000 rpm or 14 000 x g	VWR International GmbH, Ismaning, Germany
Micro-Centrifuge Sprout, 2000 x g	Kisker Biotech GmbH & Co. KG, Steinbach, Germany
Microscope Axiovert 40C	Carl Zeiss AG, Oberkochen, Germany
Mini-Shaker PSU-2T	Biosan, Riga, Latvia
Mini-vortexer, Vortex V-1 plus	Kisker Biotech GmbH & Co. KG, Steinbach, Germany
Multiflow pump	Stöckert Instrumente, Munich, Germany
Nanophotometer 7122 V2.3.1	Implen GmbH, Munich, Germany
Neubauer counting chamber	Glaswarenfabrik Karl Hecht GmbH & Co K, Sondheim/Rhön, Germany
NovaFlow c Ultrasonic Flowcomputer	Novalung GmbH, Heilbronn, Germany
SevenEasy pH-Meter	Mettler-Toledo, Columbus, Ohio, USA
Sterile bench	Kojair, Vilppula, Finland
Thermo-Shaker	Kisker Biotech GmbH & Co. KG, Steinbach, Germany
Vakuum oven	Yamato Scientific Co., Ltd., Tokyo, Japan

Name	Reference
Water bath	Memmert GmbH + Co.KG, Schwabach, Germany

Table 4-2. Biomolecules and amino acids

Name	Reference
Alanine, L- (EP, USP)	AppliChem GmbH, Darmstadt, Germany
Anti-Adiponectin/Acpr30, 0.2 mg/ml in PBS (binds polyclonal to aa 19-244)	R&D Systems, Minneapolis, Minnesota, USA
APO010, 490 µg/ml in PBS, Active Pharmaceutical Ingredient	Oncology Venture, Hoersholm, Denmark
Arginine, L- (USP)	Carl Roth GmbH & Co.KG, Karlsruhe, Germany
Aspartic acid, L- (EP)	Carl Roth GmbH & Co.KG, Karlsruhe, Germany
Bovine Serum Albumin (BSA)	Sigma-Aldrich, St. Louis, Missouri, USA
Fas-Fc, lyophilized (extracellular part of Fas receptor fused to an Fc-domain)	kindly provided by Prof. Martin Zörnig, Georg-Speyer-Haus, Frankfurt, Germany
Glutamic acid, L- (EP)	Carl Roth GmbH & Co.KG, Karlsruhe, Germany
Glycine (EP, USP, JP)	Carl Roth GmbH & Co.KG, Karlsruhe, Germany
Glycyl-L-glutamine monohydrate (≥ 97 % HPLC)	Sigma-Aldrich, St. Louis, Missouri, USA
Glycyl-L-tyrosine (≥ 98 %)	Sigma-Aldrich, St. Louis, Missouri, USA
Histidine, L- (EP)	Carl Roth GmbH & Co.KG, Karlsruhe, Germany
Isoleucine, L- (USP)	Carl Roth GmbH & Co.KG, Karlsruhe, Germany
Leucine, L- (≥ 98 % HPLC)	Sigma-Aldrich, St. Louis, Missouri, USA
Lysine acetate salt (USP)	Sigma-Aldrich, St. Louis, Missouri, USA
Lysine, L-, HCl (EP, USP, JP)	Carl Roth GmbH & Co.KG, Karlsruhe, Germany
Methionine, L- (≥ 99 %)	Sigma-Aldrich, St. Louis, Missouri, USA
Phenylalanine, L- (EP)	Carl Roth GmbH & Co.KG, Karlsruhe, Germany
Proline, L- (EP)	Carl Roth GmbH & Co.KG, Karlsruhe, Germany
Recombumin Alpha 10% (albumin)	Novozymes A/S, Bagsværd, Denmark
rhIL-8 recombinant human	R&D Systems, Minneapolis, USA
Serine, L- (EP)	Carl Roth GmbH & Co.KG, Karlsruhe, Germany
Sodium-Heparin, 250000 IU	Rathiopharm, Ulm, Germany
Streptavidin conjugated to horseradish peroxidase (Streptavidin-HRP)	R&D Systems, Minneapolis, Minnesota, USA
Threonine, L- (EP)	Carl Roth GmbH & Co.KG, Karlsruhe, Germany

Name	Reference
Tryptophan, L- (EP)	Carl Roth GmbH & Co.KG, Karlsruhe, Germany
Valine, L- (USP)	Carl Roth GmbH & Co.KG, Karlsruhe, Germany

Table 4-3. Materials

Name	Reference
Aqua B. Braun, purging solution, sterile and pyrogen-free = H2O	B. Braun Melsungen AG, Melsungen, Germany
DuPont™ Tyvek® Steriking® Bags	Wipak Oy, Nastola Plant, Nastola, Finland
EDC (1-ethyl-3-(3-dimethylaminopropyl)carbodiimide hydrochloride)	Thermo Fisher Scientific, Waltham, Massachusetts, USA
Ethanol, 70 %	Carl Roth GmbH & Co.KG, Karlsruhe, Germany
Hydranal Coulomat AD	Sigma-Aldrich, St. Louis, Missouri, USA
Hydranal Water Standard KF-Oven	Sigma-Aldrich, St. Louis, Missouri, USA
Oxygenator	Novalung GmbH, Heilbronn, Germany
OXYPLUS®, Polymethylpentene (PMP) hollow fibers for gas exchange	Membrana, Wuppertal, Germany
PBS w/o Mg^{2+}/ Ca^{2+}	Biochrom GmbH, Berlin, Germany
Polysorbate 20	Carl Roth GmbH & Co.KG, Karlsruhe, Germany
Skim milk powder	Sigma-Aldrich, St. Louis, Missouri, USA
Sulfo-NHS (N-hydroxysulfosuccinimide)	Thermo Fisher Scientific, Waltham, Massachusetts, USA
Sulfuric acid (H2SO4), 96%	Sigma-Aldrich, St. Louis, Missouri, USA
TMB (3,3',5,5'-Tetramethylbenzidine)	Invitrogen, Carlsbad, California, USA
Trehalose Dihydrate (USP/NF, EP, JP)	Pfanstiehl, INC., Waukegan, Illinois, USA
Trypanblue, 0.4 %	Sigma-Aldrich, St. Louis, Missouri, USA

Table 4-4. Media and solution

Name	Reference
Fetal bovine serum (FBS) Superior	Biochrom GmbH, Berlin, Germany
L-Alanyl-L-Glutamine, 200 mM	Biochrom GmbH, Berlin, Germany
RPMI 1640 Medium w/ 20 mM HEPES, w/o NaHCO3, w/o L-Glutamine	Biochrom GmbH, Berlin, Germany

Table 4-5. Cell lines

Name	Cell type characteristics
Human blood	Different healthy donors

4.1.1   Isolation of neutrophils

Neutrophils were isolated as described in 2.1.2. Human blood was collected from healthy donors in neutral S-monovettes (Sarstedt) spiked with 5 U/ml Na-Heparin.

Cell culture medium: RPMI 1640 Medium w/ 20 mM HEPES 1640, 10 % FBS,

2 mM L-Alanyl-L-Glutamine

4.1.2   Chemotaxis assay

The chemotaxis assay as described in 2.1.6 was modified in this chapter to investigate the impact of the anti-inflammatory coating in direct contact to the neutrophils. Therefore, the coated PMP slides were placed in the upper compartment as shown in Figure 4-1 and were fixed by silicone rings with a cut-out of 0.5 cm x 0.5 cm in the center.

Cell culture medium or cell culture medium with chemoattractant IL-8 (1 ml, 25 ng/ml) were added into the lower compartment of the chemotaxis chamber, then the coated PMP-slide was added to the upper compartment and fixed with a silicon ring and 500 µl of cell suspension (0.1×10^6 cells/ml) were layered on top. Then the samples were incubated for 1 h at 37 °C.

After incubation, the contents of the lower compartments were transferred to a FACS tube and 125 µl of the samples were measured with the BD Accuri C6 flow cytometer (BD Biosciences). The number of events in the previously determined gate was counted. A vitality test was carried out before and after the chemotaxis incubation as described in 2.1.6. All samples were normalized to the untreated negative control for each group (with and without IL-8), respectively.
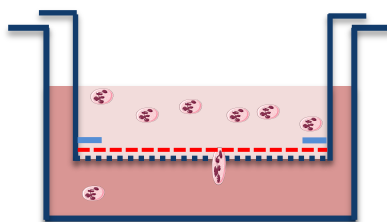
Figure 4-1. Schematic representation of the modified chemotaxis chamber.
The chamber is divided into two compartments: the upper compartment contains the neutrophil suspension and the coated PMP-slide (broken red line), which is fixed with a silicon ring (light blue lines at the edge of the upper compartment), the lower compartment contains cell culture medium (negative control) or cell culture medium with the chemoattractant IL-8. Between the two compartments there is a porous membrane with a pore size of 3 μm. The neutrophils can actively migrate through the pores and after 1 h incubation the neutrophil suspension in the lower compartment is analyzed by flow cytometry.

4.1.3 Anti-inflammatory coating

The coating of the anti-inflammatory coating is described in detail in 3.1.5 and was carried out as described there. In addition, the anti-inflammatory coating was upscaled to several medical devices.

4.1.3.1 The bench setting

The bench setting is described in 3.1.5.2.1.

4.1.3.2 The circuit setting

The circuit setting is adapted from one mat in a holder device as described in 3.1.5.2.2 to three mats in a holder device to simulate layers as in the medical device. Three mats were layered 90° to each other. The circuit setting was filled with 8 ml of each coating solutions as described below and incubated with a flow rate of 15.7 ml/min.

First, 8 ml EDC coating solution (0.5 mM in H_2O) was incubated with the PMP for 15 min and the setting was washed 1 min with H_2O. Second, 8 ml APO010 solution (20 ng/ml to 100 ng/ml in PBS) was added and incubated for 30 min. The solution was removed and the mat was washed 5 min with H_2O. Third, the reaction was quenched by adding 8 ml albumin (0.01 % in H_2O) for 15 min. The solution was removed and washed 15 min with H_2O. Afterwards, the mats were analyzed by ELISA.
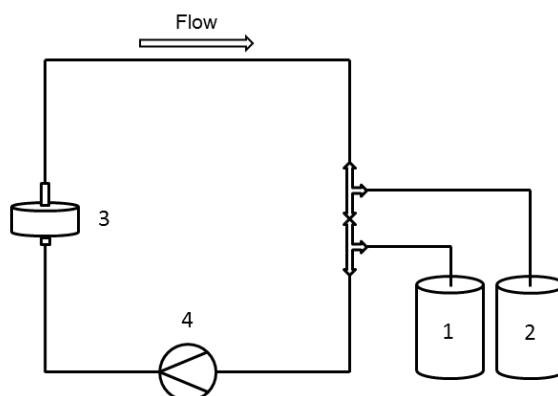
Figure 4-2. Schematic illustration of coupling approach in adapted circuit setting.
Three round PMP slides with 20 mm diameter were layered 90° to each other in the holder device (3) in the circuit. The circuit has a total volume of 8 ml (20 mm holder device) and the coating solution (1) is pumped through the circuit via a flexible-tube pump (Flexible-tube pump MCP, ISMATEC, Germany) (4) into a collecting container (2). Flow rate 15.7 ml/min.

4.1.3.3 The upscaling setting

In the upscaling setting, the coating procedure was optimized for one medical device in circuit as shown in Figure 4-3. 350 ml coating solution was used in this setting for all coating solutions.

First, 350 ml EDC coating solution (0.5 mM in H_2O) was incubated with the PMP for 15 min and the setting was washed with 350 ml H_2O. Second, 350 ml APO010 solution (20 ng/ml to 100 ng/ml in PBS) was added and incubated for 30 min. The solution was removed and the mat was washed with 1 l H_2O. Third, the reaction was quenched by adding 350 ml albumin (0.01 % in H_2O) for 15 min. The solution was removed and the setting was washed with 1 l H_2O. Afterwards, the samples were collected as described below.

For sample preparation, the medical device was opened and the samples were collected according to Figure 4-4. The 54 PMP mats contained in the device were cut out by a scalpel and were numbered from 1 to 54 in the direction of the initially flow direction. For sample preparation, three pieces (1.1 x 1.1 cm) of position A, B and C were cut out by a manual punch and were further analyzed by the different ELISAs.

A   **B**
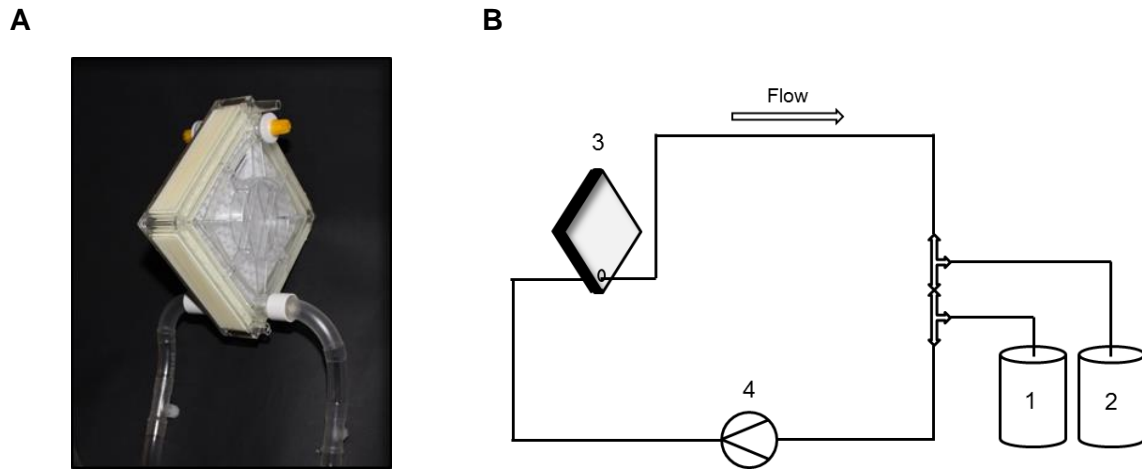
Figure 4-3. Image of the medical device and schematic illustration of the coupling approach in the upscaling setting.
A Image of the medical device without cover on the sides. The device consists of 54 PMP hollow fiber mats, whereby mat 1 is the first in flow direction. By filling the device, it is always filled from the bottom to the top. The Luer Lock ports (white with yellow caps) on the top on both sides enable the removal of air during coating and priming and can be used as pressure sensors. The 54 PMP mats are layered 90° to each other in the device, respectively. At the edge, the mats are fixed with PU (light yellow) to keep the mats in the middle of the device in the right position.
B The circuit has a total volume of 350 ml and the coating solution (1) is pumped through the medical device (3) via a flexible-tube pump (Multiflow pump, Stöckert Instruments, Germany) (4) into a collecting container (2). The medical device is filled from the bottom to the top by the port indicated by the circle. The medical device consists of 54 PMP mats, whereby mat 1 is the first in flow direction. Flow rate 0.5 – 1 l/min.
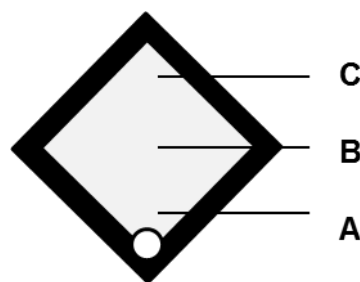
Figure 4-4. Illustration of the sample collection of the medical device from the top view.
As the medical device is filled from the bottom to the top by the port indicated by the circle, the PMP mats were numbered serially from 1 to 54, whereby mat 1 is the first in flow direction. For homogeneity coating studies, the PMP mat numbers **2, 10, 27, 44** and **54** were analyzed at **three different positions A, B** and **C**. The position **A** indicates the area on the mats, which was coated first, then the area which was coated second (position **B**) and third (position **C**). By analyzing these three positions and the different mat numbers in the device, it can be investigated, if the whole device is coated homogenously or not.

4.1.3.4 The upscaling to serial production scale

In the serial productions runs the anti-inflammatory coating was upscaled to several medical devices. The coating was performed as in the other settings, but here three different amino acid (aa)-based stabilization formulations were used as last protection layer during sterilization and storage as indicated in Table 4-6.

Table 4-6. AA-based stabilization formulations

AA-based stabilization formulations	Content
F1 (aa-based formulation with 7 aa), 20 g/l	Ala, Arg, Glu, Gly, His, Lys-HCl, Trp pH 6.5 in H_2O
F2 (aa-based formulation with 15 aa and 2 dipeptides), 30 g/l	Ala, Arg, Asp, Glu, His, Ile, Leu, Lys-Acetate, Met, N(2)-Gly-Gln, N(2)-Gly-L-Tyr, Phe, Pro, Ser, Thr, Trp, Val pH 6.5 in H_2O
F3 (aa-based formulation with 8 aa, one sugar and Polysorbate), 30 g/l	Arg, Asp, Glu, His, Lys-HCl, Ser, Thr, Trp, Trehalose, Polysorbate 20 pH 6.5 in H_2O

First serial production run

In the first serial production run, six medical devices were coated in line with a flow rate of 2 l/min (Figure 4-5), whereby the solution was pumped in circle after the whole setting was filled. The coating solutions were used in a total volume of 5.8 l. This correlates to a theoretical ratio of 1.79 ng/cm^2 APO010 per device. In Table 4-7 the separate steps of the coating are shown.
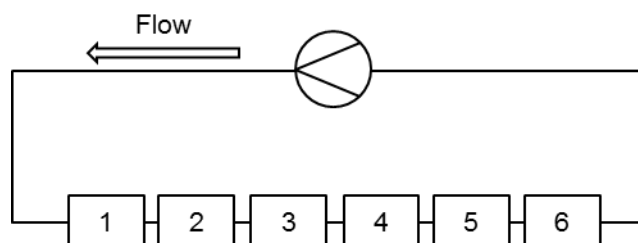
Figure 4-5. Schematic setting of the first serial production run.
In the first serial production run six medical devices were coated in a flow system, whereby no EtO treatment was performed.
Coating settings: 0.5 mM EDC, 20 ng/ml APO010, 0.01 % albumin, 20 g/l aa-based stabilization formulation F1, volume 5.8 l, flow rate 2 l/min. The flow rate was detected before #1 and #6. The pressure was detected before #1, #4 and after #6.

Table 4-7. Coating scheme of first serial production run

	Coating step / concentration	Time	Flow rate / pressure
1	Flushing with H_2O	5 min	2 l/min
2	Blowing out	20 sec	1 bar
3	EDC / 0.5 mM in H_2O (pH 5.0)	15 min	2 l/min
4	Flushing with H_2O	5 min	2 l/min
5	Blowing out	20 sec	1 bar
6	APO010 / 20 ng/ml in PBS (pH 7.2-7.5)	45 min	2 l/min
7	Flushing with H_2O	5 min	2 l/min
8	Blowing out	20 sec	1 bar
9	Albumin / 0.01% in H_2O (pH 4.5)	15 min	2 l/min
10	Flushing with H_2O	5 min	2 l/min
11	Blowing out	20 sec	1 bar
12	Stabilization formulation F1 / 20 g/l in H_2O (pH 6.5)	30 min	2 l/min
13	Blowing out	20 sec	1 bar
14	Drying 50 °C vacuum oven	o/n	vacuum

Second serial production run

In the second serial production run 1, 20 medical devices were coated in-line with APO010 (33.35 ng/ml), albumin and the aa-based stabilization formulation F2 (volume 6 l, flow rate 1.5 l/min) and in the second serial production run 2 another set of 20 medical devices was coated with APO010 (33.35 ng/ml), albumin and aa-based stabilization formulation F1 (volume 6 l, flow rate 1.5 l/min). The coating solutions were used in a total volume of 6 l. All solutions were pumped in circle after the whole setting was filled. The first flow direction was from left to right and was then changed every 5 min. The APO010 concentration used in these two runs correlates to a theoretical ratio of 0.925 ng/cm^2 APO010 per device.

In Table 4-8 separate steps of the coating are shown. After coating of medical devices 1 to 20 (stabilized with F2) and medical devices 21 to 40 (stabilized with F1) different steps were performed with the medical devices. Nine medical devices were directly investigated to test the coating, four medical devices were used for a bioburden test and 27 medical devices were EtO-treated (Table 4-9).

Second serial production run 1 with stabilization formulation F2:

Variation of flow direction every 5 min

Second serial production run 2 with stabilization formulation F1:

Variation of flow direction every 5 min
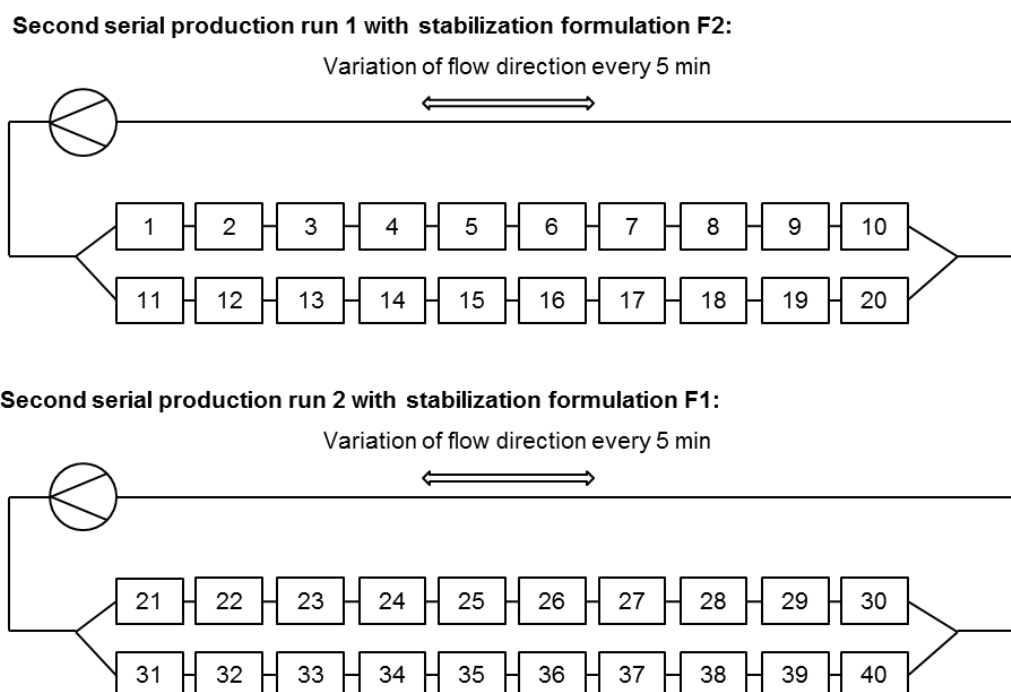
Figure 4-6. Schematic setting of the second serial production run 1 and 2.
In the **second serial production run 1** 20 medical devices were coated with APO010 (33.35 ng/ml), albumin and F2 (volume 6 l, flow rate 1.5 l/min) and in the **second serial production run 2** another set of 20 medical devices was coated with APO010 (33.35 ng/ml), albumin and F1 (volume 6 l, flow rate 1.5 l/min).
Coating settings: 0.5 mM EDC, 33.35 ng/ml APO010, 0.01 % albumin, 30 g/l F2 or F1, volume 6 l, flow rate 1.5 l/min. The flow rate was detected before #1/ #21 and #11/ #31. The pressure was detected before #1/ #21, #5/ #25 and after #10/ #30 (run 1 with F2/run 2 with F1). Afterwards, an EtO treatment and storage at different conditions were carried out.

Table 4-8. Coating scheme of second serial production run 1 and 2

	Coating step / concentration	Time	Flow rate / pressure
1	Flushing with H_2O	5 min	1.5 l/min
2	Blowing out	20 sec	1 bar
3	EDC / 0.5 mM in H_2O (pH 5.0)	15 min	1.5 l/min
4	Flushing with H_2O	5 min	1.5 l/min
5	Blowing out	20 sec	1 bar
6	APO010 / 33.35 ng/ml in PBS (pH 7.2-7.5)	45 min	1.5 l/min
7	Flushing with H_2O	5 min	1.5 l/min
8	Blowing out	20 sec	1 bar
9	Albumin / 0.01% in H_2O (pH 4.5)	15 min	1.5 l/min
10	Flushing with H_2O	5 min	1.5 l/min

	Coating step / concentration	Time	Flow rate / pressure
11	Blowing out	20 sec	1 bar
12	Stabilization formulation F1 or F2 / 30 g/l in H_2O (pH 6.5)	30 min	1.5 l/min
13	Blowing out	20 sec	1 bar
14	Drying 50 °C vacuum oven	o/n	vacuum

Table 4-9. Overview of workflow for the 2x 20 medical devices of the second serial production run 1 and 2

Number of 40			Position number	Analysis
9 of 40	**w/o EtO treatment**		# 21, 25, 30, 32, 35, 40 # 1, 15, 20	Coating efficacy assay
4 of 40	**w/o EtO treatment**		# 32, 33 # 12,13	Bioburden
27 of 40	**EtO treatment**		# 22, 23, 24, 26, 27, 28, 29, 34, 36, 37, 38, 39 # 2, 3, 4, 5, 6, 7, 8, 9, 10, 11, 14, 16, 17, 18, 19	
⌐→	*1 of 27*	*Priming test*	# 11	Coating efficacy assay detachment assay
⌐→	*2 of 27*	*Bioburden*	# 34 # 14	Bioburden

⌐→	*12 of 27*	*Storage for 20 days at different temperautres*	5°C: # 22, 39
			      # 2, 19
			RT: # 23, 38
			     # 3, 18
			55 °C: # 24, 37
			     # 4, 17
				Coating efficacy assay

⌐→	*12 of 27*	*Back-up*	# 26, 27, 28, 29, 36 # 5, 6, 7, 8, 9, 10, 16	Storage at RT

In the second serial production run 1 and 2 the stability testing of the medical devices were tested according to the norm for medical devices. Therefore, the stability testing was performed by accelerated aging until real-time aging studies are available. According to ISO 11607 the medical devices were packed in Tyvek® bags and sterilized as described in 4.1.4 [125]. The accelerated aging studies are based on the Arrhenius reaction rate function as described in the norm ASTM F 1980 [126]. By this theory an accelerated aging factor (AAF) can be calculated with an accelerated aging temperature (T_{AA}) of 55°C, a room temperature (T_{RT}) of 23°C, an aging factor (Q_{10}) of 2 which is most common.

This results in an accelerated aging time (AAT) of 20 days, which correspond to a 6 month real-time storage as depicted in the following equations (1-3):

$$AAF = Q_{10}^{[\frac{(T_{AA}-T_{RT})}{10}]} \tag{1}$$

$$AAF = 2^{[\frac{(55-23)}{10}]} = 9.19 \tag{2}$$

$$AAT = \frac{(30,4*6\ month)}{9.19} \equiv 19,8\ days \equiv 6\ month\ real-time\ storage \tag{3}$$

Third serial production run

In the third serial production run, 22 medical devices were coated with APO010 (35 ng/ml), albumin and F3 (volume 6 l, flow rate 1.5 l/min) in a circuit setting as shown in Figure 4-7. The coating solutions were used in a total volume of 6 l. All solutions were pumped in circle after the whole setting was filled. This correlates to a ratio of 0.885 ng/cm^2 APO010 per device.

As described above the medical devices were packed, sterilized and the accelerated aging protocol was designed according the ISO 11607 and ASTM F 1980 [125, 126]. By this theory an accelerated aging factor (AAF) can be calculated with an accelerated aging temperature (T$_{AA}$) of 55°C, a room temperature (T$_{RT}$) of 23°C, an aging factor (Q$_{10}$) of 2 which is most common. This results in an accelerated aging time (AAT) of 80 days, which correspond to a 2 year real-time storage as depicted in the following equations (1-3):

$$AAF = Q_{10}^{[\frac{(T_{AA}-T_{RT})}{10}]} \tag{1}$$

$$AAF = 2^{[\frac{(55-23)}{10}]} = 9.19 \tag{2}$$

$$AAT = \frac{365\ days}{9.19} \equiv 39.7 days \equiv 12\ month\ real-time\ storage \tag{3}$$
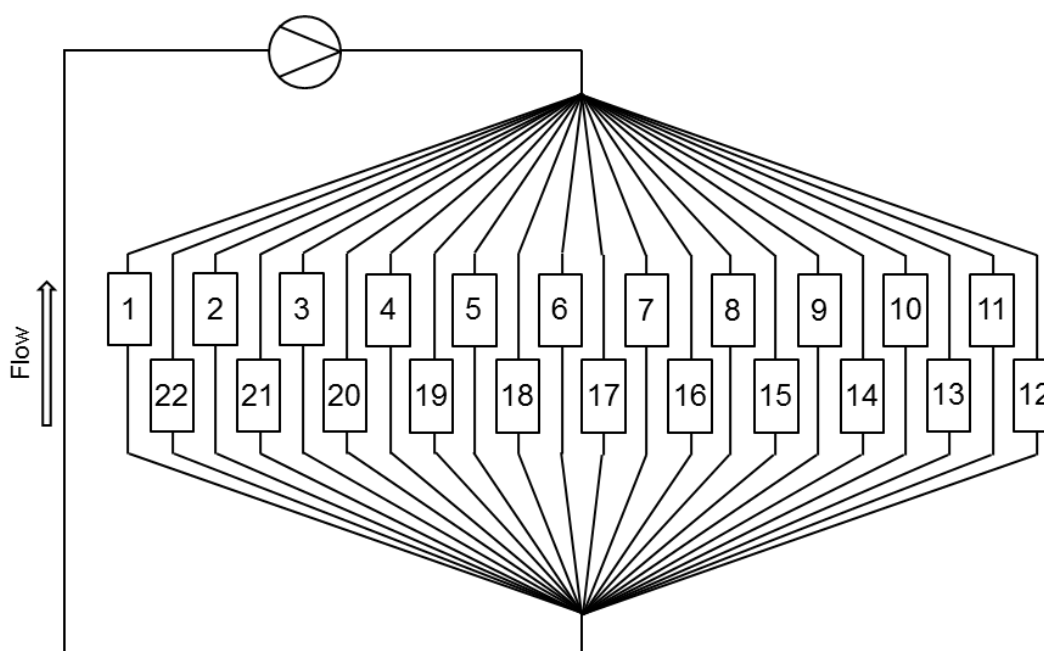
Figure 4-7. Schematic setting of the third serial production run in a circle setting.
In the third test run 22 medical devices were coated with APO010 (35 ng/ml), albumin and aa-based stabilization formulation F3 (volume 6 l, flow rate 0.2-0.3 l/min). The flow rate was detected after #5. The pressure was detected after #5 and #6. Afterwards, an EtO treatment and storage at different conditions were performed.

Table 4-10. Coating scheme of third serial production run

	Coating step / concentration	Time	Flow rate / pressure
1	Flushing with H_2O	5 min	0.2- 0.3 l/min
2	Blowing out	5 min	1 bar
3	EDC / 0.5 mM in H_2O (pH 5.0)	15 min	0.2- 0.3 l/min
4	Flushing with H_2O	5 min	0.2- 0.3 l/min
5	Blowing out	5 min	1 bar
6	APO010 / 35 ng/ml in PBS (pH 7.2-7.5)	45 min	0.2- 0.3 l/min
7	Flushing with H_2O	5 min	0.2- 0.3 l/min
8	Blowing out	5 min	1 bar
9	Albumin / 0.01% in H_2O (pH 4.5)	15 min	0.2- 0.3 l/min
10	Flushing with H_2O	5 min	0.2- 0.3 l/min
11	Blowing out	5 min	1 bar
12	Stabilization formulation F3 / 30 g/l in H_2O (pH 6.5)	30 min	0.2- 0.3 l/min
13	Blowing out	5 min	1 bar
14	Drying 50 °C vacuum oven	o/n	vacuum

Table 4-11. Overview of workflow for the 22 medical devices of the third serial production run

Number of 22			Position number	Analysis
4 of 22	**w/o EtO treatment**		# 1, 2, 3, 4	Coating efficacy assay
18 of 22	EtO treatment		# 5-22	
⌐→	*15 of 18*	*Storage and accelerated aging*	20 d, RT: # 5, 6, 7 20 d, 55 °C: # 14, 15, 16 50 d, 55 °C: # 17, 18, 19 80 d, 55 °C: # 20, 21, 22	Coating efficacy assay
⌐→	*3 of 18*	*Coating distribution*	# 11, 12, 13	Coating efficacy assay
⌐→	*3 of 18*	*Back-up*	# 8, 9, 10	Storage at RT

4.1.4   EtO Sterilization

An EtO sterilization process was carried out from an external service provider (Rose GmbH, Tier) with selected medical devices after coating and drying of the anti-inflammatory coating. The devices were treated with EtO in the cycle B 01 according to DIN EN ISO 11135-1:2007. The main conditions of EtO treatment for medical devices were as followed: pre-conditioning (10 – 48 h, 45 °C – 53 °C, 45 % – 80 % relative humidity), sterilization (100 vol% EtO for 4 – 5 h, 45 °C – 53 °C, and several flushing cycles), and post-conditioning (22 – 54 h, 45 °C – 53 °C, and >7-fold/h air change).

4.1.5   Read-out for monitoring coating efficacy

The coating efficacy assay, previously called non-functional ELISA, is carried out in this chapter to monitor the coating efficacy and the homogenous distribution of the coating. The coating efficacy assay is described in 3.1.8.

4.1.6   Functional Enzyme-linked Immunosorbent Assay (ELISA)

The functional ELISA is carried out in this chapter to investigate the functional coupling of APO010 and is described in 3.1.7.

4.1.7   Detachment assay

The detachment ELISA is carried out in this chapter to investigate the stability of the coating and is described in 3.1.9.

4.1.8 Residual moisture

The residual moisture was measured by Karl-Fischer-titration using an 831 KF Coulometer and an 832 KF Thermoprep by Metrohm. The assay was done with HYDRANAL®-Coulomat AD and HYDRANAL®-Water Standard KF-Oven at 140°C to 160°C. The residual moisture from the water standard was extracted at 160°C. The moisture content of the 1.1 x 1.1 cm PMP mats was extracted at 120°C. Therefore, approximately 150 mg of each sample was weighed into 6R glass vials.

4.2 Results

This section describes the upscaling of the anti-inflammatory coating to a serial production scale. Several intermediate steps were included, whereby the bench setting was transferred to the circuit setting. The circuit setting was transferred to the coating of one medical device called upscaling setting here and this was transferred to the coating of 6, then 20 and then 22 medical devices.

4.2.1 Transfer of the bench setting to circuit setting

The transfer of the coating protocol in the bench setting to circuit setting was a crucial step in the upscaling process. In this step, the settings were performed parallel to each other and were compared with two analytical methods to evaluate the coating process: the functional ELISA and the non-functional ELISA. The functional ELISA was used to detect the functional FasL domain of the APO010 and thereby to detect the amount of functional coupled APO010. The non-functional ELISA was used to detect the amount of coupled APO010 via the Adiponectin domain of APO010.

In the circuit setting, different APO010 concentration were investigate in order to test, which is the lowest detectable APO010 concentration in both ELISAs. We aimed at a preferably low APO010 concentration, because it is known from chapter 2 that only 2 ng/ml APO010 results in high activity in the apoptosis assay. When APO010 is coated to PMP, APO010 concentrations from 20 to 1000 ng/ml were used in chapter 3.

In this chapter, APO010 concentrations of 20 ng/ml, 50 ng/ml, 75 ng/ml and 100 ng/ml shall be tested. The results of these investigations are presented in Figure 4-8. It is shown that the approaches of the bench and the circuit setting can be distinguished from the negative controls (nc) **F** (functional (f) = 0.18 ± 0.07 RU, non-functional (nf) = 0.10 ± 0.03 RU) and **G** (f = 0.11 ± 0.03 RU; = 0.12 ± 0.01 RU).
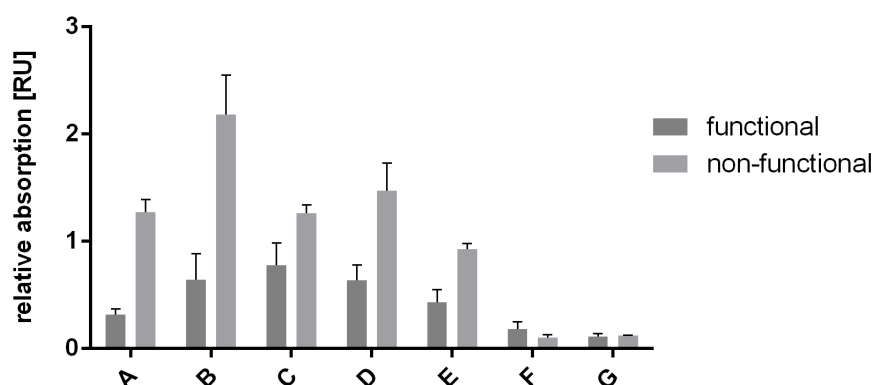
Approach	setting	Coating steps	ng APO010/cm^2
A	Bench setting	V = 0.6 ml, 0.5 mM EDC 15 min, 100 ng/ml APO010 30 min, 0.01 % albumin 15 min	8.3 ng/cm^2
B	Circuit setting	V = 8 ml, 0.5 mM EDC 15 min, 100 ng/ml APO010 30 min, 0.01 % albumin 15 min	42.5 ng/cm^2
C	Circuit setting	V = 8 ml, 0.5 mM EDC 15 min, 75 ng/ml APO010 30 min, 0.01 % albumin 15 min	31.85 ng/cm^2
D	Circuit setting	V = 8 ml, 0.5 mM EDC 15 min, 50 ng/ml APO010 30 min, 0.01 % albumin 15 min	21.2 ng/cm^2
E	Circuit setting	V = 8 ml, 0.5 mM EDC 15 min, 20 ng/ml APO010 30 min, 0.01 % albumin, 15 min	8.5 ng/cm^2
F	Bench setting	V = 0.6 ml, 0.5 mM EDC 15 min, PBS 30 min 0.01 % albumin 15 min	0 ng/cm^2
G	Non coated	-	0 ng/cm^2

Figure 4-8. Schematic illustration of different settings analyzed by functional and non-functional ELISA.
APO010 was coupled via EDC (0.5 mM) to PMP in the bench setting and circuit setting with different concentrations of APO010 (20 to 100 ng/ml). The reaction was quenched with 0.1 % albumin. The coating success was analyzed via the functional and non-functional ELISA. The bench setting has a coating volume of 0.6 ml, whereby the circuit setting has a volume of 8 ml. This results in a different APO010 to area relation. The column chart shows the relative absorbance $_{450\text{-}550 \text{ nm}}$ in relative units [RU], whereby the relative absorbance is proportional to the amount of bound APO010 (Mean ± SD from n=3).

The relative absorption signals of the bench setting **A** (f = 0.31 ± 0.06 RU, nf= 1.27 ± 0.11 RU) were lower than those of the circuit setting **B** (f = 0, 64 ± 0.24, nf = 2.18 ± 0.36 RU), which corresponds to the lower APO010 amount per area of PMP (8.3 ng/cm^2 compared to 42.5 ng/cm^2, (Figure 4-8)). In the dilution series of the circuit setting from **B** to **E** (100 ng/ml to 20 ng/ml), there was a deviation in batch **C** where the non-functional signal (nf = 1.26 ± 0.08 RU) was identical to **D** (nf = 1.47 ± 0.26 RU). At the same time, the functional signal of approach **B** (f = 0.64 ± 0.24 RU) was identical to **C** (f = 0.78 ± 0.21 RU) and **D** (f = 0.64 ± 0.14 RU). The approaches **C** and **D** do not differ strongly in the APO010 amount 31.9 ng/cm^2 and 21.2 ng/cm^2. The signal of **E** (f = 0.43 ± 0.12, nf = 0.93 ± 0.05 RU) with the lowest APO010 amount of 8.5 ng/cm^2 was comparable with the bench setting approach **A**, where 8.3 ng/cm^2 was used. Therefore, a range between 20 ng/ml and 50 ng/ml APO010 in the coating solution seems ideal for further upscaling. A higher concentration of 100 ng/ml APO010 delivers no benefit in the functional ELISA. However, the functional relevance of the whole coating has to be tested later on the end setting.

In a second step, the EDC step was varied. Sulfo-NHS can be added to EDC during crosslinking to stabilize the instable intermediate. In the previous experiments no Sulfo-NHS was added to the EDC crosslinker. To test if the crosslinking process is improved, Sulfo-NHS was mixed to EDC in a ratio of 2.5:1 in the next experiment.

Different crosslinking solutions were tested in the circuit setting (Figure 4-9): The approach **A** with 0.5 mM EDC / 1.25 mM Sulfo-NHS crosslinking solution shows the highest non-functional signal (nf = 1.19 ± 0.10 RU), whereby the functional signal (f = 0.37 ± 0.08 RU) was comparable to approach **C** with 1 mM EDC crosslinking solution (f = 0.40 ± 0.11 RU). The non-functional signal of the coating with 1 mM EDC crosslinking solution (nf = 0.87 ± 0.12 RU) was comparable to the coating with 0.5 mM EDC crosslinking solution (nf = 0.92 ± 0.03 RU), whereby the functional signal of **B** was lower (f = 0.21 ± 0.03 RU). The negative control signals **D** (nf = 0.04 ± 0.00 RU; f = 0.06 ± 0.01 RU) and **E** (nf = 0.06 ± 0.05 RU; f = 0.05 ± 0.01 RU) differed only slightly from 0 and were thus significantly lower than that of the coatings. Due to the slight differences in the results with or without Sulfo-NHS, the protocol was not changed in the following.
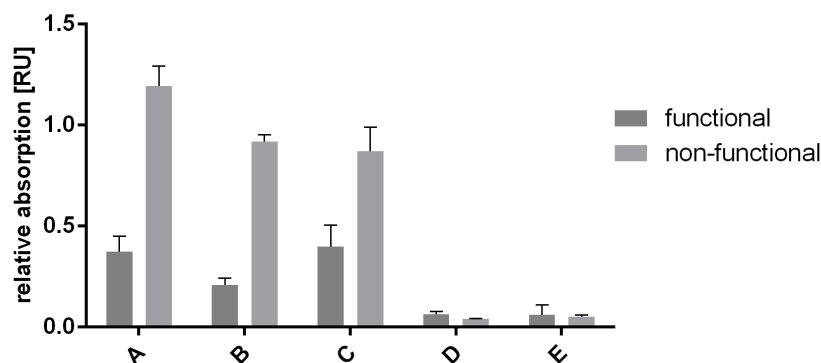
Approach	setting	Coating steps	ng APO010/cm^2
A	Circuit setting	V = 8 ml, 0.5 mM EDC + 1,25 mM Sulfo NHS 15 min, 50 ng/ml APO010 30 min, 0.01 % albumin 15 min	21.2 ng/cm^2
B	Circuit setting	V = 8 ml, 0.5 mM EDC 15 min, 50 ng/ml APO010 30 min, 0.01 % albumin 15 min	21.2 ng/cm^2
C	Circuit setting	V = 8 ml, 1 mM EDC 15 min, 50 ng/ml APO010 30 min, 0.01 % albumin 15 min	21.2 ng/cm^2
D	Circuit setting	V = 8 ml, 1 mM EDC 15 min, PBS 30 min, 0.01 % albumin 15 min	0 ng/cm^2
E	Non coated	-	0 ng/cm^2

Figure 4-9. Circuit settings with different coating procedures analyzed by functional and non-functional ELISA.
APO010 was coupled (50 ng/ml) via EDC (0.5 mM or 1 mM w/ or w/o 1.25 mM Sulfo-NHS) to PMP in the circuit setting. The reaction was quenched with 0.1 % albumin. The coating success was analyzed via the functional and non-functional ELISA. The circuit setting has a volume of 8 ml. This results to an APO010 to area relation of 21.2 ng/cm^2. The column chart shows the relative absorbance $_{450-550\,nm}$ in relative units [RU], whereby the relative absorbance is proportional to the amount of bound APO010 (Mean ± SD from n=3).

In the third step, the incubation time of APO010 was optimized. Therefore, the circuit setting was tested with 30, 45, 60 and 75 min APO010 incubation and compared by the functional and non-functional ELISA (Figure 4-10).
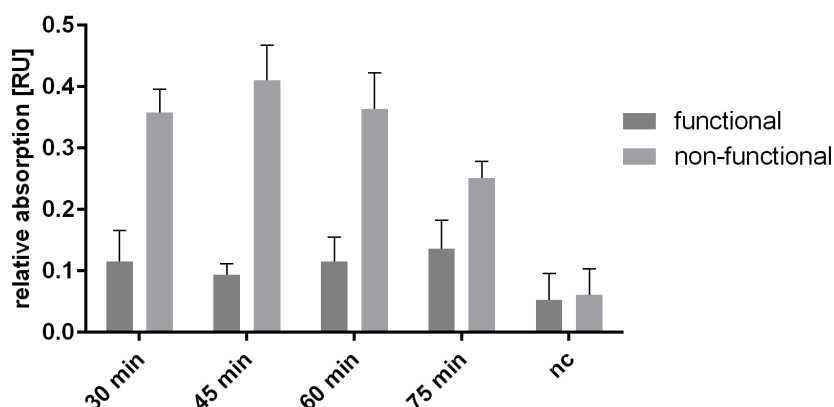
setting	Coating steps	ng APO010/cm^2
Circuit setting	V = 8 ml, 0.5 mM EDC 15 min, 20 ng/ml APO010 different incubation times (30, 45, 60, 75 min), 0.01 % albumin 15 min	8.5 ng/cm^2

Figure 4-10. Schematic illustration of different incubation times for APO010 in circuit setting.
APO010 was coupled (20 ng/ml) via EDC (0.5 mM) to PMP in the circuit setting with different incubation times (30, 45, 60, 75 min). The reaction was quenched with 0.1 % albumin. The coating success was analyzed via the functional and non-functional ELISA. The circuit setting has a volume of 8 ml. This results to an APO010 to area relation of 8.5 ng/cm^2. The column chart shows the relative absorbance $_{450-550 \, nm}$ in relative units [RU], whereby the relative absorbance is proportional to the amount of bound APO010 (Mean ± SD from n=3).

An incubation time for APO010 of 45 min indicates the highest non-functional signal (nf = 0.43 ± 0.06 RU). However, statistically, the non-functional signals of the batches with 30 min (nf = 0.37 ± 0.04 RU) and 60 min (nf = 0.38 ± 0.06 RU) incubation time are equal. In this experiment, the low APO010 concentration of 20 ng/ml results in low functional signals of all approaches, which cannot distinguished from the signals of negative control (f = 0.06 ± 0.04 RU).

In summary, the experiments indicate to use the following upscaling parameters: a range between 20 ng/ml and 50 ng/ml APO010 and an incubation time of 45 min. In addition, 0.5 mM EDC without the usage of Sulfo-NHS results in good non-functional ELISA results.

The functional ELISA results deliver too low absorption signals when 20 ng/ml APO010 was used for coating.

The coupling efficacy of APO010 to the PMP mats is very important due to the high costs of APO010. Therefore, it was investigated indirectly via the detachment assay how much APO010 is in the solution before and after the coating process. In addition, it was tested if there is any APO010 left in the washing solutions. Figure 4-11 shows that the APO010 concentration is 16.2 ng/ml APO010 before the coating and 2.0 ng/ml after the coating in the solution. This means that only 12.42 % did not bind to the PMP mats. In the washing solutions 1 to 5 no APO010 could be detected.
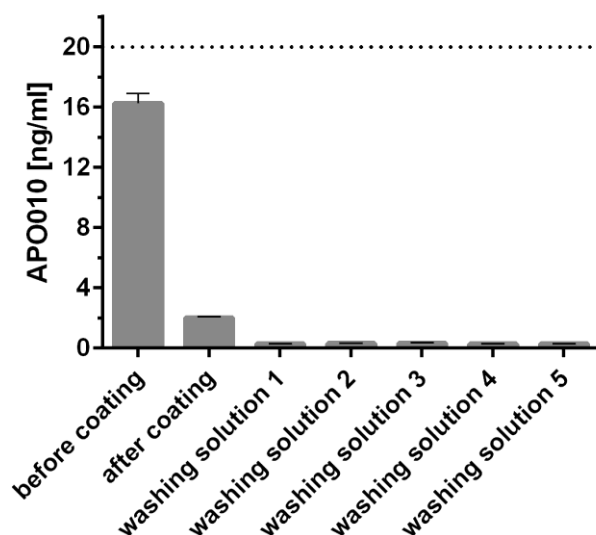
Figure 4-11. Results of the coating efficiency of APO010 before and after the coating.
The anti-inflammatory coating was carried out with the bench setting and an APO010 concentration of 20 ng/ml. After the incubation of APO010 with the PMP mats the mats were washed five times with H_2O (washing solution 1 to 5). Each solution was detected with the detachment assay. The column chart shows the amount of bound APO010 [ng/ml] (Mean ± SD from n=3).

4.2.2 Transfer from the circuit setting to the upscaling setting

For the transfer of the circuit setting to the medical devices, in the first experiment one medical device was coated with a volume flow of 0.5 l/min to test the feasibility of the coating in the flow. The flow rate corresponds to the used flow rate in the circuit setting. Then, the device was opened and tested at different mat positions in the device as described in 4.1.3.3. The non-functional absorption signals of the analyzed samples of mat 2, 10, 27, 44 and 54 of position A, B and C are shown in Figure 4-12 A. The mean value indicates a homogeneity of

the coating by low standard deviation (nf = 0.32 ± 0.07 RU) and differs from the negative control signal (nf = 0.07 ± 0.02 RU). With regard to the homogeneity, there was no trend between the different positions on the individual mats. The coating was equally distributed to the mats.

The total PMP mat area per device is approximately 10 800 cm^2, which results in a ratio of 0.65 ng/cm^2 APO010 per area. In these experiments a higher APO010 amount was not possible to use due to availability.

Due to the low absorption signals after coating with the flow rate of 0.5 l/min, it was tested, if a higher flow rate can increase this signal. In a second experiment, two devices were coated with a volume flow of 1 l/min, whereby one was tested directly after the coating and drying, the other was sterilized by EtO after it was packed in a Tvyek-bag. To stabilize the coating during this process, the devices were coated with an aa-based formulation 20 g/l F1 after the albumin treatment for 30 min and were dried without a washing process to deposit the protective formulation on the coating. The aa formulation with seven amino acids was used in this first experiment expecting good stabilization effect as known by literature [55, 124].

For the device, which was tested after coating and drying, the non-functional absorption signals of the analyzed samples of mat 2, 10, 27, 44 and 54 of position A, B and C (prepared according to Figure 4-4) are shown in Figure 4-12 B. The mean value indicates a homogeneity of the coating by low standard deviation (nf = 0.60 ± 0.05 RU) and differs from the negative control signal (nf = 0.10 ± 0.06 RU). With regard to the homogeneity, there was no trend between the different positions on the individual mats. The coating was equal distributed to the mats. By doubling the flow rate from 0.5 l/min to 1 l/min, the absorption signal is doubled as well.

In order to test whether the sterilization with EtO has an influence on the homogeneity of the coating, a second device was tested as described above. Figure 4-12 C shows the results of the device. The mean value indicates a homogeneity of the coating by low standard deviation (nf = 0.24 ± 0.05 RU) and differs from the negative control signal (nf = 0.04 ± 0.02 RU). With regard to the homogeneity, there was no trend between the different positions on the individual mats. The coating was equal distributed to the mats, but compared to the device before EtO treatment, the absolute amount of APO010 was 2.5 fold lower after EtO sterilization. This means, the coating could not be fully protected by the stabilization formulation.
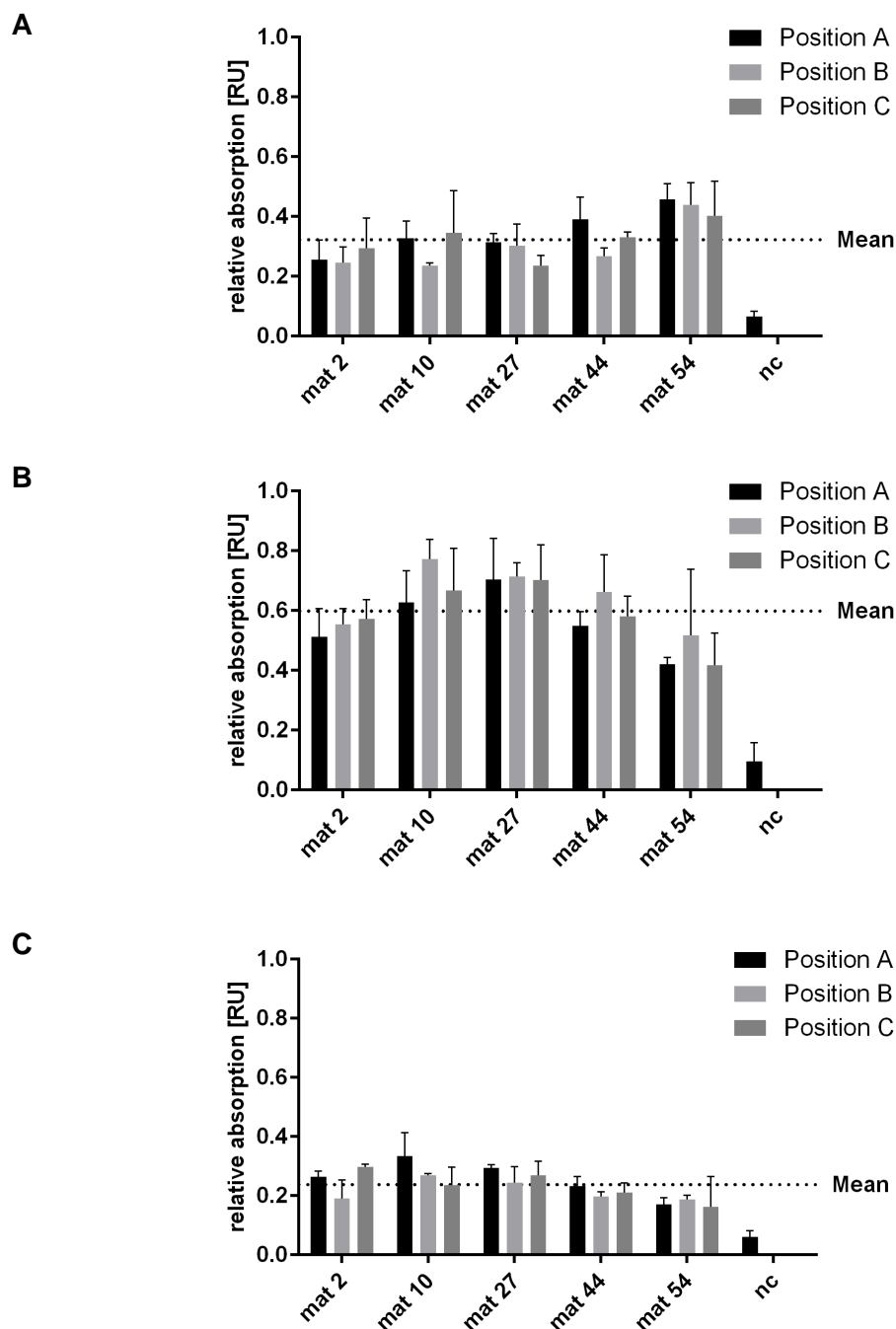
Figure 4-12. One medical device coated by the upscaling setting and analyzed by non-functional ELISA.

APO010 was coupled (20 ng/ml, 45 min) via EDC (0.5 mM, 15 min) to PMP in the upscaling setting with a flow rate of 0.5 l/min **(A)** or 1 l/min **(B, C)** which changed every 5 min. The reaction was quenched with 0.1 % albumin (15 min). 20 g/l stabilization formulation F1 was added on top of the coating for stabilization (30 min). In **C** the medical device was EtO sterilized after coating.

The coating success was analyzed via the non-functional ELISA. The column chart shows the relative absorbance $_{450-550\ nm}$ in relative units [RU], whereby the relative absorbance is proportional to the amount of bound APO010 (Mean ± SD from n=3), nc = negative control (no APO010 was coated).

4.2.3   The serial production scale

The goal of these experimental series was to transfer the coupling protocol into a serial production scale.

In a first step, the development of a routine assay to monitor the quality of the anti-inflammatory coating during serial production was necessary.

In the second step, the adaptation of the lab-scale coating procedure to the serial production procedure had to be done. A homogenous distribution of covalently coupled APO010 within each device and in different devices after serial production had to be confirmed.

Two main questions were addressed in general: Was the coating procedure efficient and is the coating stable and functional after sterilization and storage. For the monitoring of the first issue, the "coating efficacy assay" was performed. This assay is the previously described non-functional ELISA, which detects the Adiponectin domain on APO010. An additional functional assay for the quantification of the neutrophil activity was used (chemotaxis assay).

For the monitoring of the second issue, the "detachment assay" was performed. This assay is based on a sandwich-ELISA, which was previously described. It is highly sensitive in the detection of detached APO010 molecules in the washing solutions.

The overall goal is to confirm that even after prolonged storage there is no specific signal above the assay cut-off. In Figure 4-13 a workflow of the quality control (QC) assays is shown.
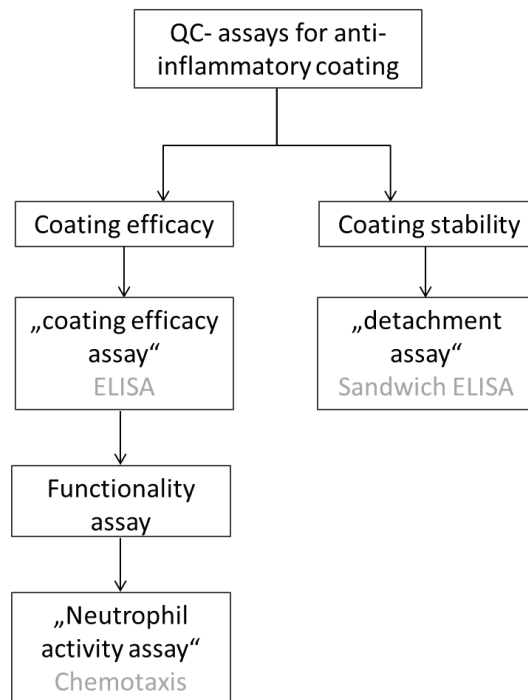
Figure 4-13. Schematic workflow of the QC assays after serial coating.

Three serial production runs were performed in order to generate a homogenous upscaling protocol. An overview of these runs is depicted in Table 4-12. In a first production test run the anti-inflammatory coating protocol, which was established in the bench and circuit setting, was transferred to the serial production scale. In this run, six medical devices were coated in line. In the second serial production run 2x 20 medical devices were coated in a similar setting as the first production run. The stabilization formulation F2 and F1 were compared with each other in this run. In the third production test run 22 medical devices were coated in a circle for better distribution of the coating solutions.

Table 4-12. Overview of the three serial production runs

Serial production run	Description
First serial production run	6 medical devices (in-line) **1.79 ng/cm^2 APO010 per Device** Coating solutions: APO010 20 ng/ml, albumin, stabilization formulation F1 Volume 5.8 l Flow rate 2 l/min
Second serial production run 1	20 medical devices (2x10 in-line) **0.925 ng/cm^2 APO010 per Device** Coating solutions: APO010 (33.35 ng/ml), albumin and stabilization formulation F2 Volume 6 l Flow rate 1.5 l/min
Second serial production run 2	20 medical devices (2x10 in-line) **0.925 ng/cm^2 APO010 per Device** Coating solutions: APO010 (33.35 ng/ml), albumin and stabilization formulation F1 Volume 6 l Flow rate 1.5 l/min
Third serial production run	22 medical devices (in circle) **0.885 ng/cm^2 APO010 per Device** Coating solutions: APO010 (35 ng/ml), albumin and stabilization formulation F3 Volume 6 l Flow rate 0.2-0.3 l/min

For composition of formulation F1, F2 and, F3 see Table 4-6.

4.2.3.1 The first serial production run

The first serial production run was carried out with six medical devices in-line, whereby positon #1, #3 and #6 were investigated further by the coating efficacy assay. The medical devices #2, #4 and #5 were tested externally specifically for their gas exchange quality. The gas exchange showed no anomalies, which means that the anti-inflammatory coating did not change the functionality of the gas exchanger (data not shown).

The results of the coating efficacy assay are shown in Figure 4-14 B. In each medical device, there is a homogenous coating distribution from mat 2 to mat 54, respectively. But from medical device #1 to #3 and from #3 to #6 there is a reduction of APO010 coating by approximately 20 %. The cut off of the ELISA was defined as 0.1 relative absorbance units (RU) due to unspecific signal on negative controls < 0.1 RU. The relative absorbance is an indirect measure for the amount of coupled APO010 on PMP. The goal to reach a homogenous distribution from medical device #1 to #6 was not fulfilled with this setting. Therefore, a second serial production had to be done in a modified setting. The amount of devices was increased in the setting to have more medical devices to analyze.

A

B
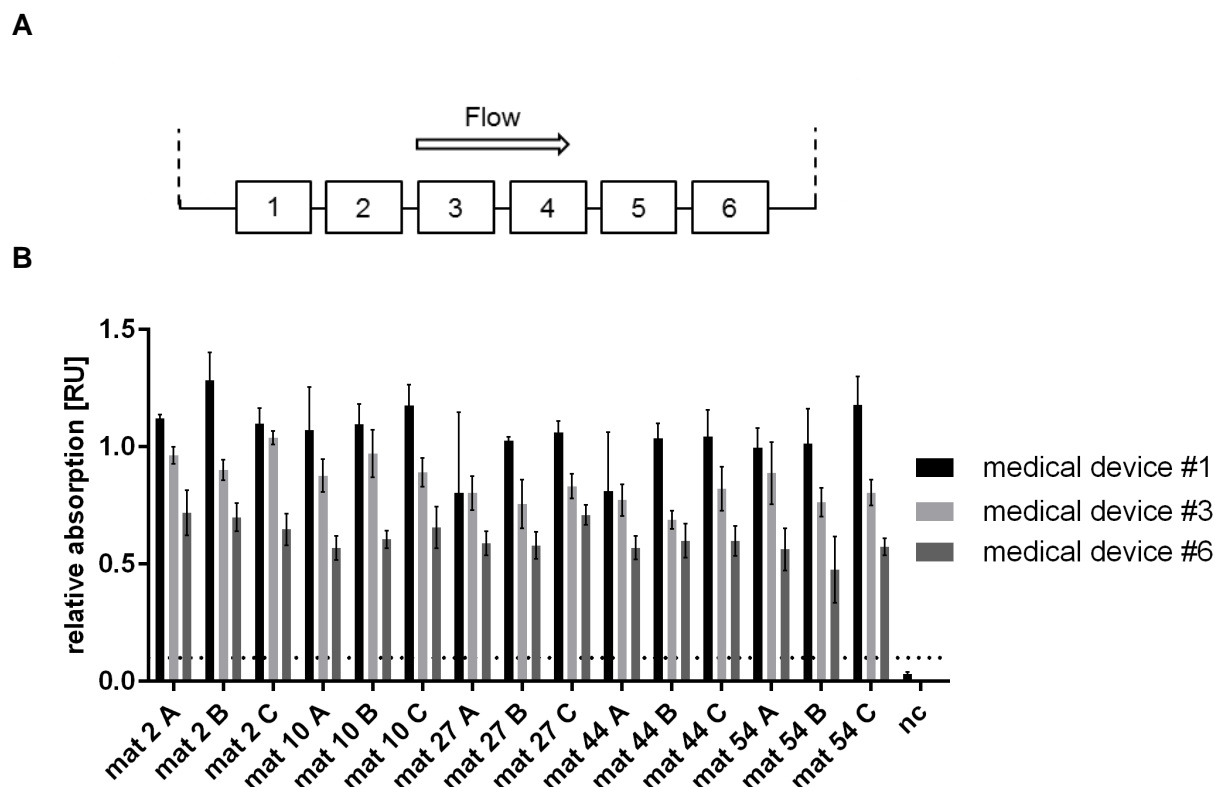
Figure 4-14. Results of the first serial production of six medical devices.
A Schematic illustration of the first serial production run. Six medical devices were coated in-line by flow (0.5 mM EDC, APO010 20 ng/ml, 0.01 % albumin, 20 g/l stabilization formulation F1, total volume 5.8 l, flow rate 2 l/min).
B Samples of different PMP mat (mat 2, 10, 27, 44, 54) of different mat positions A, B and C and different medical devices #1, #3, #6 were investigated by the coating efficacy assay (ELISA). NC means that the PMP was coated with all components except APO010. The column chart shows the relative absorption $_{450-550\ nm}$ in relative units [RU], whereby the absorption signal of the ELISA is proportional to the amount of bound APO010. Error bars represent SD from the mean of n=3 (intra-assay). The cut off was defined due to RU values <0.1 obtained for the NC.

4.2.3.2 The second serial production run

In order to avoid a flow direction dependent gradient of the coating, the flow was changed every five minutes (setting shown in Figure 4-15 A). The second serial production run 1 and 2 were carried out with 20 medical devices, respectively, whereby 2x 10 medical devices were in-line. In run 1 the medical devices (#1-20) were flushed in the last step with the stabilization formulation F2 and in run 2 the medical devices (#21-40) were flushed with the stabilization formulation F1.

To adapt the coating protocol to the larger total volume and surface area, the APO010 concentration was increased from 20 ng/ml to 33.35 ng/ml in the second serial production with 20 medical devices.

From the 40 medical devices coated with the anti-inflammatory coating, nine medical devices were tested immediately after production to determine the coating efficacy (Figure 4-15 B). Four medical devices were used in a bioburden test, which was performed externally, to confirm sterility. The remaining 27 medical devices were sterilized with EtO by the standard procedure for medical devices after packed in Tyvek® bags as described in 4.1.3.4.

After EtO treatment, twelve medical devices were stored at different temperatures (5 °C, RT and 55 °C) and tested after 20 days for stability and functionality. The accelerated aging procedure was performed according to the norm for medical devices [125, 126]. An accelerated temperature of 55 °C for 20 days correlates with six months real-time storage at RT and therefore provides important evidence for stability of the coating. The other medical devices were tested directly after the coating by means of the coating efficacy assay, bioburden tests, and by means of the detachment assay. One of those medical devices was filled with 0.9% NaCl solution, which is normally used as priming solution before filling the medical device with the patient blood and referred here as "priming test". After circulation of the NaCl priming solution, the solution was investigated by the detachment assay to analyze detached APO010. For the priming test, medical device 11 was representatively used and incubation solutions were analyzed after different time points.

Nine medical devices were directly tested by means of the coating efficacy assay. These medical devices were taken from the first, middle, and end position in the coating. The first flow direction was from left to right and was then changed every 5 min. Thus, device #1 and #11 were filled first with the coating solution, then #2 and #12, and so on. Figure 4-15 B shows, that the devices at the same position in the setting bound the same amount of APO010. Due to the low concentration of APO010 the devices on the first positions bound more APO010 than those on the last position. This results in a flow direction dependent reduction of bound APO010 from medical device #1/#11 to #10/#20 in run 1 and #21/#31 to #30/#40 in run 2, whereby in the first 5 min of flow direction from left to right the coupling of APO010 was determined. The change of flow direction every five minutes is not sufficient for a homogeneous distribution of APO010 in all devices. However, within each medical device

a homogenous coating distribution ranging from mat 2 to mat 54 was found. This result shows that the medical devices were filled completely during the coating procedure.

A   **Second serial production run 1 with stabilization formulation F2:**

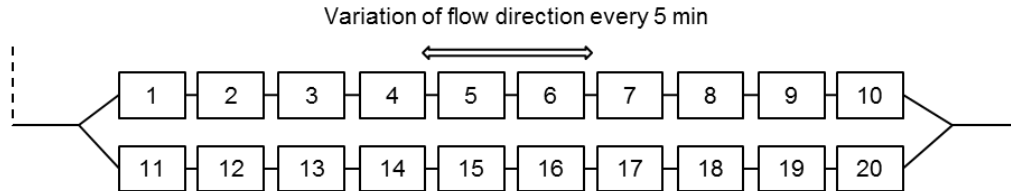**Second serial production run 2 with stabilization formulation F1:**
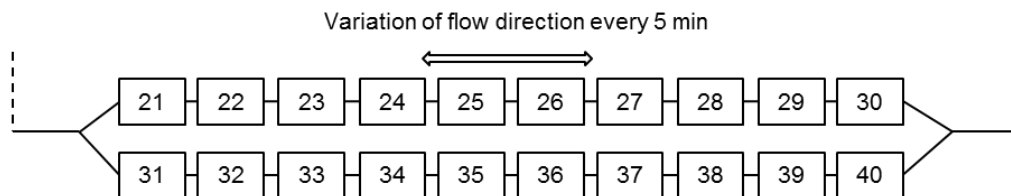
B
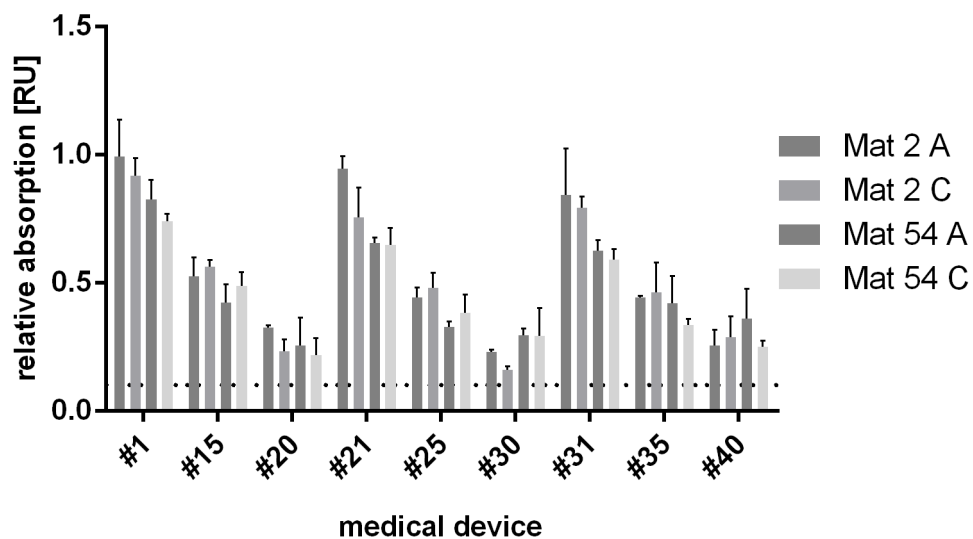
Figure 4-15. Results of the second serial production of 2x 20 medical devices.
A Schematic design of the second serial production system with 2x 20 medical devices. 2x 20 medical devices were coated via EDC 0.5 mM with APO010 (33.35 ng/ml), albumin (0.01 %) and stabilization formulation F2 (Volume 6 l, flow rate 1.5 l/min) and another set of 20 medical devices was coated via EDC 0.5 mM with APO010 (33.35 ng/ml), albumin (0.01 %) and stabilization formulation F1 (Volume 6 l, flow rate 1.5 l/min). **B** Samples of different PMP mats (2, 54) of different mat position A and C were investigated by the coating efficacy assay (ELISA). The column chart shows the relative absorption $_{450-550\,nm}$ in relative units [RU], whereby the absorption signal of the ELISA is proportional to the amount of bound APO010. Error bars represent SD from the mean of n=3 (intra-assay). The cut off was defined due to RU values <0.1 obtained for the negative control.

In addition to the relative absorption signal in Figure 4-15, in Table 4-13 the reduction of the absorption signal from the first medical device to the middle medical device in-line and from the middle medical device to the last medical device in-line is shown. The reduction of the absorption signal was found to be comparable in the second serial production run 1 and 2.

This means that both runs performed in the same way and are comparable. In addition, from this data it can be assumed that the medical devices more distal from the coating solution source receive less APO010 compared with those more proximal. But, the anti-inflammatory coating distribution is homogenous within each device. A modified coating set-up should therefore be applied to allow similar flushing of all medical devices at the same time.

Table 4-13. Reduction of absorbance in percent flow direction during coating process

	Flow direction	Reduction of absorption [%]
Batch 1	#1 to # 15	42.61
	#15 to # 20	27.83
Batch 2	#21 to # 25	45.62
	# 25 to # 30	21.86
	# 31 to # 35	41.77
	# 35 to # 40	17.80

In order to determine the potential effects of EtO sterilization on the coating efficacy, EtO-sterilized medical devices and non-sterilized medical devices were tested in the coating efficacy assay. In this experiment, medical devices with similar positions (# 1, #11, #21, #31 and #10, #20, #30, #40) in the coating process were compared, whereby only #11 and #10 were EtO sterilized (Table 4-14). No loss of absorption signals of the anti-inflammatory coating after EtO sterilization compared to non-sterilized medical devices were observed as the absorption signals for the devices # 1, #11, #21, and #31 are similar and as well for the devices #10, #20, #30, and #40.

Table 4-14. Results of coating efficacy assay of medical devices w/o and with EtO treatment

Medical device	with EtO Mean (± SD) [RU]	w/o EtO Mean (± SD)
# 1		1.05 (± 0.03)
# 11	1.19 (± 0.12)	
# 21		1.23 (± 0.21)
# 31		1.07 (± 0.03)
# 10	0.34 (± 0.16)	
# 20		0.37 (± 0.09)
# 30		0.32 (± 0.11)
# 40		0.33 (± 0.22)

The coating efficacy assay was conducted to find out, whether priming of medical devices with NaCl may result in unappreciated reduction of APO010 coupling. The priming procedure is done to fill the extracorporeal system with NaCl and to remove potential air bubbles. The results are shown in Figure 4-16. Even after 1 h washing of medical device #11 (after EtO sterilization) with 0.9 % NaCl, APO010 is homogenously distributed throughout the whole oxygenator with a mean absorption signal of 1.19 ± 0.12 RU. Compared to the previously shown ELISA results of medical devices from the same position as #11 (Table 4-14) there is no loss of APO010 observed. The filling behavior and air removal of the medical device in the priming test was unchanged to a non-coated medical device, which means that the coating has not changed the mode of action of the device.

The detachment assay was conducted to find out whether the priming of medical devices with NaCl may result in unappreciated detachment of APO010. Usually, the priming solution would reach the patient circulation and thus detached APO010 molecules will be infused into the blood circulation.

After up to 60 min washing with a flow rate of 1 l/min of the medical device #11 with 0.9 % NaCl solution no APO010 molecules were detected in the washing solutions. At a concentration of ≥ 0.098 ng/ml APO010 the detachment assay delivers stable results. As shown in Figure 4-17 B, the coating was found to be stable even after EtO sterilization and washing.
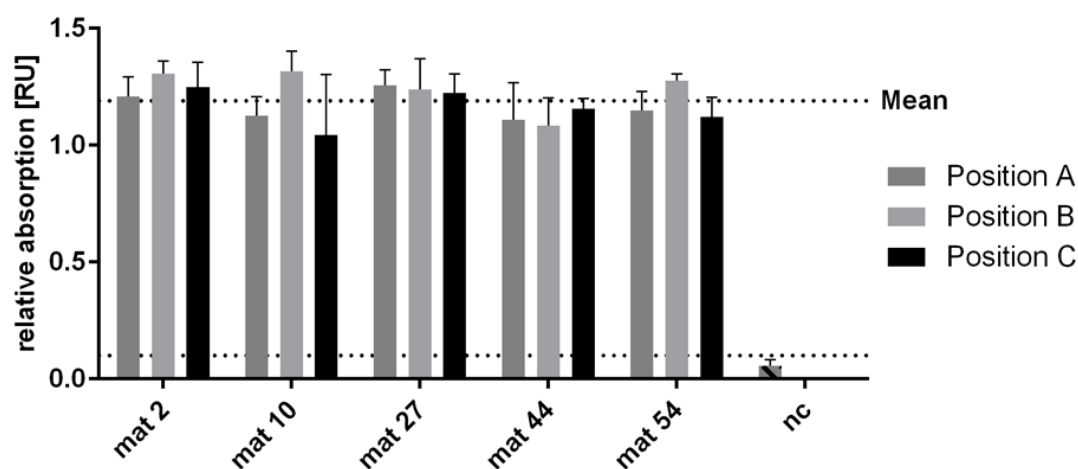
Figure 4-16. Results for device #11 after washing with NaCl for 1 h in circulation.
Device #11 was washed for 1 h with 0.9 % NaCl solution in flow (1 l/min). Afterwards, the device was opened and samples of different PMP mats (2, 10, 27, 44, 54) of different mat position A, B and C were collected and analyzed by the coating efficacy assay. Negative control (nc) means that the PMP was coated with all components except APO010. The column chart shows the relative absorption $_{450-550\ nm}$ in relative units [RU], whereby the absorption signal of the ELISA is proportional to the amount of bound APO010. Error bars represent SD from the mean of n=3 (intra-assay). The cut off (lower dotted line) was defined due to RU values <0.1 obtained for the negative control.

A

B
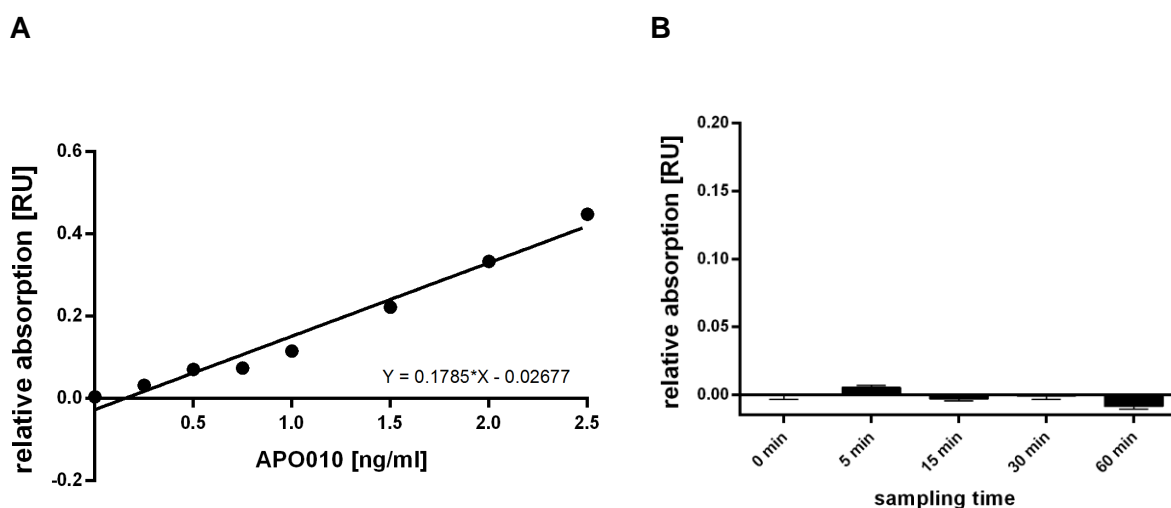
Figure 4-17. Results of the detachment assay of washing solutions of medical device #11.
A Dilution series for quantitative analysis of APO010**. B** Washing solutions of medical device #11 detected by the detachment assay. The column chart shows the relative absorption $_{450-550\ nm}$ in relative units [RU], whereby the absorption signal of the ELISA is proportional to the amount of bound APO010. Error bars represent SD from the mean of n=3 (intra-assay). The specificity of the detachment assay is ≥ 0.098 ng/ml APO010.

As mentioned above several medical devices were stored after EtO sterilization for 20 days at 5 °C, RT and 55 °C. Subsequently, the medical devices were opened and samples were collected. As shown in Figure 4-18 there was a flow direction dependent APO010 reduction from medical device in-line from left to right from about 70 % as shown in the nine medical devices analyzed directly after the coating as well. Therefore, it was assumed that no loss of APO010 after sterilization and storage was found compared to the control devices #1 and #21, which were tested previously (Figure 4-15).

As well, no difference in coating efficacy was found after storage of medical devices stabilized with the stabilization formulation F1 or F2. In order to compare medical devices flushed with different stabilization formulations, medical devices from similar positions during the coating procedure (Figure 4-18 A) were analyzed (e.g. medical device #2 with medical device #22; medical device #3 with medical device #23). The same colors in Figure 4-18 A indicate which pairs of run 1 and 2 were compared with each other (Figure 4-18 B). The results are comparable with the previously generated results in Figure 4-15. There is the same flow direction dependent APO010 reduction. Therefore, the storage for 20 days at different temperatures had no influence on the coupled APO010. Both stabilization formulations seem to protect the coating identical during sterilization and storage.

Summing up, the anti-inflammatory coating is stable with the stabilization formulation F1 and F2 after sterilization and accelerated aging at 55 °C, whereby 20 days accelerated aging corresponds to six months real-time storage.
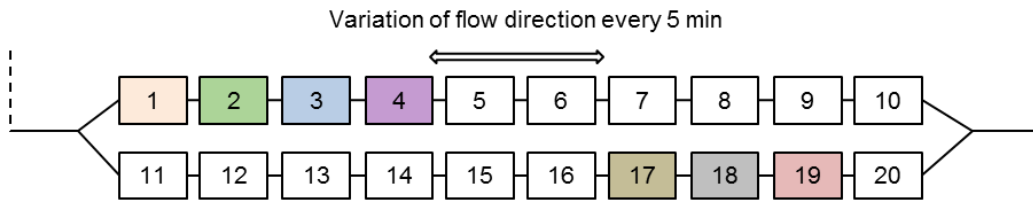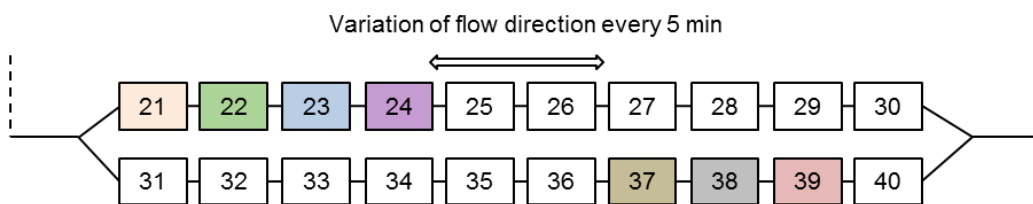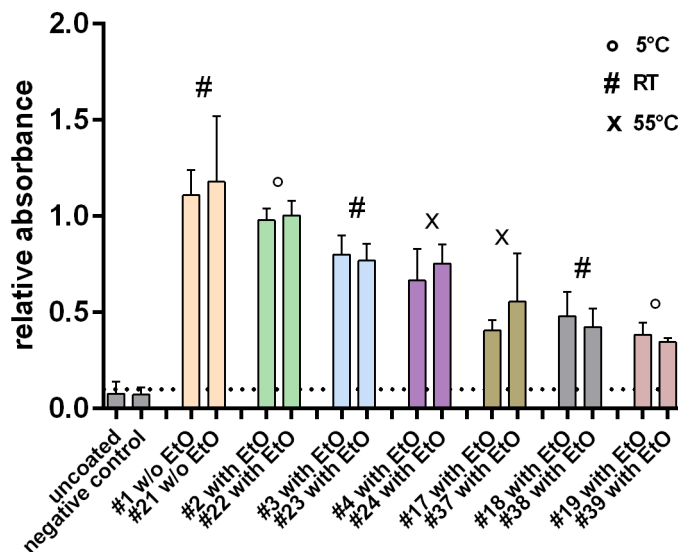
Figure 4-18. Results of the coating efficacy assay to quantify coupled APO010 on PMP after EtO treatment and after storage.
A Schematic illustration of medical device position during coating. Run 1 is #1-20 (stabilization formulation F2), run 2 is #21-40 (stabilization formulation F1). The same color indicates which pairs of batch 1 and 2 have to be compared with each other. **B** The first two columns (grey) show the control samples, whereby uncoated means that the uncoated PMP was used, negative control means that the PMP was coated with all components except APO010. The other samples were taken of PMP mat 4 of mat position A of the different medical devices. All samples were investigated by the coating efficacy assay. # 1 is a control, which was tested in earlier experiments, medical device 2, 22, 19, 39 were stored at 5 °C, medical device 3, 23, 18, 38 were stored at RT and medical device 4, 24, 17, 37 were stored at 55 °C for 20 days. The column chart shows the relative absorbance $_{450-550\ nm}$ in relative units [RU], whereby the range of 0 to 2.0 is proportional to the amount of bound APO010. Error bars represent SD from the mean of n=3. The cut off was defined due to RU values <0.1 obtained for the negative control.
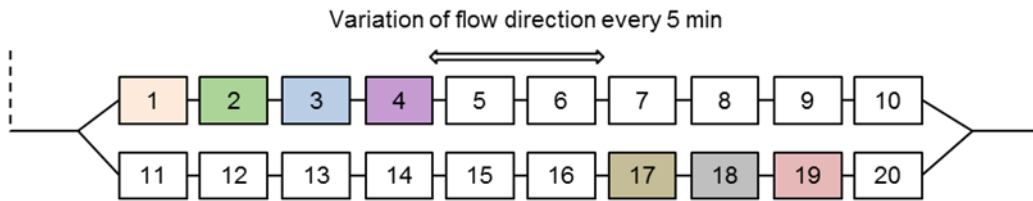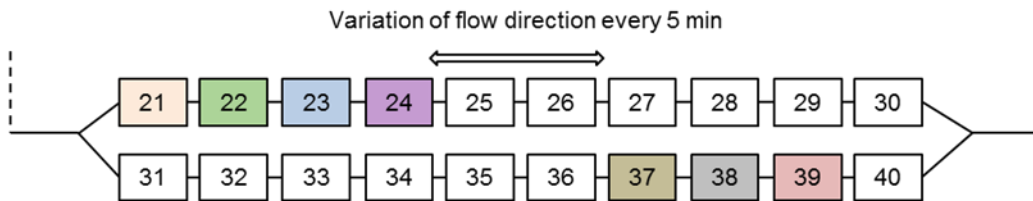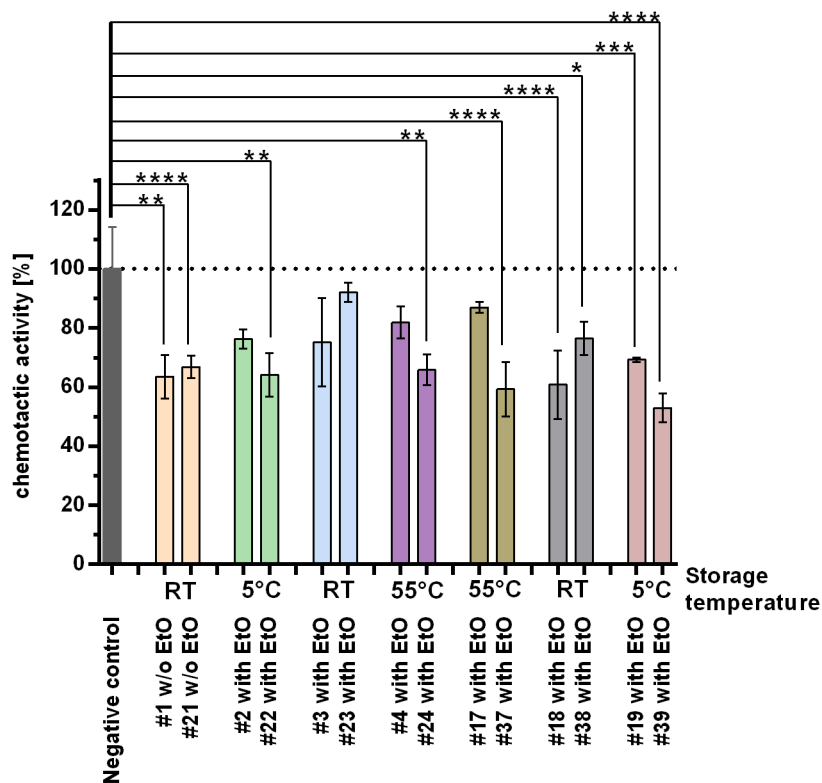
Figure 4-19. Results of chemotaxis assay to test the functionality of coupled APO010 on PMP w/o and with EtO treatment and after storage.
The same color indicates which pairs of batch 1 and 2 have to be compared with each other. The functionality of the PMP mats from medical devices w/o and with EtO treatment and after 20 days storage at 5 °C, RT and 55 °C were tested in the chemotaxis assay. Data is normalized to the negative control (100 %) in %. Error bars represent SD from the mean of n=3. Blood was donated by the same donor at two days.
Two-way ANOVA: * < 0.1, ** < 0.01, *** < 0.001, **** < 0.0001.

By the neutrophil activity assay the PMP mats from the medical devices stored at different temperatures for 20 days were additionally tested on functionality. As depicted in Figure 4-19, the anti-inflammatory coated PMP mats reduced chemotactic activity of neutrophils even after sterilization and storage. However, the reduction value of all medical devices is very similar and shows not the excepted difference dependent on the APO010 concentration as shown in Figure 4-18. In addition, the medical devices stored at 55°C perform similar than those stored at 5°C or RT. The medical devices #1 (**), #21 (****), #22 (**), #24 (**), #37 (****), #18 (****), #38 (*), #19 (***), #39 (****) show significant reduction of chemotactic activity compared to the negative control, however there is an irregular variation of chemotactic activity of the medical devices.

The medical devices #3 and #23 were stored for 20 days at RT, #2 stored at 5°C, #4 stored at 55°C, and #17 stored at 55°C showed no statistically difference to the negative control and therefore were not sufficient stabilized or had not coupled enough APO010. These results indicate the tendency, that medical devices stabilized with F1 (medical device #21-40) show stronger reduction than those stabilized with F2 (medical device #1-20). A more complex formulation is therefore not necessary for this approach. However, the goal to reduce neutrophil activity at least about 10 % could be observed for all medical devices, expect #23 which had a chemotactic activity of 92.17 % ± 3.25 %.

After the storage of selected medical devices for 20 days at different temperatures samples from the medical devices were taken as described above. These anti-inflammatory coated PMP samples were washed for 1 h with PBS. Subsequently, washing solutions were harvested and analyzed. As shown in Figure 4-20 B, no APO010 molecules were detected in the washing solutions indicating that the anti-inflammatory coating is highly stable even after sterilization and 20 days storage at different temperatures.

To confirm that there is no unappreciated non-specific coupling of APO010 to the PVC tubing of the circuits, the PVC tubing of the medical device-set were tested via the coating efficacy assay. As shown in Figure 4-21, the PVC tubing which is connected to the medical devices were negatively tested on the presence of APO010. As an internal positive control, PMP from medical device 11 was included. This data shows that, based on the anti-inflammatory protocol, APO010 specifically binds to PMP and not to the PVC tubing.

A

$Y = 0.06390*X + 0.04451$

B
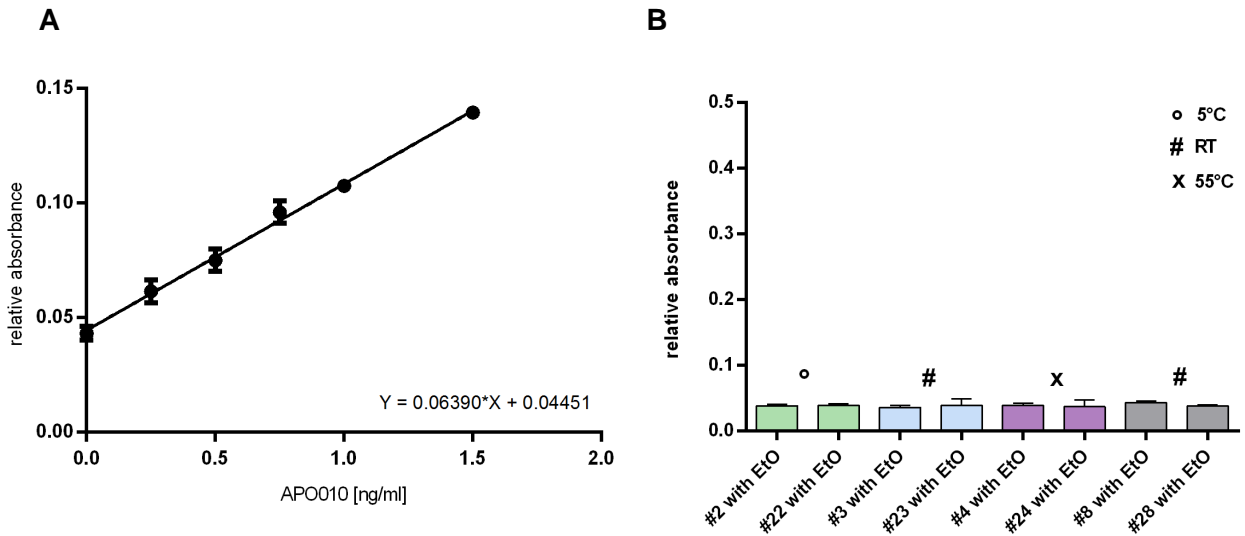
Figure 4-20. Results of the detachment assay to detect detached APO010 molecules after sterilization and 20 day storage.
A Dilution series for quantitative analysis of APO010. **B** Washing solutions of differently stored (5°C, RT, 55°C for 20 days) medical devices detected by detachment ELISA. Error bars represent SD from the mean of n=3.
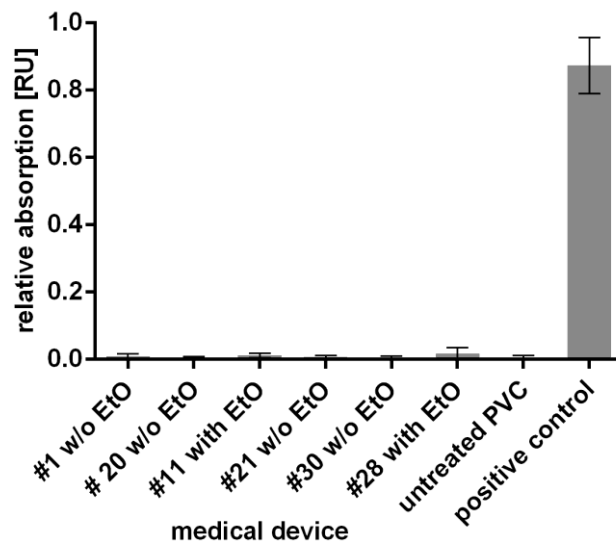
Figure 4-21. Results of the coating efficacy assay with PVC tubing with and without EtO sterilization.
12 mm pieces of tubing of different medical devices were prepared and analysed by the coating efficacy assay. PMP mats of medical device 11 served as positive control. The column chart shows the relative absorption $_{450-550nm}$ in relative units [RU], whereby the absorption signal of the ELISA is proportional to the amount of bound APO010. Error bars represent SD from the mean of n=3 (intra-assay).

Residual moisture is a crucial issue during sterilization and storage. In general, a residual moisture around 2 % is specified within biofunctionalized medical devices. Therefore, the goal was to limit moisture below 2 % at the end of the production process. The medical devices were dried o/n at 50°C in a vacuum oven and afterwards the residual moisture was determined by Karl-Fischer-Titration. The figure shows that residual moisture values are very low (≤ 1.1 %) for all medical devices. The positive control is medical device #11 after it was washed for 1 h with NaCl and afterwards dried at 37 °C. The high value of 6.4 % indicated that the time was not sufficient for drying the PMP mats completely (Figure 4-22), but the drying method of the medical devices in the serial production run had not to be optimized.
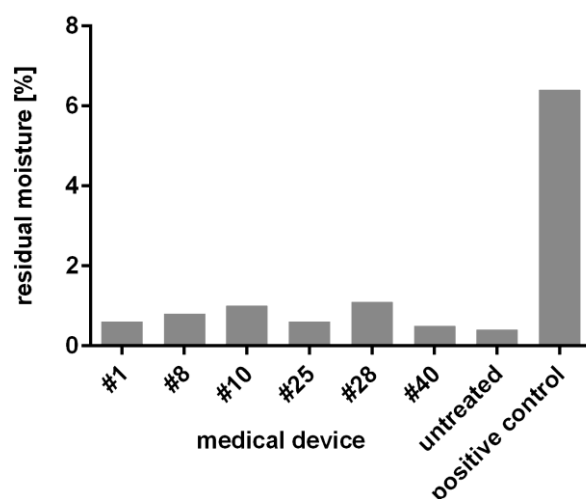
Figure 4-22. Results of residual moisture [%] of different medical devices.
Residual moisture was measured by Karl-Fischer-Titration referenced to air moisture. The positive control is medical device #11 after it was washed with 0.9 % NaCl and dried at 37 °C.

Summary of the second serial production run

The anti-inflammatory coating process was transferred to the serial production scale, however a homogenous distribution of the coating from the medical devices was not fulfilled so far. The devices, which were positioned more distal from the coating solution source receive less APO010 compared with those more proximal. The quality control (QC) assays after sterilization, storage and accelerated aging for 20 days at different temperatures were carried out successfully, but had to be repeated with the final setting. In the next serial production run the coating system was optimized to generate a homogenous distribution of the coating on all medical devices.

4.2.3.3 The third serial production run

The third serial production run was modified to obtain a more homogenous distribution of the coating efficacy compared with second serial production runs 1 and 2. Therefore, a circular approach with 22 medical devices was tested. It was expected that all medical devices receive the same amount of the coating solutions for the same time period.

After the coating of the devices, an EtO treatment and storage at different conditions were performed and the coating distribution was tested. In the third serial production run the stabilization formulation F3 was tested which includes 8 amino acids, trehalose and Polysorbate 20. Here it was tested, if sugar and Polysorbate 20 show positive effects on stabilization of the dried anti-inflammatory coating as known by literature [67, 69].

By the coating efficacy assay a homogeneous distribution of anti-inflammatory coating could be confirmed. However, the overall absorption was slightly lower compared with the second production run 1 and 2. The data of this third serial production run show that less APO010 molecules (0.885 ng/cm^2 APO010 per device) bound per area PMP when 22 devices were homogenously flushed at once by the circular setting compared to first serial production run (1.79 ng/cm^2 APO010 per device) and the second serial production run (0.925 ng/cm^2 APO010 per device).

In Figure 4-23, the homogenous distribution of APO010 between all medical devices is depicted with a mean of 0.64 ± 0.14 RU. The mean values of all samples show that the APO010 distribution between different medical devices is homogenous, however partly with high standard deviations. A reason for this relatively high deviation might be the unexpected loss of pressure during the EDC coating step due to technical reasons. The lower flowrate of 0.3 l/min is due to the round settings, whereby the flow is reduced by the several medical devices. In this setting, it was not possible to increase the pressure in order to increase the flow rate.

The accelerated aging procedure shows that the medical devices show no crucial difference in absorption after the different storage condition. The accelerated aging for up to 82 days at 55 °C shows no loss of absorption signal, which corresponds to 2 years real-time storage.

A

B
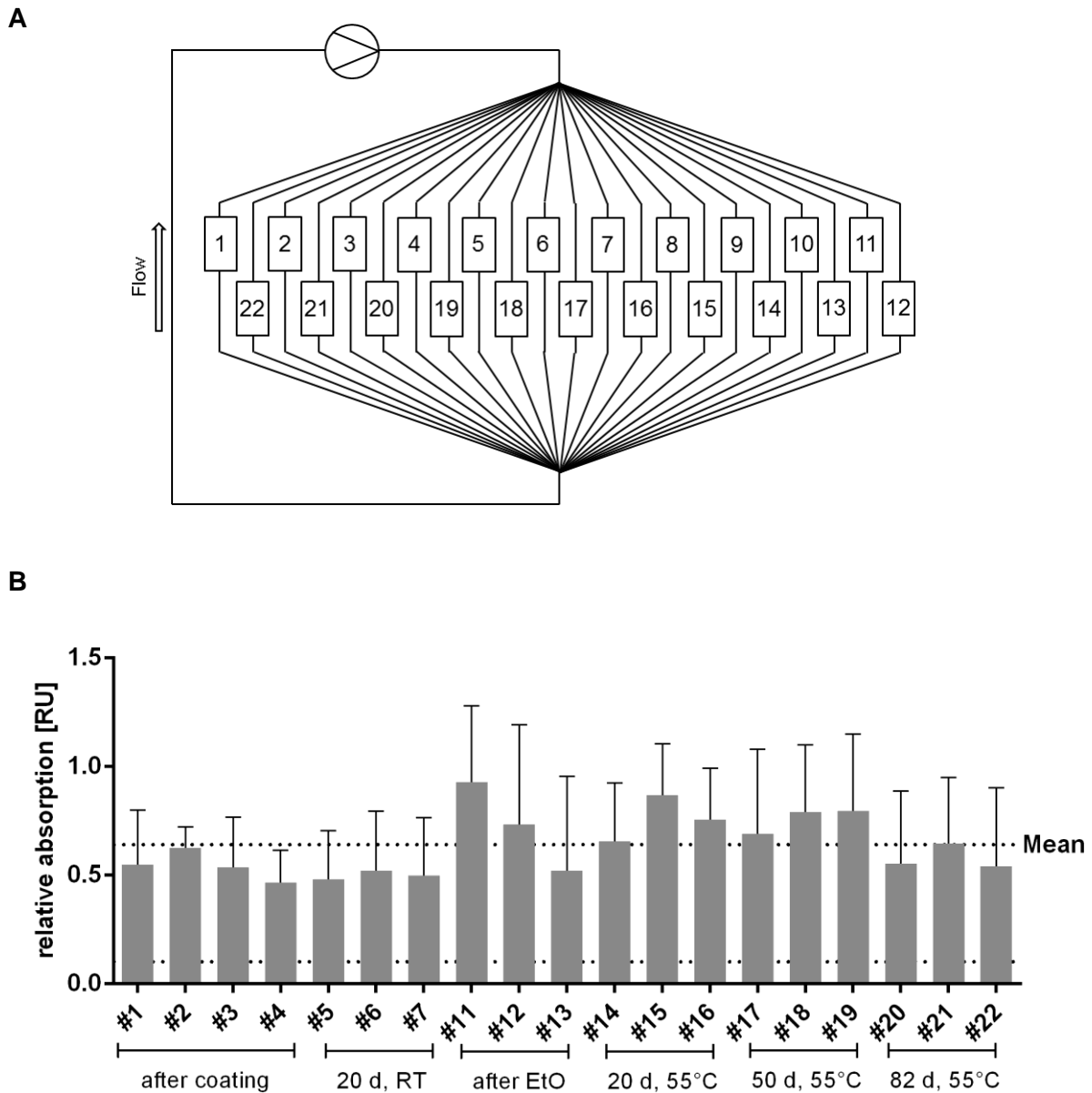
Figure 4-23. Results of the coating efficacy assay to quantify coupled APO010 on PMP after third serial production run.

A Schematic illustration of medical device position during coating.The 22 medical devices were coated with APO010 (35 ng/ml), albumin and aa-based stabilization formulation F3 (volume 6 l, flow rate 0.2 - 0.3 l/min). The flow rate was detected after #5. The pressure was detected after #5 and #6.

B PMP pieces were cut from positions A, B and C out of mat 2 and 54 from the medical device 1 to 22. The medical devices were different treated. The column chart shows the relative absorbance $_{450\text{-}550\,nm}$ in relative units [RU], whereby the range of absorption is proportional to the amount of bound APO010. Error bars represent SD from the mean of n=3.

Summary of the third serial production run

In summary, the third serial production run was the most successful one. It was the first time that a homogenous coating of all medical devices was reached. The lower absorption signal is due to the lower APO010 amount to PMP area. The concentration of APO010 can be increased, when a higher number of medical devices are coated at the same time. Furthermore, the coating flow rate could be increased by using a setting where a higher pressure is feasible.

4.3 Discussion

The upscaling of the anti-inflammatory coating to a serial production scale was a crucial step in finishing of this work. Due to the very low concentration of the anti-inflammatory molecule APO010, the upscaling had to be performed in several steps to ensure efficient coupling.

In the beginning, the bench setting was transferred to a circuit setting and different APO010 concentrations were tested in the functional and non-functional ELISA. It became clear that in the circuit setting both ELISAs generated detectable results in a range of 20 to 50 ng/ml APO010, whereby the functional ELISA needs a higher APO010 concentration than the non-functional ELISA. At this step in the upscaling it was difficult to decide for a final concentration, because this decision depends on functional behavior, which can differ on the final setting. The total amount of coupled APO010 is depending on the APO010 concentration and the surface area of PMP. Therefore, the development range was defined by two main points: First, what can be measured by ELISA? Second, is the chosen concentration of APO010 sufficient for the desired anti-inflammatory effect?

Therefore, in the next steps the crosslinking reagent Sulfo-NHS was added for optimal coupling of APO010 and the incubation time of APO010 was tested, to enable the most efficient coupling strategy in the circuit setting. The efficiency was analyzed indirectly in the coupling solution to show if APO010 is completely coupled and to investigate if material is wasted. Due to the slight differences in the results with or without Sulfo-NHS, the protocol was not changed. All these steps were necessary for economic efficiency.

Then, one medical device was coated with a flow rate of 0.5 l/min, another with a flow rate of 1 l/min and the above defined parameter. Interestingly, it was shown that a higher flow rate doubles the amount of coupled APO010. After incubation with F1 as stabilization formulation, drying the device, and EtO sterilization the coating was analyzed again. After the sterilization the absorption signal was 2.5 fold lower than without EtO, which means that the stabilization was not as successful as basically described before [55]. One reason could be that here EtO was used as sterilization method and in previous work beta sterilization was performed [55].

Hence, the sterilization stress is very different for each method and it is necessary to adapt the formulation in regard to the stress model. In literature it was shown that up to 250-1,000 mg EtO/l, temperatures of 40-60°C, and relative humidities of 50-90 % were used to inactivate Bacillus subtilis [127]. This means a protein, sterilized by EtO, has to be stabilized for medium temperatures, high humidity and as well strong chemical degradation by EtO.

EtO is highly reactive due and reacts by alkylation, which leads to denaturation of proteins and inactivation of microorganisms [128]. Therefore, the selection of a stabilization formulation is a separate development project, which could not be covered in this thesis. Thus, only three different formulations were used as basis for further development.

When upscaling to 6 medical devices in-line no homogeneous distribution of APO010 could be found from device #1 to #6. A reduction of 20 % from #1 to #3 and #3 to #6 shows that the setting is not optimal for the coupling. One main problem is that APO010 is not saturated in the coupling solution and therefore the device on first position (#1) gets the biggest amount due to the fast crosslinking process with EDC.

In order to increase the amount of devices for analysis and for further upscaling, a setting with 20 medical devices was tested. The setting was in-line with 2x 10 devices. The flow direction was changed every 5 min to increase the homogeneous distribution of the coating solution. However, the same picture as in the first run was seen. Interestingly, in this setting each medical device on the same position in-line showed the same absorption signal. This observation made clear, that the only setting, which can generate a homogeneous distribution of the coating can be a setting where every medical device gets the same amount of the coating solution at the same time. Therefore, the third setting was designed in a circle with 22 devices.

Due to the flow dependent decrease of APO010 coupled to the medical devices in the second serial production run form the first to the last device, it was suspected that due to the different APO010 concentrations on the medical devices a loss of functionality due to sterilization or storage would be difficult to interpret. But the medical devices were tested as planned in the workflow and performed very successful. Fortunately, the same pattern of flow dependent decrease in APO010 was observed after the different treatments. Overall no loss of absorption signal after EtO sterilization was observed in comparison with the results generated with one medical device during the upscaling transfer. There, a 2.5 fold decrease after EtO treatment was shown.

The idea for two runs in the second serial production run was to test a second stabilization formulation F2. The more complex formulation F2 includes more excipients than F1 and therefore the amount of different substances could improve the anti-inflammatory coating stability especially during drying and subsequent EtO sterilization [75]. As it was shown by the second serial production run, there were no differences shown after EtO sterilization with

both formulations in the non-functional ELISA. One reason should be the optimized performance during the manufacturing of the medical device, which lead to shorter handling times and therefore less stress on the anti-inflammatory coating.

The medical devices were tested on their washing performance with the result that there was no loss of the anti-inflammatory coating as no APO010 molecules could be detected in the detachment assay. After storage of the medical devices at 5°C, RT and 55°C for 20 days no loss of absorption signal was detectable. In this case the problem was that there was already a loss in absorption signal form device #1 to #20 and from #21 to #40 due to the inhomogeneous coating, as described above. Therefore, the shown pattern complicates to distinguish the different stress treatments. This was even more difficult when considering the results of the functionality assay. The functionality assay, which measures the chemotactic activity of neutrophils, showed a different pattern than the coating efficacy assay for the same stored medical devices. Not all medical devices could reduce the neutrophil activity significantly compared to the negative control. There is a tendency that the medical devices, which were stabilized with F1 performed better than those which were stabilized with F2, but overall the effect is small.

However, the goal to reduce neutrophil activity at least about 10 % could be observed for all medical devices, except #23 which had a chemotactic activity of 92.17 % ± 3.25 %. The corresponding incubation solutions of the stored medical devices showed no detached APO010 in the detachment assay after storage at different temperatures, which confirms the stability of the coating.

In addition to the experiment with neutrophils, functional blood experiments would be of great interest, because they would show the functional effect in blood as it will be in the medical use. But working with freshly prepared neutrophils or with blood involves a lot of problems. Biological material is extremely different form each donor, for which reason the results can differ and different settings need to be performed with the same sample to enable comparison. To test the anti-inflammatory effect fresh blood and to ensure statistical relevant data a clinical study with trauma patients with an activated immune system would be of great interest as these kind of patients would need this application.

Not only the functionality of the anti-inflammatory coating in blood is of great interest, but the anti-inflammatory coating itself. It is known that the oxygenator with PMP generates a biofilm of fibrin, thrombocytes, erythrocytes, and blood proteins which lowers the efficacy of the gas

exchange. The biofilm can extend up to 50 µm, whereby the wall thickness of the PMP hollow fiber is 70 µm. By extension of the wall thickness the gas exchange is disturbed and the oxygenator has to be exchanged. As well the cellular detachment is very strong on the woven thread and the contact points of the neighbored fibers [12]. The same observation was shown in chapter 3 in the SEM images, where the stabilization formulation built a film like structure on the woven thread.

The third serial production setting was performed with 22 medical devices in a circular set-up. The 22 devices were tested directly after the coating, after EtO sterilization and after storage of 20 days at RT and after 20 days, 50 days and even 82 days at 55 °C. All tested devices generated the same result in the coating efficacy assay.

For in vivo use in humans of the anti-inflammatory coating it is essential that the anti-inflammatory coating is specifically bound to the PMP surface. Therefore, it was tested if there were any APO010 molecules bound to the PVC tubing. The result was that no APO010 was bound to the PVC tubing, therefore it is assumed that as well no other components of the device are affected. Residual moisture of the coating delivers insight of a stable drying process, whereby for each device the same residual moisture should be observed. This was the case for the second serial production scale. Low residual moisture is important to reduce a loss of the coating before sterilization. No relevant residual moisture within medical devices was found after production.

In external investigations no relevant changes in the function of the gas exchange were found after anti-inflammatory coating (data not shown) and sterility of anti-inflammatory coating was confirmed by bioburden assays (data not shown).

To sum up, in this work an anti-inflammatory coating on an inert PMP hollow fiber was established from bench setting to a serial production scale. The coating is stable during circulation as shown in the priming test and as well during blood contact as shown in chapter 3. In the serial production runs the aa-based stabilization formulations were able to stabilize the coating during drying, sterilization, and storage, but could be further investigated for more detailed information. The serial production scale was optimized to a circular setting in order to generate a homogenous distribution in all medical devices. Due to the very low amount of APO010 on the surface the most known analytical methods are not sensitive enough. Therefore, the established ELISAs are the best available methods to qualify the anti-inflammatory coating.

GENERAL SUMMARY AND OUTLOOK

5   General summary

This work deals with the question how to design an anti-inflammatory surface coating, which avoids or reduces material-mediated innate immune responses on the example of the material polymethylpentene (PMP). PMP is a polymer, which can be manufactured as hollow fibers and is used in medical devices like oxygenators and enables the exchange of oxygen and carbon dioxide in the blood.

In **chapter 1** the background, especially for the design of an anti-inflammatory coating, was discussed in detail. Five potential anti-inflammatory molecules were selected based on the idea that activated neutrophils expressing Fas on their surface can be inactivated by contact with the selected molecules. Those five molecules are anti-Fas molecules, which have optimal binding and trimerization properties to Fas: SuperFasL, MegaFasL, Fc-FasL, E09 and CH11. SuperFasL, MegaFasL (two variants) and Fc-FasL are recombinant proteins, which trimerize to homotrimers. Three FasL domains are located in spatial proximity enabling the induction of apoptosis in all Fas positive cells. This structure makes the proteins extremely efficient because it enables the trimerization of the Fas receptor, which allows the activation of the extrinsic apoptosis pathway. IgG1 E09 and IgM CH11 are monoclonal antibodies. E09 has been reported to induce apoptosis in an effective way although the affinity to the Fas receptor is relatively weak [60]. CH11 has been used previously for anti-

inflammatory approaches [61] but was shown to be instable over a longer period of storage time. Therefore, CH11 was only used as a control molecule for establishing the assays.

In **chapter 2** the five anti-inflammatory molecules were investigated on their efficiency to induce apoptosis in the Jurkat cell line and neutrophils. Therefore, read out models for the investigation process were developed. Apoptosis and neutrophil activity assays have been established as the anti-inflammatory molecules have pro-apoptotic function. Soluble and immobilized effector molecules were systematically evaluated on their potential to induce apoptosis and to reduce neutrophil activity. Except the E09 antibody, each anti-Fas molecule induced apoptosis in > 20 % of target cells and impaired neutrophil activity in > 10 % of target cells. Therefore, the defined goals were reached. The APO010 is the most suitable molecule due to its availability in Good Manufacturing Practice (GMP) quality. In addition, clinical safety data for systemic application are available for APO010 as well [102, 103].

In **chapter 3** it was focused on the design of the anti-inflammatory coating. For the anti-inflammatory coating, first, the polymethylpentene (PMP) hollow fiber was plasma activated with O_2 to generate carboxyl groups. Second, the plasma activated PMP reacts with EDC. The activated PMP can react in a third step with APO010, which results in a stable amid bond. Afterwards, the reaction was quenched with recombinant albumin. Crosslinking with EDC results in covalent coupling of APO010 and albumin to the PMP. Albumin interacts as blocking reagent with free PMP groups and avoids unwanted binding of blood components. In the last step an amino acid-based stabilizing formulation was added to the coating and will protect the coating during drying, sterilization, and storage. Each compound has already been approved to be safe for clinical applications.

Covalent and stable binding of APO010 to PMP was shown in leaching experiments. Five washing steps are recommended after crosslinking APO010 with EDC for removing residual non-covalently bound APO010 from PMP. Functionality was shown by reduced chemotactic activity of neutrophils after challenging with the anti-inflammatory coating. Hemocompatibility of PMP coated with the anti-inflammatory coating was shown in the circuit setting with human blood. Moreover, no cytotoxic effects of fluid samples harvested from circuits with the anti-inflammatory coating could be observed. The characterization of the surface in general was not possible due to the low APO010 concentrations. Most characterization methods as FTIR

need smooth surfaces and high protein concentrations of at least 1 mg/ml. The contact angle method to differ the surface properties before and after coating of the anti-inflammatory coating showed only differences by adding the stabilization formulation. Therefore, only the developed ELISAs, apoptotic and chemotactic assays could determine the coating quality.

In **chapter 4** the upscaling process to serial production scale is reported. Therefore, the coating had to be adapted from bench setting to several medical devices, whereby three upscaling steps were necessary to generate a homogeneous distribution of the coating. In the first and second serial production runs there was a flow dependent decrease of APO010 coupled to the medical devices.

However, it could be demonstrated that in the second serial production run 1 and 2 the anti-inflammatory coating is stable after EtO sterilization analyzed by the coating efficacy assay, as well as after storage, and prolonged washing for up to 1 h. The anti-inflammatory coating is functional even after EtO sterilization and storage of 20 days at different temperatures, whereby not all medical devices delivered the same functionality data in chemotaxis assay with freshly isolated neutrophils.

In the third serial production run the medical devices were coated in a circular setting which generated a homogenous distribution of APO010 in all 22 medical devices. After storage for up to 82 days at 55 °C there was no loss of APO010 in the coating efficacy assay, which correlates to 2 years real-time storage, the normal minimal durability of medical devices.

It was investigated that the anti-inflammatory coating can be analyzed easily by the coating efficacy assay after the coating procedure, as well as after sterilization, and storage. Washing experiments after 1 h washing delivered no detached APO010. The APO010 detachment can be quantified by the detachment assay at a concentration of ≥ 0.098 ng/ml. In addition, the anti-inflammatory coating is specific to the PMP hollow fibers as no unspecific binding to PVC tubings after serial production could be detected. The performed drying process was optimal for the medical devices as no relevant residual moisture within medical devices was found after production. As well the mode of action of the medical device, the gas exchange of the PMP hollow fibers, was investigated externally with the result that no relevant changes in the function of the gas exchange were found after anti-inflammatory coating. The sterility of the anti-inflammatory coating was ensured by externally sterility tests.

142

In summary, in this work an anti-inflammatory coating on an inert PMP hollow fiber was established from bench setting to a serial production scale. The coating is stable during circulation and as well during blood contact as shown in chapter 3. The aa-based stabilization formulations were able to stabilize the coating during drying, sterilization, and storage. The serial production setting was optimized to a circular setting in order to generate a homogenous distribution in all medical devices.

However, due to the very low amount of APO010 on the surface the most known analytical methods are not sensitive enough to detect the molecule on the surface directly. Therefore, the established ELISAs are the optimal methods to qualify the anti-inflammatory coating.

Anti-inflammatory coatings are used for implants or prostheses [119, 120], hernia repair [121], disorders [122] or are used in general to differentiate monocytes into macrophages [123]. This anti-inflammatory coating is an innovative approach for a medical device with blood contact, with high requirements in stability and functionality. Thus, it can possibly show the way for new biofunctional coatings in the medical device sector.

5.1 Outlook

As the third serial production in a circular setting delivered the best results with a homogeneous anti-inflammatory coating even after storage at accelerated temperatures at 55 °C for 82 days, the setting should be further validated.

In addition, it is necessary to test the functionality of the coating with blood of patients, preferably of trauma patients, to investigate the reduction of inflammatory signal in the blood. For this study, the blood needs to be fresh, in order that all components behave as natural as possible. To ensure statistical relevant data a clinical study would be of great interest. On basis of these experiments the anti-inflammatory coating can be further developed for a usage in medical devices.

The biofunctional anti-inflammatory coating is a novel technology to reduce unappreciated material-induced immunogenic responses. In principle, it should be possible to transfer this technology to other surfaces. This could allow for expansion of the positive effects to other medical devices in direct blood contact.

6 References

1. Gorbet, M.B. and M.V. Sefton, *Biomaterial-associated thrombosis: roles of coagulation factors, complement, platelets and leukocytes.* Biomaterials, 2004. **25**(26): p. 5681-703.
2. Asimakopoulos, G., *Mechanisms of the systemic inflammatory response.* Perfusion, 1999. **14**(4): p. 269-77.
3. Asimakopoulos, G., *Systemic inflammation and cardiac surgery: an update.* Perfusion, 2001. **16**(5): p. 353-60.
4. Asimakopoulos, G. and T. Gourlay, *A review of anti-inflammatory strategies in cardiac surgery.* Perfusion, 2003. **18 Suppl 1**: p. 7-12.
5. Scholz, M. and J. Cinatl, *Fas/FasL interaction: A novel immune therapy approach with immobilized biologicals.* Medicinal Research Reviews, 2005. **25**(3): p. 331-342.
6. Gibbon, J.H., Jr., *The gestation and birth of an idea.* Phila Med 1963. **59**: p. 913.
7. Gibbon, J.H., Jr., *Application of a mechanical heart and lung apparatus to cardiac surgery.* Minn Med, 1954. **37**(3): p. 171-85; passim.
8. Lillehei, C.W., *A personalized history of extracorporeal circulation.* Trans Am Soc Artif Intern Organs, 1982. **28**: p. 5-16.
9. Miller, G.W., *King of Hearts: The True Story of the Maverick Who pioneered Open Heart Surgery.* 2000, New York: Crown Publishers.
10. Meisner, H., *Milestones in surgery: 60 years of open heart surgery.* Thorac Cardiovasc Surg, 2014. **62**(8): p. 645-50.
11. FDA. [cited 2016 20.11.2016]; Available from: http://www.fda.gov/MedicalDevices/ProductsandMedicalProcedures/default.htm.
12. Philipp, A., et al., *Langzeitfunktion von Oxygenatoren bei extrakorporaler Lungen Unterstützung.* Kardiotechnik, 2009. **1**.
13. Cao, L., et al., *Plasma-deposited tetraglyme surfaces greatly reduce total blood protein adsorption, contact activation, platelet adhesion, platelet procoagulant activity, and in vitro thrombus deposition.* J Biomed Mater Res A, 2007. **81**(4): p. 827-37.
14. Shen, M., et al., *PEO-like plasma polymerized tetraglyme surface interactions with leukocytes and proteins: in vitro and in vivo studies.* J Biomater Sci Polym Ed, 2002. **13**(4): p. 367-90.
15. Ishihara, K., et al., *Hemocompatibility on graft copolymers composed of poly(2-methacryloyloxyethyl phosphorylcholine) side chain and poly(n-butyl methacrylate) backbone.* J Biomed Mater Res, 1994. **28**(2): p. 225-32.
16. Liefeith, K., et al., *Surface Characteristics and Biofilms*, in *Biofunctional Surface Engineering*, M. Scholz, Editor. 2014, Pan Standford Publishing: Singapore. p. 71-120.
17. Vogler, E.A., *Interfacial chemistry in biomaterials science*, in *Wettability*, J.C. Berg, Editor. 1993, Marcel Dekker, New York, Basel, Hong Kong: New York. p. 183-250.
18. Morra, M., *On the molecular basis of fouling resistance.* j Biomater Sci Polym Ed, 2000. **11**(6): p. 547-569.
19. Ascione, R., et al., *Inflammatory response after coronary revascularization with or without cardiopulmonary bypass.* Ann Thorac Surg, 2000. **69**(4): p. 1198-204.
20. el Habbal, M.H., et al., *Cardiopulmonary bypass tubes and prime solutions stimulate neutrophil adhesion molecules.* Cardiovasc Res, 1997. **33**(1): p. 209-15.
21. Paparella, D., T.M. Yau, and E. Young, *Cardiopulmonary bypass induced inflammation: pathophysiology and treatment. An update.* Eur J Cardiothorac Surg, 2002. **21**(2): p. 232-44.
22. Vohra, H.A., et al., *The inflammatory response to miniaturised extracorporeal circulation: a review of the literature.* Mediators Inflamm, 2009. **2009**: p. 707042.
23. Jaffer, I.H., et al., *Medical device-induced thrombosis: what causes it and how can we prevent it?* J Thromb Haemost, 2015. **13 Suppl 1**: p. S72-81.

24. Wilson, C.J., et al., *Mediation of biomaterial-cell interactions by adsorbed proteins: a review.* Tissue Eng, 2005. **11**(1-2): p. 1-18.
25. Levy, J.H. and K.A. Tanaka, *Inflammatory response to cardiopulmonary bypass.* Ann Thorac Surg, 2003. **75**(2): p. S715-20.
26. Amulic, B., et al., *Neutrophil function: from mechanisms to disease.* Annu Rev Immunol, 2012. **30**: p. 459-89.
27. Dancey, J.T., et al., *Neutrophil kinetics in man.* J Clin Invest, 1976. **58**(3): p. 705-15.
28. Cassatella, M.A., *The production of cytokines by polymorphonuclear neutrophils.* Immunol Today, 1995. **16**(1): p. 21-6.
29. Pillay, J., et al., *In vivo labeling with 2H2O reveals a human neutrophil lifespan of 5.4 days.* Blood, 2010. **116**(4): p. 625-7.
30. Leliefeld, P.H., et al., *The role of neutrophils in immune dysfunction during severe inflammation.* Crit Care, 2016. **20**: p. 73.
31. Lord, J.M., et al., *The systemic immune response to trauma: an overview of pathophysiology and treatment.* Lancet, 2014. **384**(9952): p. 1455-65.
32. McLean, J., *The discovery of heparin.* Circulation, 1959. **19**(1): p. 75-8.
33. Messmore, H.L., et al., *Heparin to pentasaccharide and beyond: the end is not in sight.* Semin Thromb Hemost, 2004. **30 Suppl 1**: p. 81-8.
34. Björk, I. and U. Lindahl, *Mechanism of the anticoagulant action of heparin.* Mol Cell Biochem, 1982. **48**(3): p. 161–182.
35. Lever, R. and C.P. Page, *Novel drug development opportunities for heparin.* Nat Rev Drug Discov, 2002. **1**(2): p. 140-8.
36. Xenios AG. 20.11.2016]; Available from: http://www.xenios-ag.com/novalung-products/.
37. Ahmed, I., A. Majeed, and R. Powell, *Heparin induced thrombocytopenia: diagnosis and management update.* Postgrad Med J, 2007. **83**(983): p. 575-82.
38. Kang, I.K., et al., *Immobilization of proteins on poly(methyl methacrylate) films.* Biomaterials, 1993. **14**(10): p. 787-92.
39. Kim, S.W., et al., *Platelet adhesion to polymer surfaces.* Trans Am Soc Artif Intern Organs, 1974. **20 b**: p. 449-55.
40. Park, K., D.F. Mosher, and S.L. Cooper, *Acute surface-induced thrombosis in the canine ex vivo model: importance of protein composition of the initial monolayer and platelet activation.* J Biomed Mater Res, 1986. **20**(5): p. 589-612.
41. Hartmann, H. and B. Schlosshauer, *Polyelectrolyte Multilayers as Functional Coatings for Controlled Biomolecular Interactions*, in *Biofunctional Surface Engineering*, M. Scholz, Editor. 2014, Pan Standford Publishing: Singapore. p. 27-46.
42. Xiong, X., et al., *Polyelectrolyte Multilayers as Functional Coatings for Controlled Biomolecular Interactions*, in *Biofunctional Surface Engineering*, M. Scholz, Editor. 2014, Pan Standford Publishing: Singapore. p. 47-69.
43. Bodensteiner, D.C., *Leukocyte depletion filters: a comparison of efficiency.* Am J Hematol, 1990. **35**(3): p. 184-6.
44. Matheis, G., et al., *Leukocyte filtration in the early reperfusion phase on cardiopulmonary bypass reduces myocardial injury.* Perfusion, 2001. **16**(1): p. 43-9.
45. Leal-Noval, S.R., et al., *Effects of a leukocyte depleting arterial line filter on perioperative morbidity in patients undergoing cardiac surgery: a controlled randomized trial.* Ann Thorac Surg, 2005. **80**(4): p. 1394-400.
46. Sahlman, A., et al., *No impact of a leucocyte depleting arterial line filter on patient recovery after cardiopulmonary bypass.* Acta Anaesthesiol Scand, 2001. **45**(5): p. 558-63.
47. Mair, P., et al., *Effects of a leucocyte depleting arterial line filter on perioperative proteolytic enzyme and oxygen free radical release in patients undergoing aortocoronary bypass surgery.* Acta Anaesthesiol Scand, 1999. **43**(4): p. 452-7.

48.   Boodram, S. and E. Evans, *Use of leukocyte-depleting filters during cardiac surgery with cardiopulmonary bypass: a review.* J Extra Corpor Technol, 2008. **40**(1): p. 27-42.

49.   Cinatl, J., Jr., et al., *Decreased neutrophil adhesion to human cytomegalovirus-infected retinal pigment epithelial cells is mediated by virus-induced up-regulation of Fas ligand independent of neutrophil apoptosis.* J Immunol, 2000. **165**(8): p. 4405-13.

50.   Scholz, M., et al., *First efficacy and safety results with the antibody containing leukocyte inhibition module in cardiac surgery patients with neutrophil hyperactivity.* Asaio j, 2005. **51**(2): p. 144-7.

51.   Abdel-Rahman, U., et al., *Inhibition of neutrophil activity improves cardiac function after cardiopulmonary bypass.* J Inflamm (Lond), 2007. **4**: p. 21.

52.   Paunel-Gorgulu, A., et al., *Increased serum soluble Fas after major trauma is associated with delayed neutrophil apoptosis and development of sepsis.* Crit Care, 2011. **15**(1): p. R20.

53.   Paunel-Gorgulu, A., et al., *Stimulation of Fas signaling down-regulates activity of neutrophils from major trauma patients with SIRS.* Immunobiology, 2011. **216**(3): p. 334-42.

54.   Paunel-Gorgulu, A., et al., *Mcl-1-mediated impairment of the intrinsic apoptosis pathway in circulating neutrophils from critically ill patients can be overcome by Fas stimulation.* J Immunol, 2009. **183**(10): p. 6198-206.

55.   Tscheliessnig, R., et al., *Nano-coating protects biofuntional materials.* Materials Today, 2012. **15**(9): p. 394-404.

56.   Mincheff, M., et al., *Fas and Fas ligand expression on human peripheral blood leukocytes.* Vox Sang, 1998. **74**(2): p. 113-21.

57.   Hengartner, M.O., *The biochemistry of apoptosis.* Nature, 2000. **407**(6805): p. 770-776.

58.   Paunel-Gorgulu, A., et al., *Molecular mechanisms underlying delayed apoptosis in neutrophils from multiple trauma patients with and without sepsis.* Mol Med, 2012. **18**: p. 325-35.

59.   Holler, N., et al., *Two adjacent trimeric Fas ligands are required for Fas signaling and formation of a death-inducing signaling complex.* Mol Cell Biol, 2003. **23**(4): p. 1428-40.

60.   Chodorge, M., et al., *A series of Fas receptor agonist antibodies that demonstrate an inverse correlation between affinity and potency.* Cell Death Differ, 2012. **19**(7): p. 1187-95.

61.   Logters, T.T., et al., *Extracorporeal immune therapy with immobilized agonistic anti-Fas antibodies leads to transient reduction of circulating neutrophil numbers and limits tissue damage after hemorrhagic shock/resuscitation in a porcine model.* J Inflamm (Lond), 2010. **7**: p. 18.

62.   Wang, W., *Lyophilization and development of solid protein pharmaceuticals.* Int J Pharm, 2000. **203**(1-2): p. 1-60.

63.   Chi, E.Y., *Excipients used in biotechnology products*, in *Pharmaceutical Excipients: Properties, Functionality, and Applications in Research and Industry*, O.M.Y. Koo, Editor. 2017, Wiley: Hoboken, New Jersey. p. 145-198.

64.   Arakawa, T., et al., *Factors affecting short-term and long-term stabilities of proteins.* Adv Drug Deliv Rev, 2001. **46**(1-3): p. 307-26.

65.   Arakawa, T., et al., *Biotechnology applications of amino acids in protein purification and formulations.* Amino Acids, 2007. **33**(4): p. 587-605.

66.   Carpenter, J.F., et al., *Rational design of stable lyophilized protein formulations: some practical advice.* Pharm Res, 1997. **14**(8): p. 969-75.

67.   Chang, L.L. and M.J. Pikal, *Mechanisms of protein stabilization in the solid state.* J Pharm Sci, 2009. **98**(9): p. 2886-908.

68.   Frokjaer, S. and D.E. Otzen, *Protein drug stability: a formulation challenge.* Nat Rev Drug Discov, 2005. **4**(4): p. 298-306.

69.   Jones, L.S., et al., *The effects of Tween 20 and sucrose on the stability of anti-L-selectin during lyophilization and reconstitution.* J Pharm Sci, 2001. **90**(10): p. 1466-77.

70.   Manning, M.C., K. Patel, and R.T. Borchardt, *Stability of protein pharmaceuticals.* Pharm Res, 1989. **6**(11): p. 903-18.

71.   Ohtake, S., Y. Kita, and T. Arakawa, *Interactions of formulation excipients with proteins in solution and in the dried state.* Adv Drug Deliv Rev, 2011. **63**(13): p. 1053-73.

72.   Sarciaux, J.M., et al., *Effects of buffer composition and processing conditions on aggregation of bovine IgG during freeze-drying.* J Pharm Sci, 1999. **88**(12): p. 1354-61.

73.   Cromwell, M.E., E. Hilario, and F. Jacobson, *Protein aggregation and bioprocessing.* Aaps j, 2006. **8**(3): p. E572-9.

74.   Rathore, N. and R.S. Rajan, *Current perspectives on stability of protein drug products during formulation, fill and finish operations.* Biotechnol Prog, 2008. **24**(3): p. 504-14.

75.   Yancey, P.H., et al., *Living with water stress: evolution of osmolyte systems.* Science, 1982. **217**(4566): p. 1214-22.

76.   Crowe, J.H., F.A. Hoekstra, and L.M. Crowe, *Anhydrobiosis.* Annu Rev Physiol, 1992. **54**: p. 579-99.

77.   Crowe, L.M. and J.H. Crowe, *Anhydrobiosis: a strategy for survival.* Adv Space Res, 1992. **12**(4): p. 239-47.

78.   Timasheff, S.N., *The control of protein stability and association by weak interactions with water: how do solvents affect these processes?* Annu Rev Biophys Biomol Struct, 1993. **22**: p. 67-97.

79.   Timasheff, S.N., *Protein-solvent preferential interactions, protein hydration, and the modulation of biochemical reactions by solvent components.* Proc Natl Acad Sci U S A, 2002. **99**(15): p. 9721-6.

80.   Scholz, M., *Personal communication.* 2016.

81.   Farrokh-Siar, L., et al., *Human fetal retinal pigment epithelial cells induce apoptosis in the T-cell line Jurkat.* Invest Ophthalmol Vis Sci, 1999. **40**(7): p. 1503-11.

82.   Peterson, E.J., K.M. Latinis, and G.A. Koretzky, *Molecular characterization of a CD95 signaling mutant.* Arthritis Rheum, 1998. **41**(6): p. 1047-53.

83.   Schneider, U., H.U. Schwenk, and G. Bornkamm, *Characterization of EBV-genome negative "null" and "T" cell lines derived from children with acute lymphoblastic leukemia and leukemic transformed non-Hodgkin lymphoma.* Int J Cancer, 1977. **19**(5): p. 621-6.

84.   Boyum, A., *Separation of leukocytes from blood and bone marrow. Introduction.* Scand J Clin Lab Invest Suppl, 1968. **97**: p. 7.

85.   Binder, T., D. Heinz, and F. Roland, *Pappenheim-Färbung. Beschreibung einer hämatologischen Standardfärbung-Geschichte, Chemie, Durchführung, Artefakte und Problemlösungen.* J Lab Med, 2012. **5**(36): p. 293-309.

86.   Pappenheim, A., *Zur Blutzellfärbung im klinischen Bluttrockenpräparat und zur histologischen Schnittpräparatfärbung der hämatopoetischen Gewebe nach meinen Methoden.* Folia Haematologica, 1912. **13**: p. 339-45.

87.   May, R. and L. Grünwald, *Über Blutfärbungen.* Centralbl Inn Med, 1902(11): p. 1-6.

88.   Giemsa, G., *Färbemethoden für Malariaparasiten.* Centralbl Bakteriol 1902. **31**: p. 429-30.

89.   Welsch, U. and M. Mulisch, *Mikroskopische Technik.* 18 ed. 2010, Heidelberg: Spektrum Akademischer Verlag.

90.   Degel, J. and M. Shokrani, *Validation of the efficacy of a practical method for neutrophils isolation from peripheral blood.* Clin Lab Sci, 2010. **23**(2): p. 94-8.

91.   Barclay, N.A., M.H. Brown, and M.L. Birkenland *The Leukocyte Antigen FactsBook.* 1997, San Diego, CA, USA: Academic Press.

92.	Stroncek, D.F., *Neutrophil-specific antigen HNA-2a, NB1 glycoprotein, and CD177.* Curr Opin Hematol, 2007. **14**(6): p. 688-93.

93.	Nicoletti, I., et al., *A rapid and simple method for measuring thymocyte apoptosis by propidium iodide staining and flow cytometry.* J Immunol Methods, 1991. **139**(2): p. 271-9.

94.	Riccardi, C. and I. Nicoletti, *Analysis of apoptosis by propidium iodide staining and flow cytometry.* Nat Protoc, 2006. **1**(3): p. 1458-61.

95.	BD Biosciences, *FITC Annexin V Apoptosis Detection Kit I.* 2015.

96.	Niesen, F.H., H. Berglund, and M. Vedadi, *The use of differential scanning fluorimetry to detect ligand interactions that promote protein stability.* Nat Protoc, 2007. **2**(9): p. 2212-21.

97.	Freitas, M., et al., *Isolation and activation of human neutrophils in vitro. The importance of the anticoagulant used during blood collection.* Clin Biochem, 2008. **41**(7-8): p. 570-5.

98.	Kim, G.D., et al., *beta2 integrins (CD11/18) are essential for the chemosensory adhesion and migration of polymorphonuclear leukocytes on bacterial cellulose.* J Biomed Mater Res A, 2015. **103**(5): p. 1809-17.

99.	Beyrau, M., J.V. Bodkin, and S. Nourshargh, *Neutrophil heterogeneity in health and disease: a revitalized avenue in inflammation and immunity.* Open Biol, 2012. **2**(11): p. 120134.

100.	Hu, N., et al., *Coexpression of CD177 and membrane proteinase 3 on neutrophils in antineutrophil cytoplasmic autoantibody-associated systemic vasculitis: antiproteinase 3-mediated neutrophil activation is independent of the role of CD177-expressing neutrophils.* Arthritis Rheum, 2009. **60**(5): p. 1548-57.

101.	Vermeer, A.W. and W. Norde, *The thermal stability of immunoglobulin: unfolding and aggregation of a multi-domain protein.* Biophys J, 2000. **78**(1): p. 394-404.

102.	Eisele, G., et al., *APO010, a synthetic hexameric CD95 ligand, induces human glioma cell death in vitro and in vivo.* Neuro Oncol, 2011. **13**(2): p. 155-64.

103.	Verbrugge, I., et al., *Combining radiotherapy with APO010 in cancer treatment.* Clin Cancer Res, 2009. **15**(6): p. 2031-8.

104.	Simon, M., U. Zangemeister-Wittke, and A. Pluckthun, *Facile double-functionalization of designed ankyrin repeat proteins using click and thiol chemistries.* Bioconjug Chem, 2012. **23**(2): p. 279-86.

105.	Weetall, H.H., *Preparation of immobilized proteins covalently coupled through silane coupling agents to inorganic supports.* Appl Biochem Biotechnol, 1993. **41**(3): p. 157-88.

106.	Martins, M.C., et al., *Albumin and fibrinogen adsorption on PU-PHEMA surfaces.* Biomaterials, 2003. **24**(12): p. 2067-76.

107.	Lu, Q.-W., T.R. Hoye, and C.W. Macosko, *Reactivity of common functional groups with urethanes: Models for reactive compatibilization of thermoplastic polyurethane blends.* J Polym Sci A Polym Chem, 2002. **40**: p. 2310–2328.

108.	Jóźwiak, A.B., C.M. Kielty, and R.A. Black, *Surface functionalization of polyurethane for the immobilization of bioactive moieties on tissue scaffolds.* J. Mater. Chem., 2008. **18**(19): p. 2240-2248

109.	Mühlhan, C., *Plasmaaktivierung von Polypropylenoberflächen zur Optimierung von Klebverbunden mit Cyanacrylat Klebstoffen im Hinblick auf die mechanischen Eigenschaften.* 2002.

110.	Earle, W.R., *Production of malignancy in vitro. IV. The mouse fibroblast cultures and changes seen in the lining cells.* J Natl Cancer Inst, 1943. **4**: p. 165-212

111.	Sanford, K.K., W.R. Earle, and G.D. Likely, *The growth in vitro of single isolated tissue cells.* J Natl Cancer Inst, 1948. **9**(3): p. 229-46.

112.	Gallati, H. and I. Pracht, *[Horseradish peroxidase: kinetic studies and optimization of peroxidase activity determination using the substrates H2O2 and 3,3',5,5'-tetramethylbenzidine].* J Clin Chem Clin Biochem, 1985. **23**(8): p. 453-60.

113. DIN-EN-ISO-10993-1:2009, *Biological evaluation of medical devices; Part 1: Evaluation and testing within a risk management system.*
114. DIN-EN-ISO-10993-5:2009, *Biological evaluation of medical devices; Part 5: Tests for in vitro cytotoxicity.*
115. DIN-EN-ISO-10993-12:2012, *Biological evaluation of medical devices; Part 12: Sample preparation and reference materials*
116. Stefan, N., et al., *DARPins recognizing the tumor-associated antigen EpCAM selected by phage and ribosome display and engineered for multivalency.* J Mol Biol, 2011. **413**(4): p. 826-43.
117. Stumpp, M.T., H.K. Bint, and P. Amstutz, *DARPins: A new generation of protein therapeutics.* Drug Discov Today, 2008. **13**: p. 695-701.
118. Winkler, J., et al., *EpCAM-targeted delivery of nanocomplexed siRNA to tumor cells with designed ankyrin repeat proteins.* Mol Cancer Ther, 2009. **8**(9): p. 2674-83.
119. Kasemo, B., *Biological surface science.* Surface Science, 2002. **500**(1–3): p. 656-677.
120. Roger, Y., et al., *Grid-like surface structures in thermoplastic polyurethane induce anti-inflammatory and anti-fibrotic processes in bone marrow-derived mesenchymal stem cells.* Colloids Surf B Biointerfaces, 2016. **148**: p. 104-115.
121. Gil, D., et al., *Anti-inflammatory coatings of hernia repair meshes: A pilot study.* J Biomed Mater Res B Appl Biomater, 2017.
122. Blanco-Garcia, E., et al., *Development and characterization of anti-inflammatory activity of curcumin-loaded biodegradable microspheres with potential use in intestinal inflammatory disorders.* Int J Pharm, 2017. **518**(1-2): p. 86-104.
123. Correia, C.R., et al., *The influence of surface modified poly(l-lactic acid) films on the differentiation of human monocytes into macrophages.* Biomater Sci, 2017. **5**(3): p. 551-560.
124. Margraf, S., et al., *Stabilizing compositions for immobilized biomolecules.* 2012, Google Patents.
125. ISO-11607-1:2014-11, *Packaging for terminally sterilized medical devices; Part 1: Requirements for materials, sterile barrier systems and packaging systems.*
126. ASTM-F-1980:2016, *Standard Guide for Accelerated Aging of Sterile Barrier Systems for Medical Devices.*
127. Mendes, G.C., T.R. Brandao, and C.L. Silva, *Modeling the inactivation of Bacillus subtilis spores by ethylene oxide processing.* J Ind Microbiol Biotechnol, 2011. **38**(9): p. 1535-43.
128. Mendes, G.C.C., T.R.S. Brandão, and C.L.M. Silva, *Ethylene oxide sterilization of medical devices: A review.* American Journal of Infection Control, 2007. **35**(9): p. 574-581.